This is to certify that the
dissertation entitled

DETECTION OF EMERGING PANDEMIC INFLUENZA STRAINS BY SURFACE PLASMON RESONANCE AND ELECTRICALLY-ACTIVE MAGNETIC NANOPARTICLE-BASED BIOSENSOR

presented by

TRACY KAMIKAWA

has been accepted towards fulfillment
of the requirements for the

Ph.D. degree in Biosystems Engineering

EC Slonlja

Major Professor's Signature

July 26, 2010

Date

MSU is an Affirmative Action/Equal Opportunity Employer

DETECTION OF EMERGING PANDEMIC INFLUENZA STRAINS BY SURFACE PLASMON RESONANCE AND ELECTRICALLY-ACTIVE MAGNETIC NANOPARTICLE-BASED BIOSENSOR

By

Tracy Kamikawa

A DISSERTATION

Submitted to
Michigan State University
in partial fulfillment of the requirements
for the degree of

DOCTOR OF PHILOSOPHY

Biosystems Engineering

2010

ABSTRACT

DETECTION OF EMERGING PANDEMIC INFLUENZA STRAINS BY SURFACE PLASMON RESONANCE AND ELECTRICALLY-ACTIVE MAGNETIC NANOPARTICLE-BASED BIOSENSOR

By

Tracy Kamikawa

Rapid detection technologies including surface plasmon resonance (SPR) and nanomaterial based biosensors are emerging as sensitive, specific, and rapid diagnostic tools for the detection of highly pathogenic viruses. This research demonstrates the novel application of SPR and nano-biosensors for Influenza A virus (FLUAV) detection, utilizing specificity of binding between FLUAV hemagglutinin (HA) and host sialic acid (SA) receptors, which determines viral infectivity and transmissibility. In SPR, SA receptors functionalize a gold sensor surface and a microfluidic system passes over recombinant HA, with binding indicated by a measurable increase in mass at the surface. In the nano-biosensor, nanostructured materials serve as both magnetic concentrator and biosensor transducer. Aniline monomer is coated around gamma iron oxide cores and made electrically active by acid doping. The synthesized electrically active polyaniline coated magnetic (EAM) nanoparticles are adapted in an electrochemical biosensor. Biologically modified EAMs immunomagnetically concentrate target HA bound to SA capture probes, and 10-minute electrochemical detection follows application of glycan/HA/EAM complexes to screen printed carbon electrodes. Experimental results indicate that the SPR and biosensor systems are able to detect FLUAV HA at 31.4 nM in 2% mouse serum and 1.4 μM in 10% mouse serum, respectively.

ACKNOWLEDGEMENTS

I sincerely thank everyone who contributed to this research over the years. I offer especial appreciation towards Dr. Evangelyn Alocilja for her tireless and unconditional support, not only during my graduate program but from the beginning of my undergraduate work, when she offered a home and family to me when mine was many miles away. Her guidance has shaped not only my scientific career but also my personal character, and I will carry her passion for improving the lives of others throughout my life. I am also thankful for the patience and encouragement from Dr. Dorothy Scott, who tirelessly supported my work at the FDA and strengthened the biologics side of my research. Both mentors have fostered supportive and encouraging work environments, and I thank them as well as the members of their labs for the help that they have given me in my research. They have made this process enjoyable! I also thank the members of my Ph.D. guidance committee: Dr. Shantanu Chakrabartty, Dr. Daniel Grooms, and Dr. Bradley Marks for their continuous support.

I would like to also express my unending gratitude to my family and friends who have offered guidance, patience, and love throughout this long journey. All that I have and will accomplish is because of and for you all!

Tracy Kamikawa

I would like to thank E. Torres-Chavolla, A. Pastor-Lecha, and the Center for Advanced Microscopy at Michigan State University for providing TEM assistance and expertise, and E. B. Setterington, H. Miller, D. Zhang, M. Huarng, and S. Pal for input and use of cyclic voltammetry reagents. I also thank Dr. N. Razi, A. Tran-Crie, and Dr. D. Smith of The Consortium for Functional Glycomics for helpful advice and assistance with biotinylated carbohydrate compounds.

This work was supported by Critical Path Funding from the U.S. Food and Drug Administration, Center for Biologics Evaluation and Research (FDA CBER). "The findings and conclusions in this publication have not been formally disseminated by the Food and Drug Administration and should not be construed to represent any Agency determination or policy."

TABLE OF CONTENTS

LIST OF TABLES

LIST OF FIGURES

Images in this dissertation are presented in color.

CHAPTER 1: INTRODUCTION

On June 11, 2009, the World Health Organization declared a global pandemic of novel H1N1 Influenza A virus (FLUAV). Novel H1N1 FLUAV was first observed in humans in Mexico and the United States beginning in March, 2009, and since then the virus has spread rapidly across all 50 states. At the time of the pandemic declaration, novel H1N1 FLUAV had been reported in 70 countries across the globe (CDC, 2009). The emergence of swine origin H1N1 from natural animal reservoirs brought the devastating capabilities of FLUAV viruses into public consciousness, although these viruses have been plaguing global economies for decades. Prior to the H1N1 pandemic, global pandemics had previously occurred throughout history, with varying causes and consequences. Of particular note was the H1N1 pandemic of 1918, referred to as the "Spanish flu," which was extremely virulent and led to 20-40 million deaths worldwide (Reid *et al.*, 2001).

The H1N1 pandemics of 1918 and 2009 differ in their characteristics. Both strains caused pandemics, but for different reasons. The 1918 H1N1 strain was widespread, infecting one third of the world's population, and was also the most virulent of all historical pandemic strains, leading to case fatality rates of >2.5% (Burnet and Clark, 1942; Marks and Beatty, 1976; Reid *et al.*, 2001; Taubenberger and Morens, 2006). The 2009 H1N1 strain also experienced rapid spread, but was relatively less severe, with the cumulative total number of cases worldwide at 380,000 with a <1% death rate (as of 4 October 2009; see WHO, 2009). The ability of a FLUAV strain to transmit from human-to-human is thus essential for a pandemic to occur, whether or not the strain is highly lethal. Typically, FLUAV strains must be specific for the human receptors high in the

respiratory tract, so that transmission by aerosol or surface contact is facilitated, as opposed to those strains specific for the receptors deeper in the respiratory tract. Animal FLUAV strains are typically specific for the less-accessible receptors.

The highly pathogenic avian influenza virus subtype H5N1 is one such strain. H5N1 has caused serious losses in the poultry industry and continues to affect wild fowl populations across the world, but particularly throughout Asia. The receptor recognition of H5N1 does not lend itself to human-to-human transmission. However, the ability of FLUAV viruses to easily mutate could lead a highly pathogenic avian strain to achieve human infectivity via specificity for the upper respiratory tract receptor, eventually leading to a pandemic with casualties of 1918 proportions. This could occur naturally via existing animal reservoirs, or as a result of bioterrorism efforts. Pathogenic H5N1 has been generated in the laboratory, and by similar methods of recombinant DNA technology, a highly pathogenic FLUAV could also gain human-to-human transmissibility, and thus pandemic potential (Hatta *et al.*, 2001a,b).

H5 has been identified as a subtype of FLUAV that could most likely be transmitted to humans (Webby and Webster, 2003). In fact, in those cases where humans have been infected by close contact with H5N1 infected birds, >30% of cases were fatal (Webby and Webster, 2003). If H5N1 were to become more easily transmitted from human-to-human, like an epidemic of "seasonal flu" which is carried by sneezing and casual contact, the world population would be at risk for widespread and highly fatal infection.

Vaccine development and production have proven challenging, especially when demand is high in the face of a worldwide crisis. Vaccine design is based on assumptions of which strains could gain prevalence in the following year, and as demonstrated by the

inability of the 2009 vaccine to prevent the H1N1 pandemic, these assumptions are not always correct.

In association with FLUAV epidemics, the United States experiences annual direct and indirect costs of up to $12 billion, associated with doctor's office visits, hospitalizations, medications, and work productivity losses (Solvay, 2010). Epidemic FLUAV strains are in general far less virulent and severe than pandemic strains, and the costs associated with a pandemic could be far greater. As reported by the U.S. Department of Health and Human Services, production of over 125 million doses of pandemic H1N1 vaccine has cost approximately $8 billion (Newborg, 2009). During the height of the H1N1 pandemic, many public schools were forced to halt all operations to prevent further spread. The Brookings Institute predicts that a nationwide school closure for four weeks could lead to $10-47 billion in lost economic activity, which represents 0.1-0.3 percent of the GDP. The Congressional Budget Office predicts that loss of GDP could reach 4.5 percent in the event of a pandemic on the scale of the 1918 Spanish Influenza pandemic (Amico, 2009).

Understanding the infectivity of FLUAV is essential in preventing the next pandemic. A method of rapidly testing emerging pandemic viruses could be the first line of defense against a historically non-human-transmissible strain which has gained human transmissibility by natural or unnatural routes. Targeted vaccine development could then proceed before wide spread, or other preventative measures such as quarantine or medicinal treatment could be undertaken. Current human and animal diagnostic methods for virus detection are generally based on internationally recognized methods of isolation culture with immunocytological confirmation of viral antigen (Alexander *et al.*, 2005;

Charlton *et al.*, 2009). The entire process could take up to 21 days, involving high costs of reagents and labor. The development of rapid detection devices has thus become increasingly necessary for environmental and agricultural disease surveillance, and to provide early detection of potentially human pandemic FLUAV strains for limiting spread and severity.

Biosensors are attractive alternatives for early identification of infectious pathogens such as FLUAV, and offer low cost, speed, and ease of operation as compared to their conventional counterparts. A wide range of detection platforms and targets are under investigation, spanning all fields of public health, and major advances have been made in recent years, with evolution still continuing.

Nanotechnology has offered a whole new world of possibilities to biodetection systems. Nanostructured materials such as gold and magnetic nanoparticles have been demonstrated to be effective biosensor transducer materials. A recent advancement is the development of nanostructures with both magnetic and conductive properties. Typically, these are presented with a core/shell (c/s) of magnetic/electrically active materials. One application exploits the conductive nature of polyaniline and the magnetic nature of iron (III) oxide to generate electrically active polyaniline coated magnetic nanoparticles (EAMs) with optimal combined properties of strength, flexibility, and electrochemical activity. Current literature indicates that these EAMs have not yet been applied in the detection of highly pathogenic FLUAV.

This dissertation describes the characterization of binding between the FLUAV surface glycoprotein responsible for host infectivity, hemagglutinin (HA), and the host cell carbohydrate (glycan) receptor. Surface plasmon resonance (SPR) and an

electrochemical biosensor platform were investigated as compatible assays using the same glycan/HA pairs. Because a disposable biosensor technology has not yet been reported, the SPR system was utilized to ploy the interactions between H5N1 HA and appropriate glycan receptors, as well as to identify H5-targeted antibodies with the ability to neutralize this binding. Serum matrix effects were also evaluated in the SPR system performance. Once high avidity binding pairs were identified on the SPR system, an electrochemical biosensor was designed and fabricated, utilizing immunofunctionalized EAMs as both the magnetic concentrator of the target glycan/HA complex and the transducer in the electrochemical detection of EAM nanoparticles on a screen printed carbon electrode. The binding between Influenza hemagglutinin and glycan receptors was then characterized on the biosensor platform for correlation to SPR results. Once the biosensor platform fabrication technique was established, other glycan/HA pairs were investigated, including human targets.

CHAPTER 2: LITERATURE REVIEW

2.1 INFLUENZA VIRUS

Influenza virus A (FLUAV) is an acute viral disease agent of the respiratory tract (Stevens *et al.*, 2006a), which is classified as a genus of the *Orthomyxoviridae* family (WHO, 2006). Millions of people worldwide are affected annually by FLUAV, either by epidemics of "seasonal flu," or, less commonly, by infection with a pandemic strain such as H5N1, "bird flu," or H1N1, "swine flu." The 2009 swine-origin H1N1 pandemic exemplifies the speed with which a human-transmissible FLUAV can spread worldwide. The strain had circulated in pig herds for decades, but once humans became infected, the virus achieved global spread in a matter of weeks (Michaelis, 2009).

Hemagglutinin (HA) and neuraminidase (NA) are integral membrane proteins. M2 ion channel protein is inserted through the lipid bilayer. Virion matrix protein M1 underlies the lipid bilayer. The segmented genome exists as eight RNA single-strands, to form ribonucleoproteins with transcriptase proteins PB1, PB2, and PA (Figure 1).

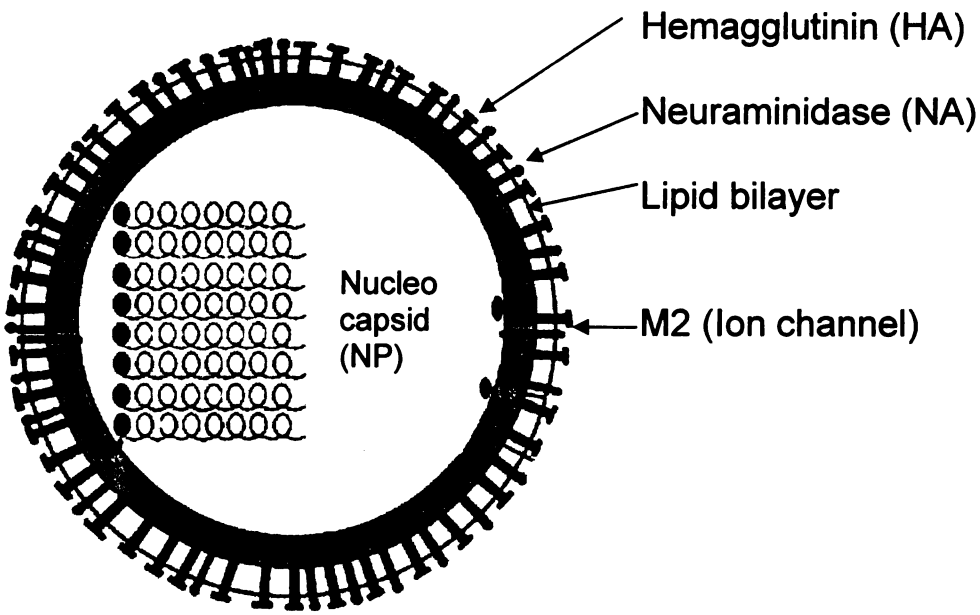

Figure 1. Schematic representation of the structure of the Influenza A virion (adapted and modified from Zhuang, 2009).

2.1.1 Viral Infectivity

The viral surface glycoproteins hemagglutinin (HA) and neuraminidase (NA) are used to name and characterize each FLUAV strain, as they are largely responsible for viral infectivity (Stevens *et al.*, 2006a). HA mediates FLUAV host specificity and host cell entry (Stevens *et al.*, 2006a; Wiley and Skehel, 1987). Of the sixteen known HA and nine known NA serotypes, only three HA and two NA have adapted sufficiently to become pandemic in humans. Pandemics recorded in history have included H1N1 in 1918 and 2009, H2N2 in 1957, and H3N2 in 1968. Birds are thought to act as the main reservoir for FLUAV, because all identified serotypes circulate in the avian population (Neumann and Kawaoka, 2006; Stevens *et al.*, 2006a; Stevens *et al.*, 2006b; Taubenberger *et al.*, 2005).

2.1.2 Epidemic Spread

Epidemics of FLUAV are largely facilitated by the ease and speed of human-to-human transmissibility by aerosol (Wright and Webster, 2001). These "seasonal flu" epidemics are responsible for 36,000 deaths and 200,000 hospitalizations in the U.S. annually, leading to costs for the nation of over $10 billion (HSC, 2005). These epidemics are caused by antigenic drift, by which the HA undergoes relatively minor changes that result from the selection of mutant viruses by antibodies generated against the prominent HA antigenic type currently circulating in the human population (Wright and Webster, 2001). Each year, the body produces antibodies against the prominent FLUAV strain, either naturally or after vaccination. Once the targeted HA antigen mutates to a form no longer recognizable by the antibodies, the body loses resistance and an annual epidemic results (NIAID, 2005).

2.1.3 Pandemic Spread

Of even greater concern are FLUAV pandemics, or global disease outbreaks, which result in high mortality rates (WHO, 2004; Wright and Webster, 2001). The FLUAV strains that have adapted to produce human pandemics include H1N1 (1918, 2009), H2N2 (1957), and H3N2 (1968) (Stevens *et al.*, 2006a). The most virulent of these was the 1918-1919 outbreak of H1N1, known as the "Spanish flu," which resulted in 20-40 million deaths worldwide (Reid *et al.*, 2001). It is believed that the extreme virulence of the virus was the main cause of the high mortality rate, as opposed to other factors such as lack of antimicrobial agents. RNA sequencing has not revealed the reason for such high pathogenicity (Neumann and Kawaoka, 2006). Such human pandemics are

caused by antigenic shifts in the HA of FLUAV, which occur less frequently than the antigenic drifts associated with FLUAV epidemics (Wright and Webster, 2001).

2.1.4 Antigenic Shifting

Antigenic shifts result from a replacement of the genomic RNA segment encoding HA, and allow FLUAV strains to jump from one animal species to another. An antigenic shift may occur by one of three ways. In the first route, an avian strain and a human strain are both passed to an intermediate host such as a chicken or pig. When the viruses co-infect the same cell, genes from the avian and human strains mix to yield a new strain that can spread to humans (NIAID, 2005). The avian strain provides the new HA genomic segment via reassortment with the human strain (WHO, 2006). FLUAV lends itself to such reassortment because the segmented nature of its genome allows for the exchange of entire genes between different viral strains when they cohabitate the same cell (Shaw *et al.*, 1992). When the reassortant strain further evolves to gain human-to-human transmissibility, a pandemic could arise (NIAID, 2005). It is commonly presumed that the 1918, 1957, 1968, and 2009 pandemic strains were the result of such reassortments (Stevens *et al.*, 2006a). An antigenic shift may also occur when an avian strain jumps directly from a bird or duck to a human without undergoing a genetic change, or when an avian strain jumps from a bird to an intermediate host and then to humans without undergoing a genetic change. When any of these new strains gain human-to-human transmissibility, a FLUAV pandemic could arise (NIAID, 2005).

2.1.5 Emergence of Highly Pathogenic Influenza Strains

2.1.5.1 Natural Reservoirs

The emergence of highly pathogenic FLUAV from natural animal reservoirs is a likely threat, as evidenced by the 2009 swine-origin H1N1 pandemic. Historically, human infections by avian FLUAV strains including H5N1, H9N2, H7N7, and H7N3 have been more commonplace, and could serve as a model for animal-to-human infection mechanisms with applicability for avian, swine, or other emerging primary hosts (Matrosovich M.N. *et al.*, 2004). H5N1 in particular has become epizootic in domestic fowl throughout Asia since 2003, is spreading to European and African bird populations, and has been confirmed in human cases. Since 2003, 385 confirmed human cases of H5N1 have been reported to the World Health Organization (WHO), including 243 deaths (as of 19 June 2008, see WHO, 2008). While human-to-human transmission has not yet shown effectiveness, the high mortality rate is cause for concern (Stevens *et al.*, 2006c).

2.1.5.2 Human-to-Human Transmissibility

Human-to-human transmission of these infections, and thus the potential for pandemic, is dependent upon HA receptor specificity (Matrosovich M.N. *et al.*, 2004; Stevens J. *et al.*, 2006a). HA mediates FLUAV host specificity and host cell entry, and binds to glycan receptors with terminal sialic acids (Stevens J. *et al.*, 2006a; Wiley and Skehel., 1987). Avian FLUAV preferentially bind to sialic acids (Figure 2) connected to galactose by α2.3 linkages on lower respiratory tract ciliated cells, whereas human FLUAV preferentially bind to α2.6-linked sialic acids on nonciliated cells found in the nose and throat (Matrosovich M.N. *et al.*, 2004; Stevens J. *et al.*, 2006a).

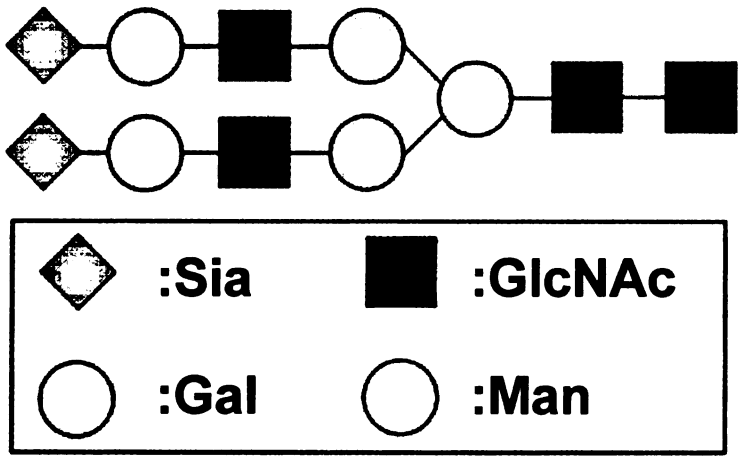

Figure 2. General structure of glycan receptor with terminal sialic acids (adapted and modified from Blixt *et al.*, 2004).

The specificity for the α2.6 receptor of isolates from the 1957 (H2N2) and 1968 (H3N2) pandemics is the primary reason that human-to-human transmission was possible (Matrosovich M.N. *et al.*, 2004; Tumpey T.M. *et al.*, 2007). It can be assumed that the 1918 (H1N1) pandemic FLUAV strains were also specific for the α2.6 receptor. Conversely, human infection by avian FLUAV that preferentially bind to the α2.3 receptor will not transmit efficiently from human-to-human and will thus not yield a pandemic. The H5N1 outbreak in Hong Kong in 1997 was specific for the α2.3 receptor (Matrosovich M.N. *et al.*, 2004). In this instance, the FLUAV strain was highly virulent but transmission between humans did not occur (Class *et al.*, 1998; Suarez *et al.*, 1998; Subbarao *et al.*, 1998; Yuen *et al.*, 1998).

Humans possess both α2.3 and α2.6 receptors, with a greater density of α2.3 in the lower respiratory tract, and α2.6 in the upper respiratory tract. It is believed that in those cases where avian FLUAV has infected humans, via the handling of dead poultry or other

close contact with contaminated materials or infected people, the avian virus has not switched receptor specificity, but has bound its α2.3 receptors deep in the respiratory tract, where they are able to efficiently replicate. This may explain the so far inefficient human-to-human transmission of H5N1. If an avian FLUAV mutates to achieve recognition of the human α2.6 receptor in the upper airway, the virus will be easily transmitted by the sneezing and coughing seen with current epidemics (Shinya *et al.*, 2006). As shown in the Vietnam and Turkey outbreaks, the virus obtained a greater affinity to the α2.6 receptors due to mutations or reassortment of genes with circulating human FLUAV (Krug, 2003; Stevens J. *et al.*, 2006c). Indeed, the 1918, 1957, and 1968 pandemic FLUAV strains are thought to have been alterations of avian FLUAV strains with α2.3 specificities (Tumpey T.M. *et al.*, 2007).

2.1.6 The Need for a Novel Biosensor Technology

FLUAV continues to circulate in Asian poultry markets, and in all plausibility, once a lethal FLUAV strain is transmitted from poultry to humans it may not be possible to prevent the virus from acquiring human-to-human transmissibility via antigenic shifts (Krug, 2003; Webster *et al.*, 2002). A detection method for rapidly identifying α2.6 specificity will be essential in this event, so that an avian FLUAV not previously known to be transmissible among humans can be identified as pandemic immediately after such transmissibility is acquired. Preventative measures against widespread human infection can then occur in a timely manner. For example, patients infected with α2.6 strains may be quickly treated with antiviral drugs or placed under stringent quarantine before the infection is passed along to others (Krug, 2003). Pandemic viruses thus emerge from avian progenitors via HA receptor specificity alteration, but because the underlying

mechanism of these shifts is unclear, it is difficult to predict such a progression with certainty. Thus, a method of rapidly determining the binding specificity of an emerging FLUAV strain will help to predict the potential for human-to-human transmission and the likely emergence of a pandemic strain.

The development of a biosensor technology that functions on the differential and specific binding of FLUAV HA to host SA is a significant initiative with regard to disease monitoring and homeland security. Such a FLUAV biosensor can probe the infection path of an emerging FLUAV strain, providing a starting point for environmental virus monitoring useful in tracking the course of virus circulation. Should FLUAV be engineered for use as a bioterrorism agent, such a biosensor could detect the appearance of a virus strain lethal to humans and perhaps possessing a novel HA subtype (Amano and Cheng, 2005).

The high death rates associated with past pandemics and the ease of human-to-human transmission could make human FLUAV attractive to bioterrorists. Even if a progression from α2.3 to α2.6 specificity does not occur by the natural mechanisms described above, lethal human FLUAV may be generated by the reverse genetic system by which transfection of multiple DNAs occurs without a helper virus (Fodor *et al.*, 1999; Neumann *et al.*, 1999). Recombinant DNA techniques have been used to generate pathogenic H5N1 virus in the laboratory (Hatta *et al.*, 2001a,b), and it is likely that such methods could also transfer human-to-human transmissibility or antiviral resistance to a pandemic avian influenza virus (Hay *et al.*, 1985; Pinto *et al.*, 1992; Air *et al.*, 1999).

There is great interest in maximizing the availability of blood and blood components during a pandemic. The FDA and the American Association of Blood Banks

(AABB) Pandemic Influenza Task Force have been working to anticipate the impact of a major FLUAV pandemic on the sustained availability of blood supplies in the U.S. (Williams, 2007). A FLUAV biosensor capable of identifying the human infectivity and transmissibility of a novel FLUAV strain would be useful as a screening tool. Quick identification of a human transmissible FLUAV strain could initiate preventative measures such as the mobilizing of blood supplies before irreversible spread of the disease. In the event that a highly pandemic FLUAV strain is identified, the AABB request for relaxation of certain current regulatory standards related to donor eligibility and testing may be considered.

2.2 INFLUENZA IMMUNE GLOBULIN

2.2.1 Applications

One of the unique abilities of influenza viruses, and the reason there is such great concern about future pandemics, is their ability for quick mutation, as described in *2.1.3* and *2.1.4*. By the same mechanisms of antigenic drift and shift that allow FLUAV strains to change receptor specificity and host range, a FLUAV strain could also achieve drug-resistance. Because vaccines may take several weeks to become effective, therapies are needed that could be used pre- and post-exposure, and as treatment, for pandemic influenza in settings where vaccines would not have time to take effect. To this end, passive antibody-based therapies have shown promise with their versatility, specificity, and low toxicity, with applications for both prophylaxis and treatment of FLUIGIV infections. In fact, the versatility of antibodies makes antibody-based therapies potentially useful against any existing pathogen (Casadevall, 1996). Immune sera therapy was first reported by Behring and Kitasato (1890) for treatment of diphtheria and tetanus, followed by treatment of bacterial infections such as those caused by *Streptococcus pneumoniae* and *Haemophilus influenzae*, as well as viral infections such as those caused by measles, Poliomyelitis, and Varicella zoster (Casadevall and Scharff, 1995). Studies indicated that serum therapy was effective in reducing mortality associated with meningococcal meningitis, *Haemophilus influenzae* meningitis, and diphtheria, the last of which is still treated by antibody therapy (Alexander, 1943a; Alexander, 1943b; Casadevall and Scharff, 1994; Flexner, 1913; Fothergill, 1937; McCloskey, 1985). Serum therapy was replaced with antimicrobial chemotherapy a century later when toxicity problems associated with heterologous sera were discovered. Side effects included fever and chills

as well as the rash, proteinuria, and arthralgia typical of 'serum sickness,' and were likely due to immune complex formation (Feinberg, 1936; Rackemann, 1942). However, in recent years antimicrobial chemotherapy has also faced lowered applicability as immunocompromised individuals, old and new pathogen emergence, and antimicrobial drug resistance all showed increases (Casadevall and Scharff, 1995). Antibody-based therapies are thus regaining applicability. Human 'gamma globulin' has replaced heterologous sera, and typically is formulated as human immunoglobulin for intravenous administration (IVIG) (Barandun *et al.*, 1962; Prince *et al.*, 1986; Zolla-Pazner and Gorny, 1992). Recent technological advances in synthesizing of human antibody reagents have eliminated serum toxicity problems and have propelled antibody-based therapies forward, and they may fill the gap in infectious disease treatment (Casadevall, 1996; Casadevall and Scharff, 1995; Kohler and Milstein, 1975; Wright *et al.*, 1992).

2.2.2 FLUIGIV as Prophylaxis

In terms of public health, prevention is especially important, and indeed the use of antibodies is in general more effective for prophylaxis than for therapy (Casadevall, 1996; Cross, 1995). High-titer human anti-HIV (human immunodeficiency virus) Ig (HIVIG) was protective against viral challenge in chimpanzees, with amount of antibody administered and amount of challenge virus playing significant roles in ability to protect (Prince *et al.*, 1991). Subject animals remained free of infection and no primary immune response was detected, leading the authors to conclude that HIV vaccines should thus induce neutralizing antibody and that cell-mediated immunity induction may not be necessary for HIV protection (Prince *et al.*, 1991).

Intranasal antibody prophylaxis has shown great promise against viral respiratory tract infections in animals and is beginning to show efficacy in human clinical studies. For example, a single intranasal application of gamma globulin to mice was prophylactically effective for about 72 hr against influenza A virus (Weltzin and Monath, 1999).

In the case of antibody in mucosal secretions, protection is achieved by immune exclusion, in which antibody activity is combined with the physical barrier of the mucus blanket of the respiratory tract, and by direct neutralization of viral infectivity, in which binding of antibody to virus particles prevents them from interacting with cell receptors so they cannot infect target cells (Weltzin and Monath, 1999).

2.2.3 FLUIGIV as Treatment

In terms of treatment, antibody therapy may be useful for those infections by drug-resistant pathogens or by pathogens for which no antimicrobial drugs are available, or in the event of antiviral rationing during a severe pandemic. Antibody-based therapies as treatment are most effective when administered early in the course of disease. For example, serum administration in the treatment of pneumococcal pneumonia was most effective if within 3 days of symptom onset (Casadevall and Scharff, 1994).

To address a gap in H5N1 treatment, Luke *et al.* (2006) concluded that convalescent human H5N1 plasma could be useful as treatment for H5N1 infection, as evidenced by studies from the Spanish Influenza pandemic of H1N1 in 1918-1919 which reported that patients with influenza complicated by pneumonia experienced a reduction in mortality and symptom improvement when treated with transfusions of influenza-convalescent human blood products (Luke *et al.*, 2006).

A patient who presented flu-like symptoms and whose tracheal aspirates tested positive for H5N1 in southern China in 2006 was treated with the convalescent plasma from another patient who had recovered from H5N1 infection 4 months prior (Zhou *et al.*, 2007). Poultry in the region had suffered from infection by a predominantly clade 2.3 H5N1 variant. After the first plasma transfusion, the patient's viral load was diminished until undetectable after 32 h, and was released 2 months later after complete recovery. Viral load reduction occurred in conjunction with neutralizing-antibody titer increase, which Zhou *et al.* (2007) concluded may have been the result of the convalescent plasma treatment as well as the normal humoral immune response. Virus isolated from both the patient and the plasma donor were Fujian-like H5N1 variants which presented close genetic relation with greater than 99% homology in HA genes (Zhou *et al.*, 2007). Passive immunotherapy is thus an option of interest with regard to FLUAV infection treatment.

2.2.4 Current Applications of Antibody Therapy

Currently, antibody therapy is used for reducing infections in immunocompromised patients; for postexposure prophylaxis against measles and hepatitis; for treatment of botulism, diphtheria, and snake bites; and for prophylaxis and treatment of viral infections caused by cytomegalovirus (CMV), parvovirus, rotavirus, enterovirus, and varicella (Barnes *et al.*, 1982; Bodensteiner *et al.*, 1979; Brunell *et al.*,1972; Bussel and Cunningham-Rundles, 1985; Conti *et al.*, 1994; Frickhofen *et al.*, 1990; McCloskey, 1985; Pennington, 1990; Reed *et al.*, 1988; Tacket *et al.*, 1984; Watt, 1978; Wilfert *et al.*, 1977). High-risk patients, such as those with AIDS or organ transplant recipients, also

may be effectively treated with polyclonal antibody to reduce incidence of infection (Mofenson *et al.*, 1994; Stratta *et al.*, 1992; Yap, 1994).

2.2.5 Potential Applications of Antibody Therapy

2.2.5.1 Antivirals

Antibodies are inherently able to neutralize virus, typically by binding to the virus within its host receptor binding domain, or by otherwise blocking attachment to this region. Antibodies as prophylaxis against viruses such as CMV, HIV, respiratory syncytial virus, and parvovirus are under current study (Aulitzky *et al.*, 1991; Barbas *et al.*, 1992; Kim, 1987; Zolla-Pazner and Gorny, 1992).

2.2.5.2 Resistant or Highly Virulent Pathogens

There are also an increasing number of pathogens which have achieved drug-resistance, such as *Pseudomonas aeruginosa, S. pneumoniae, and E. Faecium*, for which antibiotics have become obsolete (Austrian, 1994; Cameron *et al.*, 1993; Casadevall and Scharff, 1995; Pier *et al.*, 1989; Schlaes *et al.*, 1993). Various highly virulent pathogens such as methicillin-resistant *Staphylococcus aureus* are also lacking in effective antimicrobial agents. *C. parvum* and vancomycin-resistant enterococcus have no available antimicrobial therapy (Casadevall, 1996). Antibody therapy has shown promise for treatment of pneumococcus and staphylococcus (Casadevall and Scharff, 1994; Correa *et al.*, 1994; Ramisse *et al.*, 1993). In such cases, conjunctive effects of antibody therapy and chemotherapy could slow resistance development (Casadevall and Scharff, 1995).

2.2.5.3 Immunocompromised Individuals

Antibody therapies may be useful to target pathogens such as invasive fungi that affect primarily immunocompromised patients for whom antimicrobial therapy is ineffective (Casadevall, 1996). In such individuals, low-virulence organisms could cause infection that is either difficult or impossible to treat, and antibody therapy is optimal for the enhancement of immune function (Casadevall and Scharff, 1995).

2.2.5.4 Toxin Neutralization

Antibody therapies could be useful for neutralization of toxins, such as those introduced by snake bites, spider bites, diphtheria, or tetanus. Toxic shock syndrome is also a potential target, and IVIG administration has been shown to improve toxic shock syndrome due to Streptococcus pyogenes (Barry *et al.*, 1992; See and Chow, 1989; Talkington *et al.*, 1993).

2.2.5.5 Antibody Therapy as Combined with Chemotherapy

Antibody therapy could stand alone for prophylactic purposes, but for treatment of infection, a combination with chemotherapy is attractive. Antibodies promote microbial killing, implying that a combination of both treatments would cause an amplified joint response. Also, a combined response would require less of the toxic antibiotic as well as less of the costly antibody therapy (Casadevall and Scharff, 1995).

Table 1. Applications for which antibody therapy combined with chemotherapy has shown preliminary effectiveness.

Pathogen	Chemotherapy	Antibody
Cytomegalovirus (Wilson *et al.*, 1987; Reed *et al.*, 1988)	Ganciclovir	Murine immune sera
Haemophilus influenzae (Alexander, 1943a,b)	Sulfonamide	Rabbit, horse immune sera
Herpes simplex virus (Cho *et al.*, 1976)	Acycloguanosine	Human immune globulin
Lassa virus (Jahrling *et al.*, 1984)	Ribavirin	Monkey immune sera
Neisseria meningitidis (Branham, 1935; Branham, 1937)	Sulfanilamide	Horse immune sera
Staphylococcus aureus (Sonea *et al.*, 1958)	Penicillin	Human gamma globulin
Staphylococcus aureus (Fisher, 1957)	Chloramphenicol	Human gamma globulin
Streptococcus pneumoniae (Powell and Jamieson, 1939)	Sulfapyridine	Rabbit immune sera

2.2.6 Shortcomings of Immune Sera

Immune sera in its current state of development presents deficiencies. Monoclonal antibody preparations, which are homogeneous immunoglobulins generated in vitro by hybridoma or recombinant DNA technologies, recognize one epitope and could offer 100 to 200 times the activity of polyclonal immune globulin (Lang *et al.*, 1993). In contrast, immune sera contains antibodies of varying specificities and isotypes. Shortcomings have included lot-to-lot variation and low specific antibody content (Felton, 1928; Weisman *et al.*, 1994). Each lot of IVIG could include plasma from more than 2000 donors and is produced by multiple alcohol precipitations and centrifugations, as well as further manufacturer-specific processing (Cohn *et al.*, 1944; Kistler and Nitschmann, 1962). An evaluation of 100 lots of IVIG from several products to determine opsonic activity for *Staphylococcus epidermidis*, *Haemophilus influenzae*, *Escherischia coli*, and various serotypes of *Streptococcus*, revealed lot variability as dependent on organism and manufacturer. Variation in opsonic activity within one IVIG lot was significantly affected by donor pool as opposed to manufacturing method (Weisman *et al.*, 1994). Clinical reports of IVIG inefficacy could be improved if pathogen-specific antibody content of IVIG products is known (Weisman *et al.*, 1993; Weisman *et al.*, 1994).

2.3 VIROLOGICAL METHODS

2.3.1 Viral Isolation Culture

Conventional virological methods for virus analysis are well established (Amano and Cheng, 2005). The "gold standard" for virus detection is viral isolation culture with immunocytological confirmation of viral antigen, which follows internationally recognized methods (Alexander *et al.*, 2005; Charlton *et al.*, 2009). Isolation and propagation of influenza virus A, B, and C requires a biosafety level 3 (BSL-3) diagnostic laboratory as well as certain reagents, which often reserves the process for national reference or research laboratories. Virus is inoculated into the chorioallantoic sac of embryonated eggs and after 24-48 h incubation, undergoes two to three blind passages, which may take up to 21 days. The specimen produces a cytopathic effect (CPE), which is then confirmed as FLUAV by hemagglutination inhibition (HI), immunofluorescent antibody (IFA) staining, or reverse-transcriptase polymerase chain reaction (RT-PCR) with the use of reference antisera or monoclonal antibody (Amano and Cheng, 2005; WHO, 2007b; WHO SEARO, 2007). Pathotyping typically necessitates experimental inoculation of 4-8-week-old chickens (Alexander *et al.*, 2005; Charlton *et al.*, 2009). These methods each require bench times of approximately 2-4 hours (Boon *et al.*, 2001). Serological or molecular biological characterization methods may follow, which would require approximately 48-72 hours each (Amano and Cheng, 2005). By definition, virus isolation has a sensitivity and specificity of 100%, but does depend on virus viability. Time to report including isolation and typing is 2-4 weeks.

2.3.2 Complement Fixation

The complement fixation (CF) test mainly detects antibodies to type-specific nucleoproteins (Ziegler *et al.*, 1997). The test is based on the use of complement, a biological substance present in normal animal sera (Amano and Cheng, 2005). Complement reacts with almost any antigen-antibody complex because it lacks specificity. Sheep red blood cells (sRBC) are the indicators. A positive result occurs when the complement is bound to an antigen-antibody complex and cannot react with sRBC, leaving sRBC unlysed. A negative result occurs when there is no antigen-antibody complex for sRBC to bind to, allowing complement to cause lysis of sRBC. The CF test requires experienced personnel and laboratory time (Amano and Cheng, 2005). Prince and Leber (2003) have shown that CF gives false-negative antibody response results following influenza virus vaccination. CF is less sensitive than ELISA (Masihi and Lange, 1980). Full fixation requires 4 hours at 0 degrees C (Kahn, 1921).

2.3.3 Hemagglutination Inhibition

The hemagglutination inhibition (HI) method is more sensitive than CF for detecting antibody responses to naturally occurring influenza A and B (Prince and Leber, 2003). HI is a serological assay, detecting antibodies to strain-specific hemagglutinins. Hemagglutinin can cause agglutination in the presence of erythrocytes. The HA agglutination test traditionally identifies influenza, and the HI test is used to determine hemagglutinin subtype. To perform the HI test, specimen is mixed with antisera to known HA subtypes. Agglutination is inhibited when the antisera type matches the test sample. In the presence of an HA binding molecule, the observed HI is proportional to the concentration of the inhibitor (Alvarez *et al.*, 2010; Salk *et al.*, 1944). HI assays require

laboratory expertise and skill, but are highly reliable, universally recognized, and preferred for WHO global influenza surveillance (Amano and Cheng, 2005). However, there are limitations to the process, as HI assays for influenza virus antibodies are not widely available, are dependent upon the quality of erythrocytes used, and require the use of replication competent virus (Hassantoufighi *et al.*, 2009; Noah *et al.*, 2009; Prince and Leber, 2003; Stephenson *et al.*, 2003). Thus BSL-3 facilities are required as is a very large supply of virus (Allwinn *et al.*, 2010; Hancock *et al.*, 2009; Miller *et al.*, 2010; Schultsz *et al.*, 2009). Additionally, HI is limited by low sensitivity, subtype cross-reactivity, and variability, and because it does not distinguish between infectious and non-infectious virus particles, may be entirely inappropriate for H5N1 work (Julkunen *et al.*, 1985; Massicot and Murphy, 1977; Tsai *et al.*, 2009; WHO, 2007a). Time to report is several hours.

2.3.4 Microneutralization

Microneutralization is another serological assay, which requires a small amount of serum to be tested in a microtitre plate for virus neutralization by FLUAV specific antibody (WHO, 2007b). Microneutralization confirmed by western blot analysis is beginning to gain preference over HI and offers consistent results (Hancock *et al.*, 2009; Kayali *et al.*, 2008; Kitphati *et al.*, 2009; Rowe *et al.*, 1999; Schultsz *et al.*, 2009; Sirskyj *et al.*, 2010; Tsai *et al.*, 2009). This is a specific and sensitive assay for detecting strain-specific antibody in serum that can typically detect lower titers than HI. Microneutralization also presents limitations with complexity of standardization, low-throughput, and extensive training requirements (Petric *et al.*, 2006; Stelzer-Braid *et al.*, 2008; Tsai *et al.*, 2009 WHO, 2007b). BSL-3 facilities are required for live virus

handling, and results are obtained within 3 days (Hancock *et al.*, 2009; Kitphati *et al.*, 2009; Schultsz *et al.*, 2009; Sirskyj *et al.*, 2010; WHO, 2007b).

2.3.5 Immunofluorescent Antibody Staining

Immunofluorescent antibody (IFA) staining directly detects influenza antigens in clinical samples by their interaction with FLUAV strain-specific monoclonal antibodies that are directly or indirectly fluorescently tagged. A fluorescent microscope is required for visualization. Compared to cell culture, IFA staining has a sensitivity of 70-100% and specificity of 80-100%, with time to report within 24 hours (WHO, 2007b).

2.3.6 Enzyme Linked Immunosorbent Assay

Enzyme linked immunosorbent assay (ELISA) methods do not require fresh erythrocytes, virus manipulation, or subjective visual results interpretation (Alvarez *et al.*, 2010). ELISA techniques are under study for detection of anti-influenza antibodies in animal or human serum samples (Blitvich *et al.*, 2003; De Boer *et al.*, 1990; Hall *et al.*, 1995; He *et al.*, 2007; Prabakaran *et al.*, 2009; Stelzer-Braid *et al.*, 2008). However, ELISA methods may be subject to false positive results as infection or seasonal FLUAV vaccination could generate cross-reactivity of antibodies (Stelzer-Braid *et al.*, 2008). This was seen in a commercial ELISA for detection of anti-H5 HA antibodies, which was used to screen vaccinated sera, with accurate identification of high levels of anti-H5 antibodies. However, antibodies against seasonal H3N2 and H1N1 cross-reacted with the H5 antigen (Stelzer-Braid *et al.*, 2008). Results from ELISA methods have also shown poor predictive value with HI or microneutralization assays (Ceyhan *et al.*, 2010; Kayali *et al.*, 2008; Rowe *et al.*, 1999).

2.3.7 RT-PCR

Reverse transcription polymerase chain reaction (RT-PCR) is becoming increasingly effective for viral detection, typing, and subtyping (Zhang and Evans, 1991). FLUAV genetic materials may be detected by RT-PCR in samples with very low levels of viral particles, because of genetic multiplication by polymerase enzyme (WHO, 2007b). Viral nucleic acids are extracted from clinical specimens and cDNA is then synthesized by in-vitro reverse transcription of viral RNA. The cDNA is amplified with specific primers and DNA polymerase. Detection of the amplified product can be achieved by fluorescence and luminescence measurements (Amano and Cheng, 2005). RT-PCR has higher sensitivity and shorter detection time than conventional methods. Compared to the "gold standard" of virus cultivation, Atmar *et al.* (1996) reported that the RT-PCR assay had a sensitivity, specificity, and efficiency of 95, 98, and 97%, respectively, compared with 75, 100, and 93%, respectively, for the best commercially available diagnostic kit (Becton Dickinson Directigen). Compared to the 2-10 days required for culture, PCR only requires 24 hours (Magnard *et al.*, 1999). RT-PCR is thus an effective alternative to virus isolation for FLUAV detection (Atmar *et al.*, 1996). Drawbacks of this method include high cost of reagents and thermocyler equipment, requirement of specific oligonucleotide primers from WHO influenza reference and collaborating centers, BSL-2 requirement, high rate of false positive results, and complicated procedure (Ellis and Zambon, 2002; WHO, 2007b). Real-time RT-PCR is also under study for FLUAV detection, utilizing a one-tube protocol and fluorogenic hydrolysis type probes, with sensitivity and specificity comparable to virus isolation and HI (Lee and Suarez, 2004; Spackman *et al.*, 2002).

2.4 COMMERCIAL DIAGNOSTIC TEST KITS

Commercial diagnostic test kits directly detect influenza A or B virus-associated antigens or enzyme in throat swabs, nasal swabs, or nasal washes. These tests generally have 70% sensitivity and 90% specificity for viral antigens (Montalto, 2003). Time to report is approximately 30 minutes (Amano and Cheng, 2005).

Directigen (Beckton Dickinson Diagnostic Systems, Sparks, Maryland) is an enzyme immunoassay (EIA) membrane test for influenza A and B (Reina *et al.*, 2002). Enzyme-conjugated monoclonal antibodies specific to influenza A or B are used. Visualization of the captured influenza antigen-antibody couple is achieved by an enzymatic color development reaction. This is the first commercially available rapid assay kit that distinguishes between viral antigens from influenza A and B. The test has a sensitivity of 75-87% and specificity of 93-97% (Gavin and Thomson, 2003). Time to report is approximately 25 minutes (Amano and Cheng, 2005).

QuickVue Influenza A/B (Quidel Corporation, San Diego, California) uses immunochromatography to detect influenza A and B without differentiation (Gavin and Thomson, 2003). Extraction is required to allow targeting of nucleoprotein from influenza. Nucleoproteins in the specimen react with reagents to produce a color change on the test strip. Manufacturer data show a specificity of 96-99% and sensitivity from 73-82%. Time to report is approximately 10 minutes (Amano and Cheng, 2005).

ZStatFlu (ZymeTx, Inc., Oklahoma City, Oklahoma) is a neuraminidase assay that achieves specificity using modified sialic acid (SA). In the presence of neuraminidase, the bromoindole that is bonded to SA is released, forming insoluble dyes that indicate a positive response (Shimasaki *et al.*, 2001). Influenza A and B are not discriminated

(Gavin and Thomson, 2003). The test has a specificity of 98.7% but a poor sensitivity of 62.2% as reported by the manufacturer. Two minutes of testing and 20 minutes of incubation are required, resulting in a time to report of approximately 22 minutes (Amano and Cheng, 2005).

The BioStar OIA Flu A/B (Inverness Medical Innovations, Louisville, Colorado) is a nucleoprotein antibody assay that detects the change in film thickness due to the binding of antigen-antibody complex to a silicon wafer surface. Any antigen in the specimen is captured by the immobilized antibodies, resulting in an increase in film thickness that is detected as a color change due to a shift in the reflected light path (Amano and Cheng, 2005). Influenza A and B are not discriminated (Gavin and Thomson, 2003). Studies have shown that the sensitivity of this test may vary from 51.4-71.8% (95% CI), depending on the source of the specimens (Schultze *et al.*, 2001). Specificity ranges from 69-79% (Gavin and Thomson, 2003). In particular, a negative result on the FLU OIA should be confirmed by direct fluorescent antibody (DFA) and culture (Hindiyeh *et al.*, 2000). Time to report is approximately 16-20 minutes (Schultze *et al.*, 2001).

Binax NOW Flu A and Flu B (Inverness Medical Innovations, Louisville, Colorado) detects influenza nucleoprotein antigen in specimens using an immunochromatographic membrane test. Influenza antigen present in the specimen bind to gold-conjugated anti-influenza antibodies in the test strip. The sample line is then formed when the antigen-conjugate complexes are captured by the immobilized antibodies (Amano and Cheng, 2005). Sensitivity is reported as 82% and specificity is 94% (Gavin and Thomson, 2003). Time to report is approximately 1-2 hours.

The conclusion to be drawn from these current rapid assay techniques is a lack of binding partner novelty; most assays depend on detecting Influenza viruses by interactions with Influenza-specific antibodies. While the sialic acid receptor has been investigated in neuraminidase binding, there lacks a biosensor technology that exploits Influenza hemagglutinin specificity for host sialic acid receptors.

2.5 BIOSENSORS

A biosensor is the integration of a biological component with an electronic, electrochemical, optical, or acoustic transducer, with the intention of quantifying a physiological or biochemical change in terms of an electrical response (Blum and Coulet, 1991; D'Souza, 2001; Ivnitski *et al.*, 1999; Jin *et al.*, 2008; Muhammad-Tahir *et al.*, 2007; Pal *et al.*, 2007; Pal *et al.*, 2008a; Pal *et al.*, 2008b; Pal and Alocilja, 2009; Turner *et al.*, 1987; Zhang and Alocilja, 2008). Biosensors for quick and reliable FLUAV detection are of interest to minimize sample handling and the need for highly skilled laboratory technicians. An attractive development is single-step direct sensing, in which separation, incubation, and signal-reporting agents are eliminated. Label-free techniques showing potential for virus detection include surface plasmon resonance (SPR) biosensors and acoustic biosensors, both of which have shown subnanogram detection limits. Alternatively, colorimetric sensors employing functional polymers are promising for direct viral analysis without the need for instruments (Amano and Cheng, 2005).

2.5.1 Surface Plasmon Resonance Sensors

SPR biosensors are optical sensors that exploit special electromagnetic wave frequencies to probe interactions between an analyte in solution and a biomolecular recognition element immobilized on the sensor surface. This direct technique utilizes these biomolecular recognition elements to recognize and capture analyte in a liquid sample producing a local increase in the refractive index at a thin metal film surface (Figure 3). Optical means can then be used to accurately measure the refractive index increase (Homola, 2003; Meeusen *et al.*, 2005). This biomolecular interaction screening technique does not require labeling of the ligand or the receptor, allowing virtually any

complex to be screened with minimal assay development. The very high sensitivity of SPR also lends itself to flexibility in application (Cooper, 2003). Schofield and Dimmock (1996) first reported the use of SPR for influenza virus detection. The sensor chip was coated with a polymer matrix coupled with monoclonal antibody for influenza virus. The influenza virus was injected into the flow system and binding affinity with the surface antibody was monitored. Dissociation and association rate constants were comparable to those from an affinity ELISA (Schofield and Dimmock, 1996). SPR has been used to study the interaction between influenza hemagglutinin (HA) and its cell surface receptor sialic acid (SA) using a sensitive microscale binding assay (Takemoto *et al.*, 1996). BHA is a soluble form of HA that results when the protease bromelain cleaves HA from the virus near the viral membrane (Brand and Skehel, 1972). Under low-pH-induced conditions, BHA trimers form soluble aggregates called rosettes which bind specifically to the fetuin-derivitized sensor surface. The tight binding due to the multivalent interaction between the BHA rosettes and the fetuin-derivatized sensor surface was quantitated using measurements of association rate, dissociation rate, and dissociation constant (Takemoto *et al.*, 1996). Time to report is 10 minutes (Yang *et al.*, 2006).

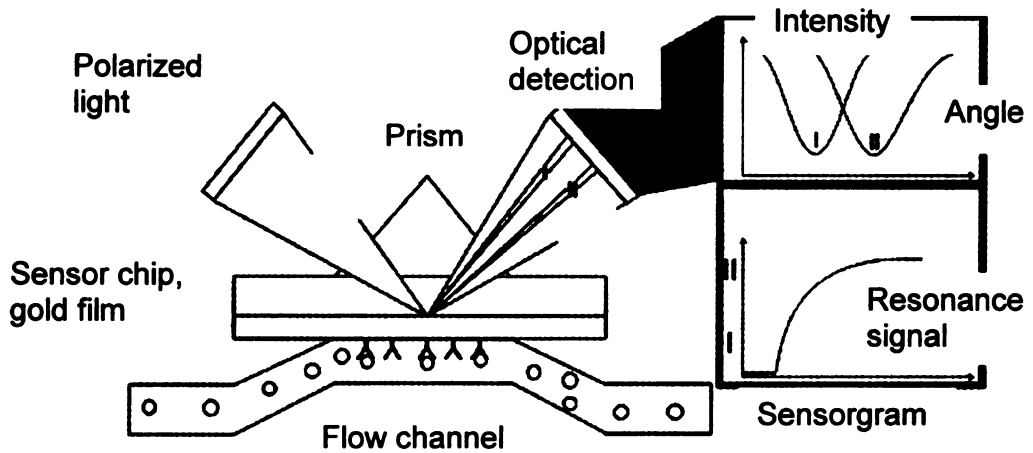

Figure 3. SPR theory based on changes in refractive index due to immobilized target, with sensorgram output (adapted and modified from GE Healthcare, 2010).

2.5.2 Quartz Crystal Microbalance

Acoustic biosensors are based on quartz crystal resonators (Cooper, 2003). Sauerbrey first demonstrated the sensitivity of the quartz crystal microbalance (QCM) towards mass changes at the surface of QCM electrodes (Bruckenstein and Shay, 1985; Henderson, 1991; Plausinaitis *et al.*, 2001; Sauerbrey, 1959). The Sauerbrey equation presents a linear correlation between the mass change and resonant frequency shift, and is dependent on the linear sensitivity factor Cf which is a fundamental property of the QCM crystal:

$$\Delta fs = - Cf \cdot \Delta m \qquad (1)$$

where, Δm is the change in mass per unit area, in g/cm2, Δfs is the observed frequency change, in Hz, and Cf is the sensitivity factor of the crystal.

The electrical behavior of a crystal resonator near series resonance is represented by the Butterworth van Dyke (BVD) electrical model of a quartz crystal resonator (Figure 4).

QCM immunosensors function on the principle that adsorption of substances on the surface of a quartz crystal changes its resonance oscillation frequency (Eun *et al.*, 2002). QCM is an attractive low-cost technique for monitoring interaction of biomolecules on functionalized surfaces. As in SPR biosensors, interaction affinity and kinetics analyses can be performed in real-time and without labeling, by monitoring changes in the crystal resonant frequency. However, QCM biosensors offer more detailed information than SPR systems, since the acoustic response also accounts for visco-elastic property and receptor-ligand complex charge changes (Cooper, 2003).

2.5.2.1 Applications

In influenza research, QCM has been applied to the study of virus/receptor interactions (Amano and Cheng, 2005). Sato *et al.* (1996) utilized QCM to study binding of FLUAV to monosialoganglioside in membranes. The receptor functions of gangliosides GM3 were found to be influenced by surrounding matrix lipids (Sato *et al.*, 1996). Cooper *et al.* (2001) developed a sensitive, economical direct method for virus detection in which type 1 herpes simplex virus interacted with specific antibodies covalently attached to the oscillating surface of a QCM. As the amplitude of oscillation of the QCM was increased, the virions were detached and the resulting acoustic noise was detected. Sensitivity approaches detection of a single virus particle (Cooper *et al.*, 2001). A QCM immunosensor for the detection of cymbidium mosaic potexvirus (CymMV) and odontoglossum ringspot tobamovirus (ORSV) utilized QCMs pre-coated with virus-specific antibodies. Binding of virions to the immobilized antibodies resulted in a reduction of resonance oscillation frequency dependent on the amount of virus bound and the resulting increase in mass at the QCM surface. The QCM assay was faster than

ELISA with comparable sensitivity (Eun *et al.*, 2002). Immunochips of QCM crystal coated with two monoclonal antibodies against dengue virus envelope protein and non-structural protein were found to have a 100-fold greater sensitivity than conventional sandwich ELISA and a shorter approximate detection time of 1 hour. Blood specimens could be used to detect virus in the viremia phase (Su *et al.*, 2003). Ultrasensitive QCM for detection of M13-phages in the liquid phase showed an increase in the signal to noise ratio by a factor of more than 6 when the resonant frequency of the quartz crystal was increased from the typical range of 5-20 MHz to the ultrasensitive range of 39-110 MHz. The detection limit was improved by a factor of 200. The ultrasensitive QCM sensors were chemically milled (Uttenthaler *et al.*, 2001). Time to report is approximately 10 minutes (Leca-Bouvier and Blum, 2005).

2.5.2.2 Rupture Event Scanning

Rupture event scanning exploits the piezoelectric property of the quartz, by which the quartz deforms under application of an electric field (Ward and Buttry, 1990). As the magnitude of the electric field is increased, the oscillation amplitude increases and acceleration of particles on the surface increases, causing the surface to exert an increasing force on the particles. Eventually the bonds between particle and surface are ruptured, and the quartz crystal can detect and convert the acoustic emission of the rupture into an electrical signal, thus providing information on particle presence, numbers, and affinity. Sample preparation is minimal, and time to report is a few minutes (Cooper *et al.*, 2001; Cooper, 2003; Dultsev *et al.*, 2000; Dultsev *et al.*, 2001).

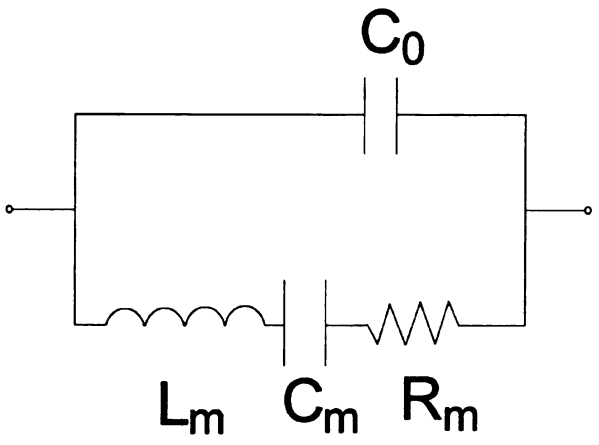

Figure 4. Butterworth van Dyke (BVD) electrical model of a quartz crystal resonator (adapted and modified from Eun *et al.*, 2002).

2.5.3. Colorimetric Sensors

Colorimetric sensors using functional polymers enable direct analysis of target analytes through a color change. "Smart" materials with desirable physical, optical or electrical properties that respond to an environmental stimulus are synthesized for the application (Amano and Cheng, 2005). A colorimetric influenza sensor has been developed that uses a polydiacetylene bilayer assembled on glass slides. The polydiacetylene layer is functionalized with an analog of SA, the natural receptor for HA recognition. The SA ligand serves as a molecular recognition element and the conjugated polymer backbone signals binding at the surface. Binding of viral HA to the SA residues results in a visible transition of blue to red film color, with color change quantified by visible absorption spectroscopy. Time to report is several minutes (Charych *et al.*, 1993).

2.5.4 Gold Nanoparticles and Quantum Dots

Nano-size gold particles (AuNPs) as well as semiconductor colloidal quantum dots (QDs) have attracted interest for sensing applications. A commercial company (Genomic Profiling Systems, Bedford, MA) has developed a strip test for influenza diagnosis

(NIAID, 2006). Influenza virus in the sample binds to antibody-coated gold particles forming complexes that are drawn up the strip via capillary action. These complexes meet and bind the antibodies on the strip, turning the line red due to the reflection of light from the gold when a sufficient number of these complexes are captured. However, the method, while easy, is not sensitive, requiring a large amount of virus, in the millions, to induce a color change. They are developing a portable MultiPath technology, which uses digital imaging to detect individual fluorescent particles instead of the large number of gold particles. By this method, fluorescent particles bound by virus can be counted individually, and virus can be detected at levels thousands of times lower than by gold particles. The company is still performing feasibility studies on this technology (NIAID, 2006).

2.5.4.1 Shortcomings

QD technology is relatively immature and limited by intermittent luminescence, influence of different dyes bound to protein linkers, influence of the colloidal nature of the sensing environment, and relatively high expense. An epitaxial quantum dot (eQD) biosensor has been proposed, in which rows of eQDs emitting at specific wavelengths are functionalized with biotinylated antibodies. Upon excitation, each eQD will emit photoluminescence radiation, which is expected to be modified in the presence of trapped viruses. eQDs avoid the intermittent luminescence effect. A prototype for influenza A virus detection utilizes a thiol-biotin-avidin-biotinylated antibody architecture (Dubowski, 2006). Cadmium telluride QDs have been used as a proton sensor to detect proton flux driven by ATP synthesis in chromatophores. QD-labeled chromatophores were applied as

a virus detector to detect the H9 avian influenza virus based on antibody-antigen reaction (Yun *et al.*, 2007).

2.5.5 Microarrays

A smart CMOS chip for influenza detection has been developed by CombiMatrix Corp. of Portland, OR. Any known flu strain can be identified in 4 hours, and the microarray does not require operation by skilled technicians. The CMOS format electronically identifies binding events. The chip can be optically scanned, but because it is an active device it can also eliminate the need for fluorescent tags and optical scanners. The system is not yet portable (Johnson, 2005).

A new ELISA test for influenza virus uses Zanamivir-biotin conjugates. Biotinylated inhibitors were fixed to an avidin-coated plate and serial dilutions of influenza virus were added. Unbound virus particles were washed off and anti-HA serum-horseradish peroxidase (HRP) conjugate and chromogenic substance were added to detect captured virus (McKimm-Breschkin *et al.*, 2003). The sensitivity was 5 hemagglutinating units (HAU), where 1 HAU is defined as the highest dilution of stock virus that completely agglutinates a standard erythrocyte suspension (WHO, 1953). Time to report for ELISA is approximately 2-4 hours (King, 2006).

2.6 TOWARDS IMPROVED TECHNOLOGY

Traditional viral assays such as MDCK cell culture, complement fixation, and hemagglutinin-inhibition are still used widely, but cannot meet the demands for fast and direct detection at the point of care and for quick screening in case of a bioterrorism event. Commercially available influenza diagnostic tests provide quick results, but their sensitivities are lower than real-time RT-PCR and virus culture. In general, rapid test sensitivity ranged from 10-70% as compared to RT-PCR for the detection of novel H1N1, and thus a negative result on a rapid test can not rule out novel influenza A infection (CDC, 2009; Hurt, 2009). A sensitive and specific biosensor technology is thus important to enable rapid and specific disease diagnosis on-site (Amano and Cheng, 2005; Muhammad-Tahir *et al.*, 2005b; Pal *et al.*, 2007; Radke and Alocilja, 2005). There is a need for a biosensor technology with a shorter detection time and comparable or superior sensitivity as compared to standard ELISA. The technology must offer speed comparable or superior to commercially available diagnostic test kits with a time to report of less than 30 minutes. Point-of-care applicability is essential. On-site handling and use may be facilitated by a single use disposable platform, and the need for only an inexpensive handheld signal reader.

2.6.1 Requirements of Biosensor Technology

New biosensor technology must improve upon commercially available test kits by decreasing definitive turnaround time and offering quantitative results as opposed to subjective color change assessments. A potential aim is the specific identification of HA receptor preference as an indicator of the pandemic potential of a FLUAV strain. Since most available test kits function on influenza antigen-antibody binding, an assessment of

binding between hemagglutinins of FLUAV to sialic acid receptors would be novel and informative. As previously described, studies have shown that human FLUAV, including pandemic and seasonal epidemic viruses, bind the specific α2.6 sialic acid receptor on host cells, whereas avian FLUAV bind the α2.3 sialic acid receptor (Matrosovich M.N. *et al.*, 2004; Stevens J. *et al.*, 2006a). This preferential binding could serve as a novel platform upon which a biosensor could identify FLUAV strains that could achieve human-to-human transmissibility and pandemic potential. Such a rapid biosensor technology would have applications for monitoring animal influenza infections and for screening emerging FLUAV strains for their potential for human infectivity for both disease monitoring and biosecurity.

2.7 CONDUCTING POLYMERS

Polymers were initially thought to be insulators, until the discovery that poly (sulphur nitride) [(SN)x] becomes superconducting at low temperatures (Suman *et al.*, 2005). Simple doping with oxidizing agents (p-doping) or reducing agents (n-doping) can enhance the electrical conductivity of [(SN)x] by several orders. In fact, a field comprised of many different conductive polymers has emerged. These polymers can be doped and undoped in reversible reactions via electrochemical techniques including changes in pH or redox potential (Malhotra *et al.*, 2006; Paul *et al.*, 1985). Yoshino *et al.* (1983) found that tetrafluorocyano-quinodimethane doping of poly-p-phenylenesulfide (PPS) increased the electrical conductivity of non-doped PPS by more than ten orders of magnitude, and double doping served to increase maximum conductivity as compared to single doping. McDiarmid and Heeger found that the electrical conductivitiy of polyacetylene could be enhanced by several orders of magnitude by doping with oxidizing and reducing agents (Gerard *et al.*, 2002). Hydrogen bromide (HBr) solution was used to dope polyacetylene, resulting in an increase of electrical conductivity by an order of six. HBr-doped polyacetylene was found to be slightly more stable than I2-doped polyacetylene under conditions of heat and air exposure (Lee *et al.*, 1989). Polymers such as polyaniline, polypyrrole, polyindole, poly-para-phenylene (PPP), polythiophene, and polyfuran have been studied to improve biomolecular stability of emerging sensor technologies, with applications in biosensors, chemical sensors, solar cells, fuel cells, diodes, field-effect-transistors, and rechargeable batteries (Ayesh, 2009; Diaz *et al.*, 1979; Gajendran *et al.*, 2008; Ivory *et al.*, 1979; Kawai *et al.*, 1991; Kim and Wamser, 2006; Kim *et al.*, 2009; Malhotra *et al.*, 2006; Rabolt *et al.*, 1980; Syritski *et al.*, 2005; Yoshino *et al.*, 1983).

Pyrrole was electrochemically polymerized on a platinum surface to produce a durable polypyrrole film of 0.8μm thickness which was used as an electrode in cyclic voltammetry measurements. Polypyrrole as an organic electrode material offers improved conductivity, good stability in electrochemical environments, and strong adhesion to the metal surface (Diaz *et al.*, 1979).

2.7.1 Electronic Structures of Conducting Polymers

In contrast to saturated polymers, conducting polymers have one unpaired electron via chemical bonding. Each carbon atom in the polymer backbone has a pi electron. There is a delocalization of electrons along the backbone due to the overlapping of orbitals of successive carbon atoms, which are in sp2pz configuration in pi bonding. These partially filled molecular orbitals cause a charge mobility which offers the polymer electrical conductivity as well as high electron affinity and low ionization potential. The pi bonds are susceptible to electrochemical and chemical oxidation or reduction (Ivory *et al.*, 1979; Malhotra *et al.*, 2006). External electric field can easily polarize the electrons in these delocalized systems, leading to attractive nonlinear optical properties (Gorman and Grubbs, 1991).

Electrical conductivity (σ) is due to the existence and ability for movement of charge carriers, and is expressed as,

$$\sigma = ne\mu \qquad (2)$$

where, n is the number of charge carriers per unit volume, e is the electronic charge, and μ is the carrier mobility. Doped conjugated polymers are good electrical conductors due to the presence of charge carriers in the p-electron polymer system, as introduced by

doping, which could potentially occur at every monomer. Charge carrier mobility results from p-electron delocalization along the polymer backbone (Heeger and Smith, 1991).

Electrical conduction properties of semiconductors can be controlled by addition of foreign atoms into the semiconductor lattice. The dopant atoms may have an electron excess or deficit, leading to corresponding *n* or *p* type semiconductors. Conducting polymers may be similarly described. The doping levels of conducting polymers are comparatively high, in contrast to those of semiconductors. Charge transfer occurs between the dopant atom and the polymer chain, which is thus partially oxidized (*p*-doping) or reduced (*n*-doping) (Lyons, 1994).

2.7.2 Nanoparticles as Biological Sensory Labels

Drug delivery, chemical sensors, biosensors, optoelectronics, and electrochemical devices are all potential applications of nanoparticles of conducting polymers (Berggren *et al.*, 2007; Burroughes *et al.*, 1988; Diaz *et al.*, 1979; Drummond *et al.*, 2003; Huang *et al.*, 2002; Jager *et al.*, 2000; MacDiarmid, 2001; Malinauskas *et al.*, 2005; Mannakos *et al.*, 1998; Potyrailo *et al.*, 2006; Smela 2003). Such nanoparticles have a high surface area and quantum size effect, offering them extraordinary physicochemical properties. When their composition, surface structure, and agglomeration are strictly controlled, the nanoparticles can have optimal electrical, mechanical, and chemical properties. Nanoparticles with uniform sizes have been achieved by the hard template method which utilizes anodized aluminum oxide or colloidal particles with empty pores. Dispersion polymerization has been used to synthesize a polymer shell around monodisperse SiO2 particles. The 150-700nm polymeric particles were hollowed by HF etching to remove the SiO2 cores. The size of the hollow core and the shell thickness were able to be varied

by size and their monodisperse nature allowed the formation of well-ordered colloidal crystals (Xu and Asher, 2004). However, hard methods are expensive, require the use of strong acids or bases, and require various template sizes. Soft template materials such as functionalized organic acids or polymeric stabilizers are also useful, but present many of the same limitations of the hard process. Surfactant micelles are self-assembled organic media that can block aggregation (Mann, 2000). A template-free, one-step chemical synthesis procedure has been developed to fabricate unagglomerated polypyrrole nanospheres with controlled size under mild conditions. The sphere sizes are controlled by manipulation of the volume ratio of two liquids, such as water and octanol, which form reversed micelle droplets (Kim *et al.*, 2009). Gold nanoparticles (AuNPs) of 1.4nm diameter linked to an oligonucleotide have been shown to be susceptible to radio frequency magnetic fields, offering remote electronic control over reversible DNA hybridization behavior. Monofunctionalization with L-lysine of AuNPs yields 2 nm nanoparticles that can serve as the building blocks for peptide chains (Hamad-Schifferli *et al.*, 2002; Sung *et al.*, 2004). Iron (III) oxide (Fe3O4) nanoparticles of 12 nm diameter have been encapsulated in large unilamellar vesicles of dipalmitoylphosphatidylcholine (DPPC) via reverse-phase evaporation (Wijaya and Hamad-Schifferli, 2007). Conjugated polymers have been applied as artificial muscles due to their electroactive nature. Use of such polymers as actuators in biomedical devices is gaining attention (Smela, 2003). Polyacetylene, a conjugated polymeric semiconductor, has been used as the basis of a semiconductor device, which operates by the presence of a surface electric field. The optical properties of the polymer are changed by the formation of charged solitons, and optical absorption occurs below the band gap. These optoelectronic effects are useful,

especially in combination with the processibility of the polymer (Burroughes *et al.*, 1988). Gold nanoparticles (AuNPs) conjugated to DNA have been shown to enhance *in vitro* protein translation by a combination of nonspecific adsorption of the ribosome to the AuNP-DNA and specific binding to the mRNA, which is a different perspective to the common belief that nonspecific adsorption is a barrier for utilizing NPs. In fact, it was shown that nonspecific adsorption was essential for expression enhancement (Park and Hamad-Schifferli, 2010).

2.7.3 Polymers in Biosensors

Electrochemical detection of selected DNA sequences or mutated genes can be achieved by electrochemistry at polymer-modified electrodes, electrochemical amplifications with nanoparticles, and electrochemistry of DNA-specific redox reporters (Drummond *et al.*, 2003). Conjugated polymer actuators are of interest for physiological applications due to their ability to be operated in aqueous media. Polypyrrole is particularly stable under these conditions. A polypyrrole-gold bilayer microactuator has been microfabricated with the ability to move other microcomponents (Jager *et al.*, 2000). Nanostructurized conducting polymers have electrochemical applications such as sensors, batteries, supercapacitors, and energy converters (Malinauskas *et al.*, 2005). Conducting polymers are useful for immobilizing and stabilizing biomolecules onto a sensor surface via physical adsorption, electrochemical entrapment and covalent attachment via coupling chemistry of ethyl-dimethyl-aminopropylcarbodiimide (EDC) and *N*-hydroxy-succinimide (NHS). The polymer itself can bind protein molecules, and electrochemical synthesis allows simultaneous direct polymer deposition onto the electrode while also trapping biomolecule targets (Bartlett and Whitaker, 1988; Gambhir *et al.*, 2001).

Polymers optimal for this application have functional groups to facilitate covalent binding. For example, polypyrrole has been galvanostatically electropolymerized to entrap anti-IgG onto a platinum surface (Andreescu and Sadik, 2004; Sadik *et al.*, 2002). Enzymes can be covalently linked to the surface of functionalized conducting polypyrrole films after carbodiimide activation (Schuhmann *et al.*, 1990). A glucose biosensor was produced by electropolymerization of pyrrole-modified biotin to enable avidin and biotin-labeled glucose oxidase (Cosnier and Lepellec, 1999). Immobilization of polyclonal antibodies onto a conducting polypyrrole membrane has exhibited improved activity compared to immunosensors made by physical entrapment or adsorption (Bender and Sadik, 1998). Electrochemical detection has been demonstrated with modified electrodes, nanoparticle amplification, and DNA-mediated charge transport (Drummond *et al.*, 2003).

2.7.4 Conducting Polymers as Transducers

Conducting polymers can have applications as biosensor transducers, serving to convert a biochemical signal that results from the interaction of a biological component into a measurable electronic signal. Physical transducers may be electrochemical, thermal, piezoelectric, and spectroscopic (Svorc *et al.*, 1997). Amperometric biosensors for example measure the current produced from the oxidation or reduction of a reactant under constant applied potential (Malhotra *et al.*, 2006).

2.7.5 Polyaniline

Polyaniline is perhaps the most studied conducting polymer in a family that also includes polypyrrole, polyacetylene, and polythiophene. As both electrical conductors and organic compounds, these materials are attractive for their flexibility and robustness. In particular, polyaniline boasts highly controllable chemical and electrical properties,

simple sythesis, low cost, good environmental stability in different solutions, and strong biomolecular interactions (Ahuja *et al.*, 2007; Feast *et al.*, 1996; Ryder *et al.*, 1997; Sarno *et al.*, 2005). Polyaniline is also unique in the appearance of a single broad polaron band deep in the gap, with a narrow band near the conduction-band edge, while all other known conducting polymers reveal two broad polaron bands (Stafstrom *et al.*, 1987). Polarons cause delocalized unpaired electrons and distortions of the polymer chain, which are confined to certain phenyl groups and adjacent NH groups (Focke *et al.*, 1987; Glarum and Marshall, 1986).

2.7.5.1 Synthesis

Synthesis of polyaniline from its monomer form, aniline, proceeds via chemical or electrochemical synthesis. Electrochemical polymerization utilizes a standard three-electrode configuration in an electrochemical bath, consisting of working, counter, and reference electrodes. Working electrodes may be composed of gold, platinum, nickel, or chromium. Polymerization may occur by potential scanning, constant potential (potentiostatic), or constant current (galvanostatic) (Ahuja *et al.*, 2007).

In chemical synthesis, aniline monomer in aqueous solution is polymerized by step-growth in the presence of an oxidizing agent and a protonating acid. Aniline cation radicals are produced and then participate in pernigraniline polyaniline chain growth or recombine into benzidine and N-phenyl-p-phenylenediamine. Oxidative polymerization converts the pernigraniline into emeraldine (Stejskal and Gilbert, 2002).

Kim and Wamser (2006) demonstrated that the use of aniline as the active redox material in a dye-sensitized solar cell using a porphyrin sensitizer leads to the formation of polyaniline, which acts as the hole transport medium. At low light intensities, the solar

cell offers 0.8% overall energy conversion efficiency (Kim and Wamser, 2006). As diagrammed in Figure 5, aniline has been polymerized in the presence of equimolar proportions of hydrochloric acid with oxidation by ammonium peroxydisulfate salt, yielding polyaniline emeraldine hydrochloride (Stejskal and Gilbert, 2002).

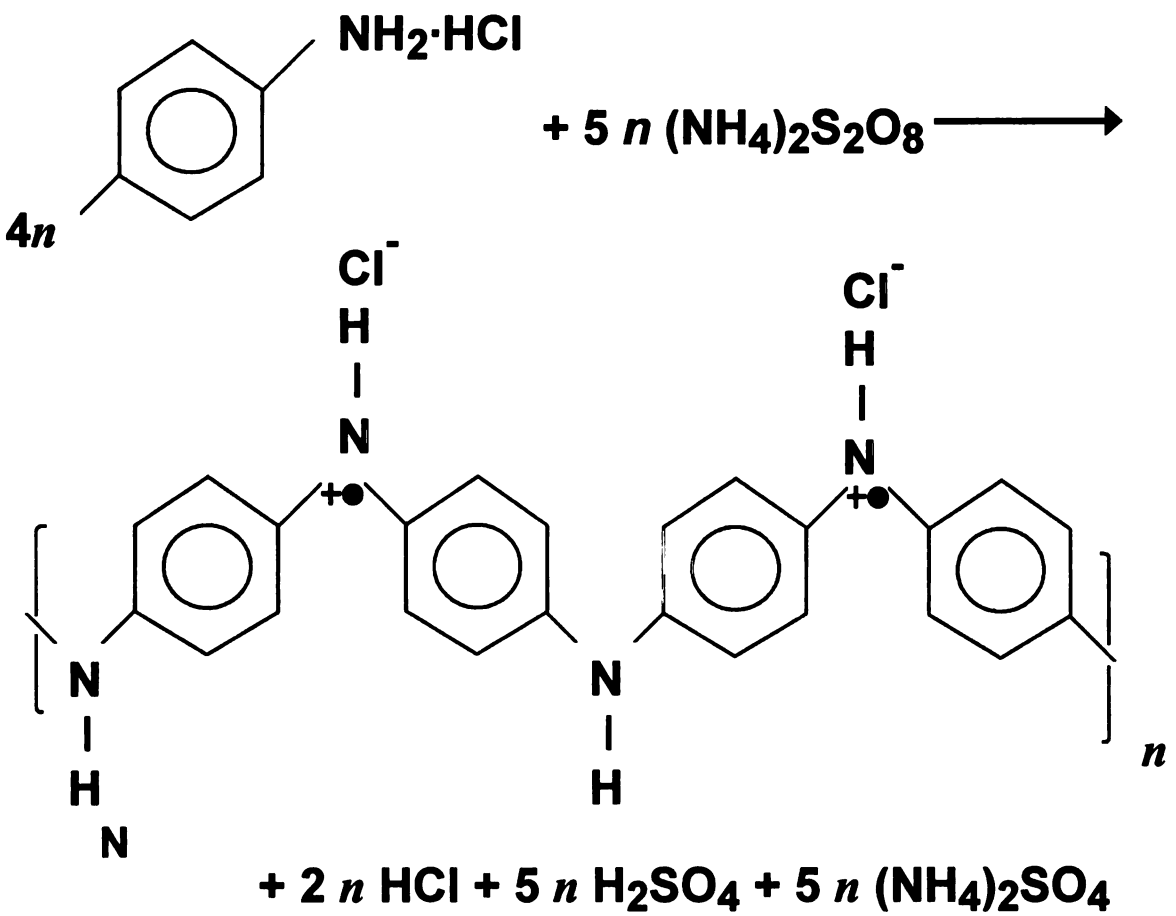

Figure 5. Aniline in the presence of hydrochloric acid, oxidized with ammonium peroxydisulfate to yield polyaniline emeraldine hydrochloride (adapted and modified from Stejskal and Gilbert, 2002).

2.7.5.2 Forms

Polyaniline may exist in various forms, with corresponding levels of electrical conductivity (Figure 6). Each structure has a characteristic color, and the forms may undergo interconversion based on the conditions. Leucoemeraldine is the fully reduced form of polyaniline, emeraldine is 50% oxidized, and pernigraniline is fully oxidized (Ray *et al.*, 1989; Stejskal *et al.*, 1996). Each of these oxidation states may exist in base form or may become protonated to its salt form by acid treatment. Of the characteristic polyaniline forms, green protonated emeraldine, as produced by oxidative polymerization of aniline, is of particular interest and importance due to its high electrical conductivity and stability. As compared to other polymers, the C6 benezenoid rings of emeraldine can rotate, causing alterations to the electronic structure. Additionally, emeraldine is not charge conjugation symmetric, and its carbon rings and nitrogen atoms form a generalized "A-B" polymer (Pouget *et al.*, 1991). Stronger oxidizing conditions generate blue protonated pernigraniline, which is also expected to be conducting. Reduction by alkali results in violet pernigraniline base or colorless leucoemeraldine, which are not electrically conducting (Stejskal *et al.*, 1996).

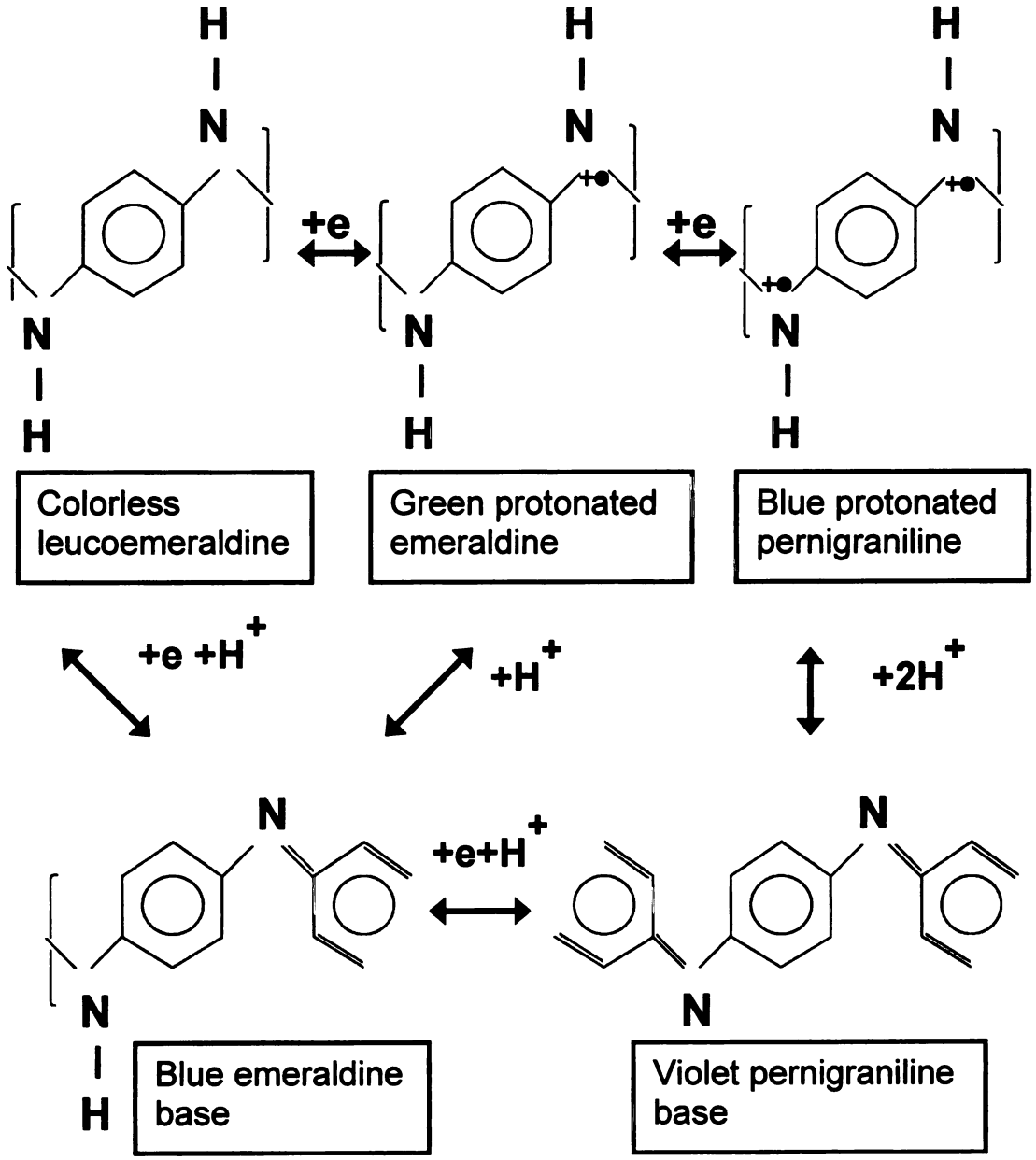

Figure 6. Forms of polyaniline (adapted and modified from Stejskal *et al.*, 1996).

2.7.5.3 Electrical Conduction Properties

The high electrical conductivity of polyaniline is determined by the polaronic state of the polymer, which in turn is determined by redox state, proton content, and stearic hindrance (Grzeszczuk and Szostak, 2003). The electronic properties of polyaniline may be modified by variation of either the number of protons, number of electrons, or both. Addition of a protic solvent such as hydrochloric acid or sulfuric acid yields a conducting form of polyaniline, with an increase in conductivity of an up to ten order of magnitude as compared to its undoped insulating form (Sarno *et al.*, 2005; Ahuja *et al.*, 2007). This is due to protonation ("proton doping") of formerly unprotonated sites. Grzeszczuk and Szostak (2003) found that hysteresis of the switching process of electrochemically produced thin films of polyaniline was highest when hydrochloric acid was used as the counterion, as compared to trichloroacetic acid or perchloric acid. The anions entered a polymer phase during the electropolymerization process that was performed in aqueous acid solution (Grzeszczuk and Poks, 1995; Grzeszczuk and Szostak, 2003; Grzeszczuk and Zabinska-Olszak, 1993; Poks and Grzeszczuk, 1997).

Green protonated emeraldine has a conductivity of the order of 1 S/cm, which places emeraldine in the semiconductor range, between common polymers ($\sigma < 10^{-9}$ S/cm) and metals ($\sigma > 10^{4}$ S/cm) (Stejskal *et al.*, 1996). The Pauli susceptibility is linearly proportional to the percentage of protonation (Stafstrom *et al.*, 1987). Protonation of the emeraldine base generates a polysemiquinone radical cation, or polaron, and a polaron conduction band is formed by coulombic repulsion (MacDiarmid *et al.*, 1987). Stafstrom *et al.* (1987) proposed that protonation causes phase segregation of unprotonated and protonated domains, and suggest a two-step transition of polyaniline in

its polyemeraldine form from undoped to proton-doped (Figure 7). Instability of bipolarons leads to formation of polarons and eventually a polaron lattice, whose single polaron band structure was shown to be accountable for observed optical transitions (Stafstrom *et al.*, 1987). Polarons occur at the midgap via removal of an electron from a neutral nonconducting polymer which has a full valence band and empty conduction band (band gap). Bipolarons are generated by further oxidation and removal of a second electron (Stafstrom *et al.*, 1987).

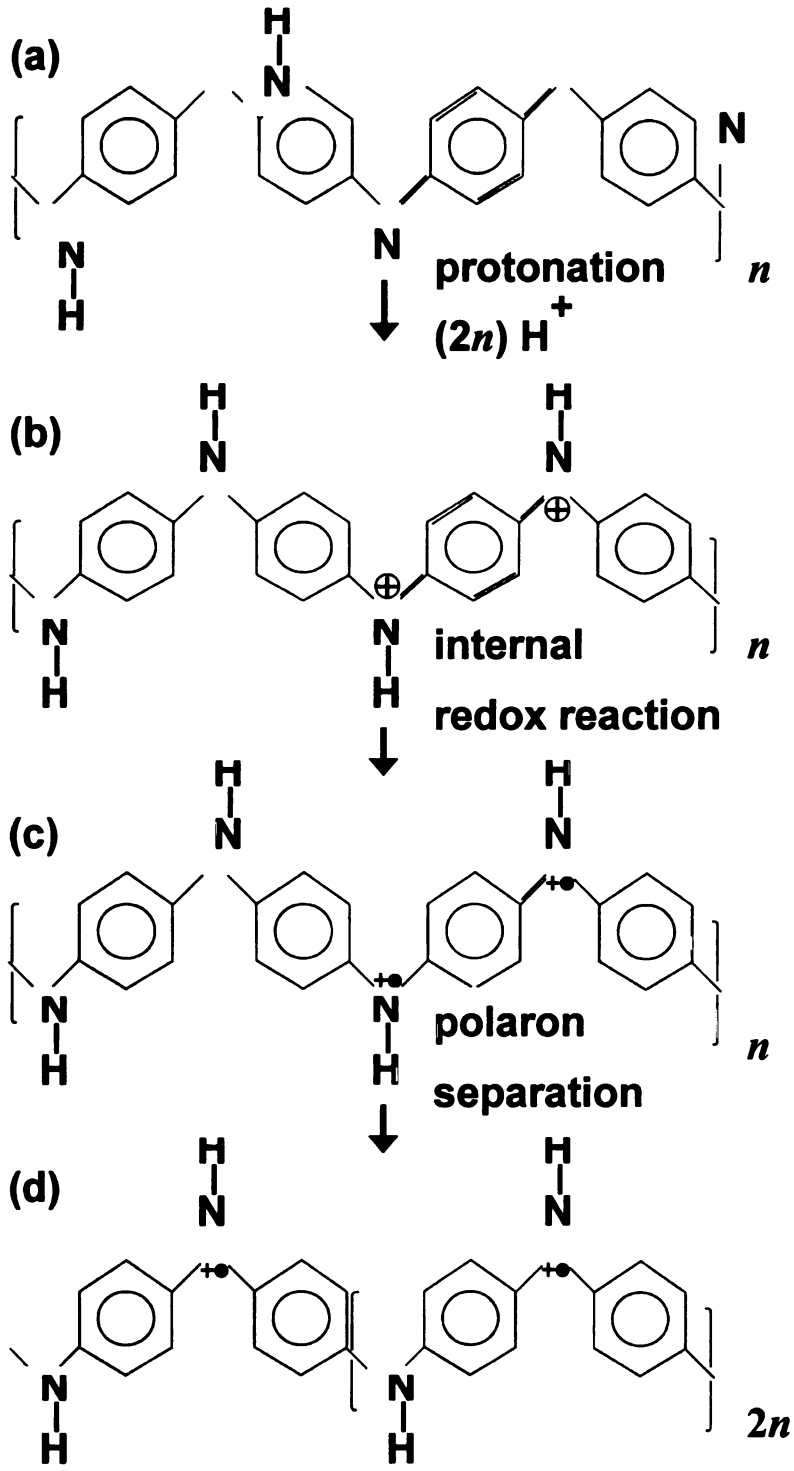

Figure 7. Geometric structure of polyaniline in polyemeraldine state. (a) Before protonation, (b) formation of bipolarons after 50% protonation, (c) formation of polarons after 50% protonation, and (d) polaron lattice formed after polaron separation (adapted and modified from Stafstrom *et al.*, 1987).

Polyaniline in the emeraldine oxidation state has been converted from insulating (σ ~ 10^-10 S/cm) to conducting (σ ~ 5 S/cm) by doping with 1M aqueous HCl, yielding emeraldine hydrochloride, the corresponding salt (MacDiarmid *et al.*, 1987). This protonic acid doping process means that the number of electrons associated with the polymer does not change. The metallic emeraldine hydrochloride was shown by MacDiarmid *et al.* (1987) to be a delocalized semiquinone radical cation with a polaron conduction band, with the nitrogen atoms holding most of the charge (MacDiarmid *et al.*, 1987).

Protonated polyaniline, in the emeraldine salt (emeraldine hydrochloride) state, has been converted to nonconducting blue emeraldine base by deprotonation in alkaline medium (Figure 8). The polyaniline transitions into polyaniline emeraldine base (Stejskal *et al.*, 1996).

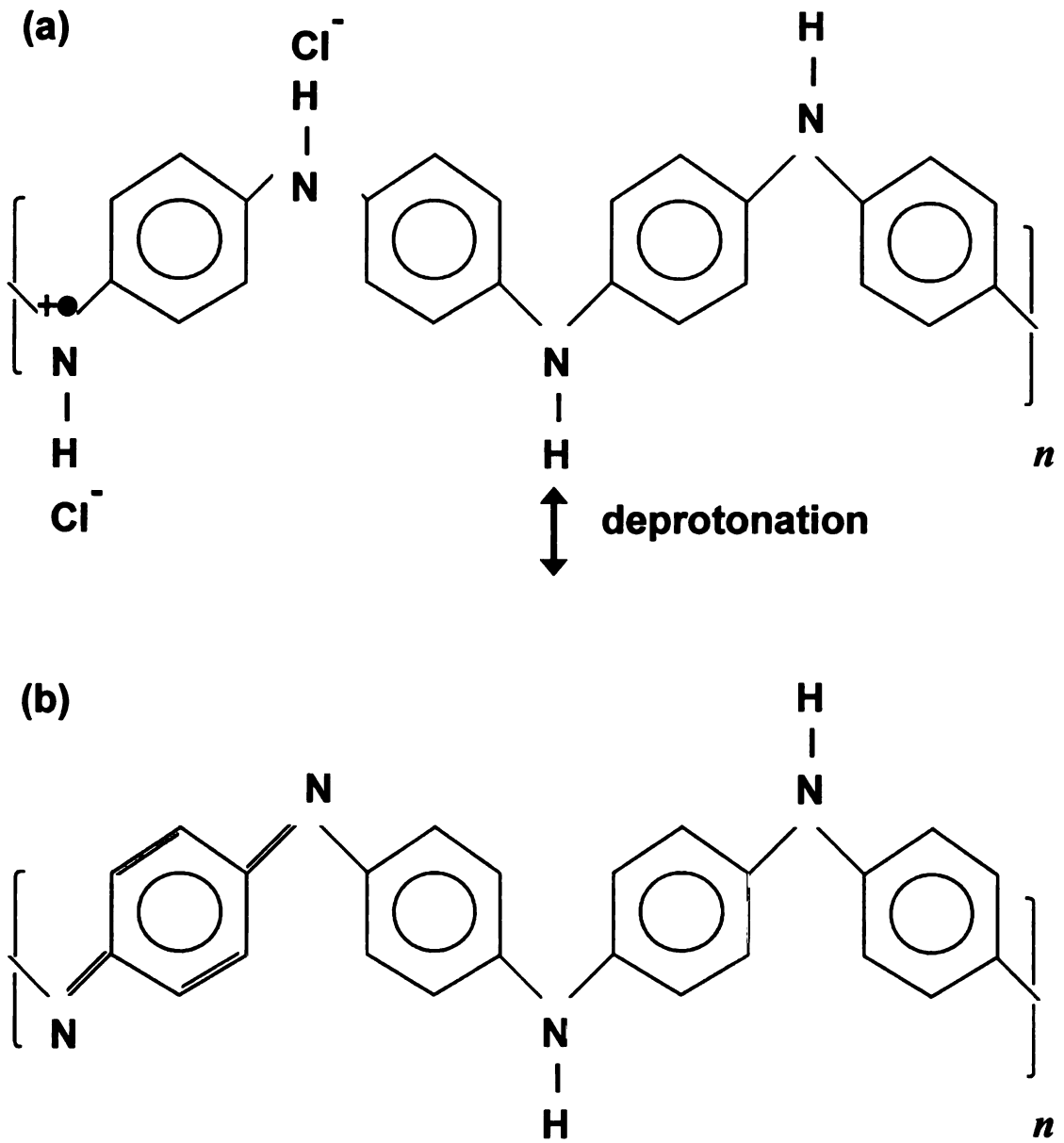

Figure 8. Deprotonation of polyaniline in presence of chloride (alkaline medium). (a) Polyaniline emeraldine salt is converted to (b) polyaniline emeraldine base (adapted and modified from Stejskal and Gilbert, 2002).

Hole-doped (p-doped) polyaniline is the more common form of conducting polyaniline. Chaudhuri and Sarma (2006) investigated electron-doping (n-doping), in which synthesis required deprotonation of the amine N atoms (-NH-) in the polymer, using a very strong base, n-butyl lithium (nBuLi). The resulting lithiated polyaniline was unstable and reacted exothermally with moisture, which was likely due to electron-rich N centers. To address instability, further complexation with electron-deficient boron trihalides was necessary. While this negated the effect of the previous n-doping, and generated a nonconducting end product, the reduced polyaniline did exhibit high efficiency deep blue photoluminescence, with applications in thin, flexible display panels. The n-doping step was able to deprotonate 75% of N atoms, leading to a strongly nucleophilic form with potential for attachment of various functional groups (Chaudhuri and Sarma, 2006).

Additionally, polyaniline offers efficient electronic charge transfer, making it attractive for use in biosensors as well as batteries, fuel cells, and electrodes (Liu *et al.*, 2005; Scott *et al.*, 2005; Grennan *et al.*, 2006). Magnetic polyaniline nanoclusters have been described in the literature as lightweight yet mechanically strong, with various combinations of magnetic cores and doping agents. Magnetic core materials include iron (II, III) oxide, hydroxyl iron, and Li Ni Ferrite, with hydrochloric acid, phosphoric acid, and toluene as doping agents (Poddar *et al.*, 2004; Zhang *et al.*, 2005; Dallas *et al.*, 2006; Jiang and Li, 2006; Xue *et al.*, 2006).

2.7.5.4 Electrochemistry

The high electrical conductivity of polyaniline is dependent on redox state, proton content, and stearic hindrance. The characteristic redox switching process of polyaniline

is important for understanding its physical and chemical properties. Switching of polyaniline from its fully reduced leucoemeraldine state to the conducting 50% oxidized emeraldine state, and then from the emeraldine state to the fully oxidized pernigraniline state, generates two peaks as observed by cyclic voltammetry. The observed emeraldine state can occur over a potential range. The redox behavior of polyaniline is fundamentally asymmetric, with oxidation transition occurring at a slower rate than reduction. Additionally, the pH of the medium is important, with electrochemical activity lost in the presence of neutral or alkaline medium (Gospodinova *et al.*, 1996; Grzeszczuk and Szostak, 2003; Hong and Park, 2005).

The redox transition of polyaniline typically occurs over the potential range from -200 to 400 mV using a saturated calomel electrode. Proton ejection or injection accompanies redox transitions. Oxidation of leucoemeraldine to emeraldine and from emeraldine to pernigraniline was shown to be accompanied by proton ejection. The proton injection that accompanies polyaniline reduction is incomplete for the transition from emeraldine to leucoemeraldine. Proton equilibration is thus a slow process. Ybarra *et al.* (2000) qualitatively demonstrated these proton ejection and injection processes by using the amperometric mode of a rotating ring-disk electrode, which exhibited significantly lower ring current during the reduction response. This indicates that the polymer is not in protonic equilibrium with the electrolytic phase (Ybarra *et al.*, 2000).

Grzeszczuk and Szostak (2003) utilized various counterions in the reversible electrochemical doping of polyaniline, and found that the thermodynamic and kinetic CV characteristics of the reversible state switching of the polymer were largely dependent on anion nature. Factors included size, geometry, hydrogen-bonding, and basicity of the

anions. Formation of transition states between reduced and oxidized states was found to require less energy when hydrogen-bonding interactions assisted the transition (Grzeszczuk and Szostak, 2003).

2.7.6 Electrically Active Magnetic Polyaniline

Nanotechnology has progressed to the point where particles can be engineering consistently at the nanoscale, for application in various biomedical and engineering fields. Properties of nanoparticles differ significantly from their bulk counterpart. Novel properties such as superparamagnetism and macroscopic quantum tunnelling emerge when the size of the particles is reduced below the single domain limit. For iron and iron oxide, this occurs at 15-20 nm (Poddar *et al.*, 2004).

Magnetic nanoparticles have applications as contrast agents in magnetic resonance imaging (MRI) and as agents of targeted drug delivery (Babes *et al.*, 1999; Lacava *et al.*, 2001; Moghimi *et al.*, 2001). A common hurdle encountered in such applications is opsonization, in which particles injected into the bloodstream become coated by plasma proteins or other biological circulatory components (Davis, 1997; Portet *et al.*, 2001; Ramge *et al.*, 2000). Particles that are resistant to such coating will be cleared more slowly, allowing improved drug performance. Such evasive particles have been developed with coatings of dextran, polyethylene glycol (PEG), poloxamers and polyoxamines (Lacava *et al.*, 2001). Small hydrodynamic radius (<20nm) is also important for the particles to reach the target cells (Gref *et al.*, 1994; Moghimi *et al.*, 2001). Iron oxide nanoparticles have been synthesized and derivatized with dextran or albumin, and the influence of their size and surface composition was assessed in vitro using human dermal fibroblasts to characterize the interaction between cells and particles.

Derivatized particles were found to induce cell behavior alterations as compared to the effects of underivatized particles, indicating that cell response can be specifically directed by the engineering of particles on the nanoparticle surfaces (Berry *et al.*, 2003).

2.7.7 Cyclic voltammetry

The electrochemical properties of a system can be explored using linear sweep voltammetry techniques such as cyclic voltammetry. In an electrochemical cell with a conventional three-electrode set-up, a potential is applied which is ramped linearly versus time at a particular scan rate (V/s or mV/s) from an initial potential, *E1*, to a final potential, *E2*, and back again to *E1*. In a reversible redox system, a redox couple will undergo a one electron oxidation-reduction process, described by the equation

$$Ox + e^- \leftrightarrow R \qquad (3)$$

The output is presented as a cyclic voltammogram (CV), which illustrates the resulting current (*I*) measured while scanning the potential range, represented with respect to the potential (*E*) (Figure 9). The oxidation process occurs at the cathode and can be represented by the cathodic peak potential, *Epc*, which corresponds to the point where the current reaches the maximum, *Ipc*. The reduction process occurs at the anode and can be represented by the anodic peak potential, *Epa*, as corresponds to the anodic maximum current, *Ipa*. These reactions create a concentration gradient at the surface of the electrode for both species, leading to a diffusion controlled mass transfer process of species Ox from the electrolyte to the surface of the electrode. This transport is referred to as ionic charge transfer or mass transfer (Vyas and Wang, 2010). Redox reactions can be quantitatively assessed by the *Ep* or *Ip* values, the ratio of peak currents, *Ipa/Ipc*, the separation of peak potentials, *Epa – Epc*, or the integral of current, ΔQ.

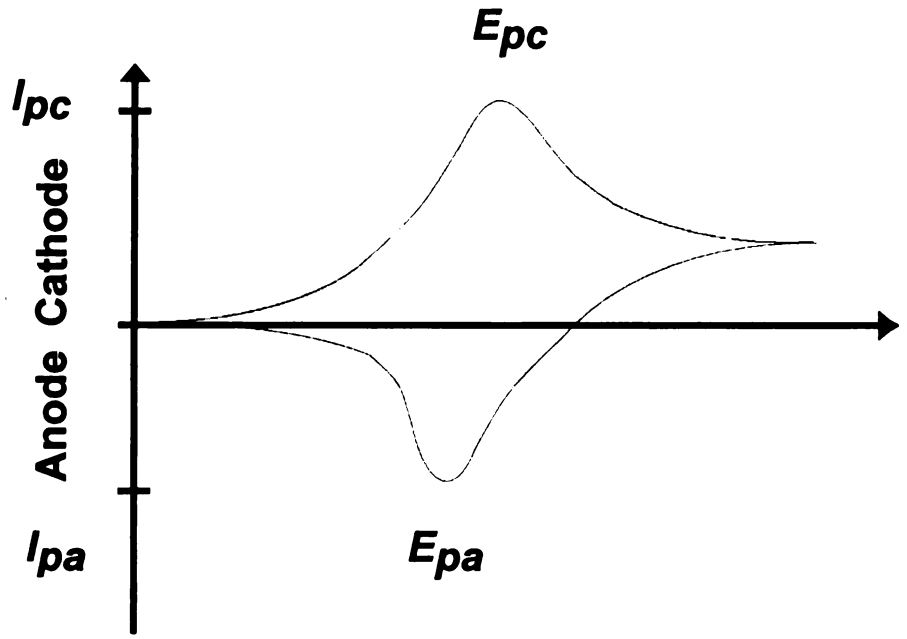

Figure 9. Schematic cyclic voltammogram for redox couple undergoing single electron oxidation-reduction process.

The peak current, I_p, in a reversible redox system is characterized by the equation

$$I_p = 0.4463\left(\frac{F^3}{RT}\right)^{1/2} n^{3/2} A D_0^{1/2} C_0^* v^{1/2} \quad (4)$$

where F = Faraday's constant (Q/mol), R = universal gas constant (J/mol·K), T = temperature (K), n = number of electrons exchanged in the reaction, A = surface area of electrode (cm2), $D0$ = diffusion coefficient of the electroactive species (cm2/s), C*= concentration of the electroactive species (mol/cm3), and v = scan rate (V/s) (Bard and Faulkner, 2000).

The peak potential, *Ep*, in a reversible redox system is characterized by the equation

$$E_p = E_{1/2} - 1.109\frac{RT}{nF} \qquad (5)$$

Mass transfer for ionic species in electrolytes near electrodes occurs between the redox couple and the electrode, and can occur by various phenomena, including diffusional transport under concentration gradients, migration transport of oppositely charged ions under electrode electric field, and convection transport due to physical electrolyte stirring. In the case of electrodes modified with electroactive or redox films, such as conducting polymer films, the redox behavior becomes more complex. Here, electron transfer from the electrode surface to the film occurs simultaneously with ionic transfer from electrolyte to film. Electro-neutrality is thereby maintained (Lyons, 1994).

Cyclic voltammetry is an effective method of characterizing electrochemical systems, and offers valuable information on redox reactions. The research described here will examine the power of cyclic voltammetry in determining the concentration of an electrically active species as an indicator of the presence of the target. Integral of current, ΔQ, and peak currents, I_p, will be used for quantitative analysis.

CHAPTER 3: RESEARCH HIGHLIGHTS

3.1 RESEARCH NOVELTY

The development of both an SPR-based assay as well as a nanoparticle-based biosensor offer innovativeness in structure and application. SPR has been used extensively in the literature as a sensitive and specific method for characterizing the avidity, specificity, and kinetics of binding between various partners. Typical reactions involve protein-protein binding, and while carbohydrate-protein interactions have been described, to date no literature has been reported that investigates the specific interaction between host carbohydrate (glycan) receptors and FLUAV hemagglutinin glycoprotein by SPR (Table 2). Protein microarray technology has been reported as an appropriate methodology for identifying this interaction; however, the indication of binding by fluorescence is less quantitative than desirable.

The biosensor architecture is novel in its preparation, with multiple crosslinkers and signal enhancers applied to achieve repeatable and sensitive binding interactions between the carbohydrates and proteins. Electrically active polyaniline coated magnetic nanoparticles (EAMs) are applied dually as magnetic concentrator of the carbohydrate—protein—antibody complex, as well as the biosensor transducer. While this dual function has been reported previously, the biosensor is novel in its design, with the molecules of interest (carbohydrate and protein) applied to the working electrode in a single step, without the need for preimmobilization of a specific antibody. The biosensor application also presents innovation in the detection of pandemic-indicative FLUAV hemagglutinin protein. Table 3 demonstrates the novelty of this research by outlining previous

contributions to the fields as well as highlighting gaps in the knowledge base that may be addressed by the current research.

Table 2. SPR assays: Gaps in research

SPR assay: monoclonal antibodies against carbohydrate epitope (Ohlson *et al.*, 2000).
SPR assay: H5N1 adjuvanted vaccine preparations against FLUAV (Khurana *et al.*, 2010).
Protein microarrays: spot printing on glass slides for protein-protein interactions (MacBeath and Schreiber, 2000).
Carbohydrate microarrays: spot printing on glass slides for carbohydrate-protein interactions as observed by fluorescence intensities (Blixt *et al.*, 2004).
Needed: SPR assay for quantitative carbohydrate-protein binding characterization
Needed: SPR assay for pandemic FLUAV H5N1 identification
Needed: SPR assay for measuring antibody-mediated inhibition of carbohydrate-protein binding

Table 3. Biosensor technology: Gaps in research

Polyaniline synthesis (Li *et al.*, 2007a): 10-50nm diameter polymerized in vanadic acid.
Electrically active polyaniline coated magnetic nanoparticle (EAM) synthesis (Li *et al.*, 2007b): Diameter of 0.5-5 μm.
Polyaniline based antibody immunochromatographic biosensor: bovine viral diarrhea virus (Muhammad Tahir *et al.*, 2005a). Polyaniline polymerized in phenylphosphonic acid (PPA), 4-hydroxybenzenesulphonic acid (HBSA), sulfobenzoic acid (SBA), hydrochloride acid (HCl), perchloric acid (PA).
Polyaniline based antibody immunochromatographic biosensor: human serum albumin detection; colloidal gold—antibody conjugates (Kim *et al.*, 2000).
Polyaniline based antibody immunochromatographic biosensor: polyaniline magnetic nanoparticles conjugated to antibody; screen printed silver electrodes (Yuk *et al.*, 2009).
Polyaniline based antibody immunochromatographic biosensor: *Bacillus anthracis* (Pal and Alocilja, 2009).
Polyaniline based enzyme amperometric biosensor: glucose oxidase immobilized on a Prussian Blue—modified platinum electrode (Garjonyte and Malinauskas, 2000).
Immunochromatographic biosensor with signal enhancement by colloidal gold conjugated to progesterone-ovalbumin (Jennes *et al.*, 1986; Laitinen and Vuento, 1996).
Immunochromatographic biosensor with signal enhancement by colloidal gold conjugated to polyclonal antibody: *Salmonella typhimurium* (Paek *et al.*, 1999).
Electrically active polyaniline coated magnetic nanoparticle as immunomagnetic concentrator of *Bacillus anthracis* endospores (Pal and Alocilja, 2009).
DNA biosensor with signal transduction and amplification by glucose oxidase catalyzed deposition of cupric hexacyanoferrate (CuHCF) NPs: FLUAV (Chen *et al.*, 2010).
Needed: EAM based carbohydrate biosensor
Needed: EAM based direct-charge transfer biosensor
Needed: EAM and gold nanoparticles as signal enhancers: carbohydrate/protein binding
Needed: EAM based biosensor for Influenza A virus detection

3.2 RESEARCH SIGNIFICANCE

The binding between host glycan receptors and the glycoprotein hemagglutinin on the FLUAV surface is essential for FLUAV infectivity and transmission, and this interaction is thus a prime target for study. Understanding the avidity and specificity of these interactions, as dependent on FLUAV strain and glycan structure, is essential to understand the mechanism of infection as well as to neutralize this binding by antibody-based therapies. SPR offers a valuable technique for binding characterization and binding neutralization studies with repeatable and quantitative results. The SPR assay requires very low concentrations and volumes of ligand and analyte, and presents the hemagglutinin analyte in a physiologically relevant aqueous system. Antibody-based therapies for prophylaxis and treatment of FLUAV infection are gaining interest to replace or augment chemotherapy techniques, and their current shortcomings, including lot-to-lot variation, variation due to donor pool, and low specific antibody content, could be circumvented by an SPR screening assay of donor plasma. Hyperimmune donor plasma could be rapidly and accurately screened by the proposed SPR assay and ranked based on glycan/protein neutralization activity to obtain a high potency FLUIGIV product.

The use of EAMs as the biosensor target concentrator and signal transducer is the result of the combination of the desirable chemical, electrical, and mechanical properties of the conducting polymer, polyaniline, and the magnetic properties of the core material, iron oxide. EAMs are valuable for their nanoscale dimensions, which provide an increased surface to volume ratio upon which biological events can occur. The magnetic property of the EAMs in conjunction with their propensity for biological surface

modification, allows the target to be quickly and easily identified and separated from irrelevant background material, reducing matrix interference. This separation technique will be advantageous for identifying low levels of target in complex samples, in particular the serum or respiratory secretions from which hemagglutinin or whole FLUAV virions are typically isolated. Ideally, the magnetic power of the EAMs will eliminate the need for time- and reagent-consuming pre-enrichment steps. The electrochemical and magnetic properties of the EAMs lend flexibility to the biosensor design, with the ability for any strain of FLUAV to be specifically identified via a compatible antibody and corresponding glycan receptor.

The strength of this research lies not only in the value of the SPR assay and biosensor individually, but also in the conjunctive applicability of both methodologies. Parallel testing of carbohydrate-protein interactions on both systems offers a basis for comparison from which improvements to both assays can be identified. The current research developed a sensitive and specific SPR assay for characterizing glycan binding to hemagglutinin from pandemic FLUAV and the neutralization of such binding. A complementary carbohydrate based biosensor platform was developed to identify H5N1 hemagglutinin based on binding to a corresponding glycan receptor. A similar biosensor platform was also investigated to differentiate between human-transmissible and non-human-transmissible FLUAV strains.

3.3 HYPOTHESIS

This research is based on the following hypothesis:

Immunofunctionalized electrically active polyaniline coated magnetic nanoparticles (EAMs) will concentrate target hemagglutinin from serum matrix by their magnetic properties, and will function as the transducer in reporting a FLUAV-specific biodetection event by their electrical properties, with results correlative to Surface Plasmon Resonance (SPR) measurements.

3.4 RESEARCH OBJECTIVES

This research is based on the following specific objectives:

Objective 1: Design of a Surface Plasmon Resonance (SPR) based binding assay.

Objective 2: Design of an SPR based assay for detection of antibody-mediated binding inhibition.

Objective 3: Design and fabrication of an EAM based electrochemical biosensor for detection of H5N1 hemagglutinin.

Objective 4: Design and fabrication of an EAM based electrochemical biosensor for identification of human-transmissible FLUAV strains.

Objective 5: Evaluation of sensitivity and specificity of the EAM based electrochemical biosensors.

CHAPTER 4: RESEARCH MATERIALS AND METHODS

4.1 OBJECTIVE 1

Surface Plasmon Resonance—based binding assay

This objective was aimed at characterizing the ability of Surface Plasmon Resonance technology to detect carbohydrate/protein binding with repeatability, sensitivity, and specificity, for application in a glycan/hemagglutinin binding assay.

4.1.1 SPR Assay Design

4.1.1.1 Reagents and Chemicals

The biotinylated carbohydrate compounds 3'SLex (B157), 3'SLN (B84), 6'SLN (B87), CT/Sda (B204), and GD2 (B184) were provided by the Carbohydrate Synthesis/Protein Expression Core of The Consortium for Functional Glycomics funded by the National Institute of General Medical Sciences grant GM62116. The following reagent was obtained through the NIH Biodefense and Emerging Infections Research Resources Repository, NIAID, NIH: H5 Hemagglutinin (HA) Protein from Influenza Virus, A/Vietnam/1203/04 (H5N1), Recombinant from baculovirus, NR-10510. 6xHis tagged H5 hemagglutinin (HA) protein from 293 cell culture, A/Vietnam/1203/04 (H5N1); C-terminal 6xHis tagged H1 hemagglutinin (HA) protein from 293 cell culture, A/South Carolina/1/18 (H1N1); and 6xHis tagged H5 hemagglutinin (HA) protein from 293 cell culture, A/Indonesia/5/05 (H5N1), were purchased from Immune Technology Corp. (New York, NY). Recombinant full-length H3 protein from baculovirus, A/Wyoming/3/03 (H3N2) was purchased from Prospec Protein Specialists (Rehovot, Israel).

HBS-P buffer; HBS-EP buffer; 10 mM glycine pH 2.0, 2.5, and 3.0; 50 mM NaOH; 10 mM sodium acetate pH 4.0 and Sensor Chip SA (Streptavidin) were purchased from GE Healthcare (Piscataway, NJ). Avidin/Biotin blocking kit was purchased from Vector Laboratories, Inc. (Burlingame, CA). Sodium chloride 5 M, ethylenediaminetetraacetic acid (EDTA), phosphoric acid, bromelain, 2-mercaptoethanol (2-ME), and Tween-20 were purchased from Sigma-Aldrich Co. (St. Louis, MO).

4.1.1.2 Equipment

The Biacore 3000 instrument offers automated Surface Plasmon Resonance detection (Jason-Moller *et al.*, 2006). Interaction analysis between proteins, carbohydrates, nucleic acids and small molecules is possible on this real-time, label-free, and contact-free system. Binding information for strong or weak, fast or slow interactions can be obtained in the form of yes/no binding, binding specificity, binding affinity or kinetics. As previously described, the Biacore-SPR system measures changes in mass at a biospecific surface that occur due to the interaction of interest. One interaction partner is immobilized onto a gold film surface, while the other is passed over in solution. The Biacore offers integrated microfluidics, with very small dead-volume, low dispersion, and fast liquid exchange rates (Figure 10). Information is output as a sensorgram of Resonance Units (RU) versus time (s) (Jason-Moller *et al.*, 2006).

4.1.1.3 SPR (Biacore) Chip Preparation and Immobilization

Previous glycan microarray analysis has been performed to probe HA specificities for glycan receptors (Blixt *et al.*, 2004; Stevens *et al.*, 2006a). From this work, corresponding glycan/HA pairs were chosen. The surface chemistry of the Biacore Sensor Chip SA consists of streptavidin covalently immobilized on a carboxymethylated

dextran matrix, and has a listed binding capacity of ≥ 1800 Resonance Units (RU) of a biotinylated oligonucleotide (Figure 10) (GE, 2004). The sealed sensor chip equilibrated to room temperature for 60 min and was docked in the Biacore 3000 instrument. The instrument was primed 3 times with filtered and degassed HBS-P buffer. Sensor Chip SA was conditioned with three consecutive 1-min injections of NaCl 1 M in NaOH 50 mM (GE, 2004). Biotinylated glycans were diluted to 1 μM in Biacore HBS-P buffer and 8 μl were injected over a Biacore SA chip at 10 μl/min. Glycans were immobilized via streptavidin/biotin interaction to saturation at approximately 300 resonance units (RU). Streptavidin has extraordinarily high affinity for biotin (K_d 10^{-14} to 10^{-16}M). The streptavidin/biotin interaction is also resilient, stable against heat, denaturants, proteolytic enzyme action, and extreme pH (Laitinen *et al.*, 2007). Flow cells 2-4 were immobilized separately by manual injection: 3'SLex on flow cell 2, CT/Sda on flow cell 3, and 3'SLN on flow cell 4. Flow cell 1 was left blank. The immobilized chip was blocked with two 30 s pulses of avidin, one 1 min pulse of HBS-P buffer, and two 30 s pulses of biotin. A second chip was immobilized with the same glycans as Chip 1 at the lowest immobilization level possible, around 20 RU. A third chip was immobilized with GD2, 6'SLN, and 3'SLN followed by avidin/biotin blocking.

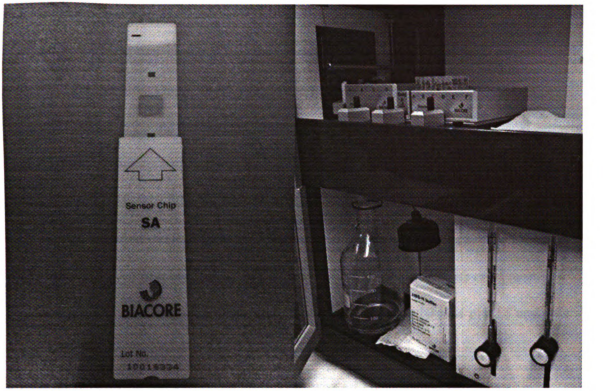

Figure 10. Biacore SA sensor chip and instrumentation.

Table 4. Glycan structure and binding predictions

Chip 1, 2	Common Name	Saccharide Name and Spacer
Fc1	blank	--
Fc2	3'SLex	Neu5Acα2-3Galβ1-4[Fucα1-3]GlcNAcβ-SpNH-LC-LC-Biotin
Fc3	CT/Sda	Neu5Acα2-3[GalNAcβ1-4]Galβ1-4GlcNAcβ-SpNH-LC-LC-Biotin
Fc4	3'SLN	Neu5Acα2-3Galβ1-4GlcNAcβ-SpNH-LC-LC-Biotin
Chip 3		
Fc1	blank	--
Fc2	GD2	Neu5Acα2-8Neu5Acα2-3[GalNAcβ1-4]Galβ1-4GlcβSpNH-LC-LC-B
Fc3	6'SLN	Neu5Acα2-6Galβ1-4GlcNAcβ-SpNH-LC-LC-Biotin
Fc4	3'SLN	Neu5Acα2-3Galβ1-4GlcNAcβ-SpNH-LC-LC-Biotin

4.1.1.4 Chip Regeneration

H5 at 280 nM was injected over the immobilized glycans at 5 µl/min to establish activity of the surface. Once binding was observed, regeneration was explored to completely remove bound H5 while retaining immobilization level and biological activity of the glycans. Regeneration buffers including glycine 10 mM at pH 3.0, 2.5, and 2.0, EDTA 50 mM + NaCl 0.5 M, NaCl 1 M, acetate 4.0, phosphoric acid 50 mM, and NaOH 50 mM were injected over the chip at 100 µl/min. A two-injection regeneration scheme consisting of 60 s of glycine 10 mM pH 2.5 and 30 s 50 mM NaOH was compared to a two-injection regeneration scheme consisting of 60 s of glycine 10 mM pH 2.5 and 18 s 50 mM NaOH.

4.1.2 SPR Binding between Glycan Receptors and Hemagglutinin

4.1.2.1 Binding Assay and Sensitivity Testing

Binding between recombinant H5 HA protein and synthetic glycan receptors was investigated by injecting H5 samples serially diluted at a 1:3 ratio over the immobilized glycans 3'SLex, CT/Sda, and 3'SLN, for 5 min at 5 µl/min, with regeneration scheme following 20 min dissociation time. The H5 molarities were 286 nM, 94.3 nM, 31.4 nM, 10.6 nM, and 3.53 nM. Regeneration included 60 s of 10 mM glycine pH 2.5 and 30 s of 50 mM NaOH at 100 µl/min. A truncated dilution series was also performed using the regeneration of 60 s of glycine 10 mM pH 2.5 and 18 s 50 mM NaOH. This binding study offered results from which the lowest detection limit of the SPR assay for H5 was obtained. Testing for each H5 molarity was performed in triplicate. Recombinant H3 HA (A/Wyoming/3/2003) was injected over the same immobilized glycans under the same conditions and concentrations, and was used as the negative control. The lowest dilution

of H5 that produced a signal distinguishable from the control was taken as the sensitivity of detection. Binding of H5 HA (A/Indonesia/5/2005) was also tested at 140 nM.

4.1.2.2 Specificity Testing

The specificity of the assay was investigated using H1, anti-H1, H3, anti-H3, and glycans nonspecific for H5, 6'SLN (α2,6 binder), GD2 (α2,8 binder), and CT/Sda (α2,3 binder). H1 HA (A/South Carolina/1/18, H1N1) at 1:3 serial dilution was injected over the glycans GD2, 3'SLN, and 6'SLN, which were immobilized to saturation. H3 HA (A/Wyoming/3/03) was injected over glycans 3'SLex, CT/Sda, and 3'SLN, which were immobilized to saturation. Testing for each dilution was performed in triplicate.

4.1.3 Characterization Studies

4.1.3.1 HA Receptor Binding Domain Binding Assessment

The binding of the HA1 segments of H5 and H3, which contain the receptor binding domains, to glycans 3'SLex, CT/Sda, and 3'SLN was investigated. HA1 H5 and HA1 H3 were prepared at 1:3 serial dilutions, with concentrations of 286 nM, 94.3 nM, and 31.4 nM, and compared to the same concentrations of full length H5. The binding experiment was repeated with running and sample buffers prepared as HBS-P with 0.1% BSA and 0.5% glycerol. HA1 H5 and HA1 H3 were compared to the positive control, H5 at 140 nM, and a glycerol concentration curve from 0-1%.

4.1.3.2 HA Preparation

To obtain a more consistent set of monomers and trimers, H5 was pretreated with heat, bromelain, 2-mercaptoethanol (2-ME), and Tween-20. H5 at 1.4 μM was heated at 37 °C for 4 h or overnight, with or without bromelain 100 μg/ml and 2-ME 0.1 M. H5 at

1.4 μM was heated at 56 °C for 10 min with or without subsequent cooling at 4 °C. H5 at 1.4 μM was also treated with Tween-20 at 0.1-0.02%.

4.1.3.3 Serum Experiments

The complexity of biological samples was considered, with the ultimate goal of a FLUIGIV screening assay in mind. The binding of H5 and H3 to glycans 3'SLex, CT/Sda, and 3'SLN as described in *4.1.2.1* and *4.1.2.2* was repeated with HA at 1:3 serial dilution prepared in mouse serum (ICR SCID) at 2% final concentration by volume. Background binding to glycans 3'SLex, CT/Sda, and 3'SLN and the blank cell was investigated using mouse serum (ICR SCID) at 0.5-10% in buffer.

4.1.3.4 Statistical Analysis

Each experiment was performed in triplicate to account for equipment or user variation. The samples were double referenced, by subtracting either the blank fc1 or nonbinders CT/Sda, GD2, or 6'SLN from the binder results, as well as subtracting a buffer run to compensate for irrelevant machine fluctuations. The SA chips were assumed to have the same physical properties, and the glycans were assumed to be immobilized to saturation. The peak RU at the end of the injection cycle was taken as an indicator of binding. The effects of different HAs, glycans, anti-HA antibodies, and HA concentration were assessed to calculate the lower detection limit and specificity of the SPR-based assay. The differences between the means for each sample peak were calculated and analyzed based on single factor analysis of variance (ANOVA) to a significance of 95% ($\alpha = 0.05$) (Tables A-1, A-2), using SAS software (SAS, Cary, NC).

4.2 OBJECTIVE 2

SPR to Detect Ab-Mediated Binding Inhibition

Although monoclonal antibodies do not mimic the complexity of immune sera or donor plasma, the ability of H5N1-specific monoclonal antibodies to neutralize previously observed binding between recombinant hemagglutinin and synthetic mimics of host glycan receptors was investigated as proof-of-concept. Also described are investigations into preparation techniques for the involved reagents for optimal binding results.

4.2.1 SPR Inhibition Assay Design

4.2.1.1 Reagents

The following reagent was obtained through the NIH Biodefense and Emerging Infections Research Resources Repository, NIAID, NIH: Monoclonal Anti-Influenza Virus H5 Hemagglutinin (HA) Protein (VN04-2), A/Vietnam/1203/04 (H5N1), (ascites, Mouse), NR-2728. Polyclonal anti-influenza virus H1 hemagglutinin (HA) protein, H1N1/Pan, (rabbit); polyclonal anti-influenza virus H5 hemagglutinin (HA) protein, A/Indonesia/5/05 (H5N1), (rabbit); and polyclonal anti-influenza virus HA2 H5 hemagglutinin (HA) protein, A/Vietnam/1203/04 (H5N1), (rabbit), were purchased from Immune Technology Corp. (New York, NY). Anti-influenza virus H3, A/Shandong/9/93 (H3N2), (mouse IgG1), was purchased from Prospec Protein Specialists (Rehovot, Israel). Mouse serum (ICR SCID) was purchased from Bioreclamation, Inc. (Liverpool, NY).

4.2.1.2 HA/glycan Neutralization by Monoclonal Antibody

H5 HA (Vietnam) at 140nM was incubated with a 1:2 serial dilution of anti-H5 monoclonal antibody (shown to be neutralizing for H5 HA in standard hemagglutination

inhibition assays) for 10 min at 25 °C and injected over the glycan chip surface to investigate the ability of the antibodies to neutralize the glycan/H5 binding. Concentrations of anti-H5 monoclonal antibody were 1:250, 1:500, 1:1000, 1:2000, and 1:4000. Binding was assessed by an increase in RU. After 25 min dissociation time, the glycan surface was regenerated with 60 s of 10 mM glycine pH 2.5 and 30 s of 50 mM NaOH at 100 µl/min.

4.2.1.3 Specificity Testing

The specificity of the assay was investigated using H1, anti-H1, H3, anti-H3, and glycans nonspecific for H5, 6'SLN (α2,6 binder), GD2 (α2,8 binder), and CT/Sda (α2,3 binder). H1 at 140 nM was preincubated with 1:2 serial dilution of anti-H1 or anti-H5 and injected over the same glycans. H5 at 140 nM was preincubated with 1:2 serial dilution of anti-H3 and injected over glycans GD2, 3'SLN, and 6'SLN to observe cross-protection. Testing for each dilution was performed in triplicate. The anti-H1 and anti-H3 antibodies were polyclonal preparations, and while this does not offer optimal comparison to the neutralizing activity of the monoclonal anti-H5, reagent availability for these different Influenza strains necessitated these comparisons for proof-of-concept. Also, the multiple-epitope recognition ability of a polyclonal population would better mimic the complexity of a natural patient plasma sample, and thus probing the cross-reactivity of these anti-H1 and anti-H3 polyclonal antibodies may in fact offer a more application-authentic evaluation.

4.2.2 Characterization Studies

4.2.2.1 Antibody Testing

An antibody that binds outside of the receptor binding domain was of interest for future application in the biosensor format. The ability of the anti-HA2 H5 polyclonal antibody to bind to the glycan/H5 precomplex was investigated. H5 at 140 nM was injected over the immobilized glycans for 10 min at 5 µl/min. After 1 min dissociation and no regeneration, a 1:2 serial dilution of anti-HA2 H5 monoclonal antibody was injected over the glycan/H5 complex for 5 min at 5 µl/min. After regeneration, the experiment was repeated with anti-H5 monoclonal antibody.

4.2.2.4 Serum Experiments

The complexity of biological samples was considered, with the ultimate goal of a FLUIGIV screening assay in mind. The neutralization experiment described in *4.2.1.2* was repeated with H5 at 140 nM prepared in mouse serum (ICR SCID) at 1% final concentration by volume. Background binding to glycans 3'SLex, CT/Sda, and 3'SLN and the blank cell was investigated using mouse serum (ICR SCID) at 0.5-10% in buffer.

4.2.2.5 Statistical Analysis

Each experiment was performed in triplicate to nullify the effect of equipment or user variation. The samples were double referenced, by subtracting either the blank fc1 or nonbinders CT/Sda, GD2, or 6'SLN from the binder results, as well as subtracting a buffer run to compensate for irrelevant machine fluctuations. The SA chips were assumed to have the same physical properties, and the glycans were assumed to be immobilized to saturation. The peak RU at the end of the injection cycle was taken as an indicator of binding. The effects of different HAs, glycans, anti-HA antibodies, and HA concentration

were assessed to calculate the lower detection limit and specificity of the SPR-based assay. The differences between the means of each sample were calculated and analyzed based on single factor analysis of variance (ANOVA) to a significance of 95% ($\alpha = 0.05$) (Tables A-1, A-2), using SAS software.

4.3 OBJECTIVE 3

H5N1—Targeted Biosensor Design

This objective is aimed towards the development of an electrochemical biosensor for the detection of the same glycan/hemagglutinin binding described in *4.1*.

4.3.1 Biosensor Design

4.3.1.1 Reagents and Chemicals

The biotinylated carbohydrate compounds 3'SLex (B157), 3'SLN (B84), GT3 (B108), and 6'SLN (B87) were provided by the Carbohydrate Synthesis/Protein Expression Core of The Consortium for Functional Glycomics funded by the National Institute of General Medical Sciences grant GM62116. The following reagent was obtained through the NIH Biodefense and Emerging Infections Research Resources Repository, NIAID, NIH: H5 Hemagglutinin (HA) Protein from Influenza Virus, A/Vietnam/1203/04 (H5N1), Recombinant from baculovirus, NR-10510 (Source A H5, referred to as H5). The following reagent was obtained through the NIH Biodefense and Emerging Infections Research Resources Repository, NIAID, NIH: Monoclonal Anti-Influenza Virus H5 Hemagglutinin (HA) Protein (VN04-2), A/Vietnam/1203/04 (H5N1), (ascites, Mouse), NR-2728. 6xHis tagged H5 hemagglutinin (HA) protein from 293 cell culture, A/Vietnam/1203/04 (H5N1) (Source B H5, referred to as H5*); C-terminal 6xHis tagged H1 hemagglutinin (HA) protein from 293 cell culture, A/South Carolina/1/18 (H1N1); and polyclonal anti-influenza virus H1 hemagglutinin (HA) protein, H1N1/Pan, (rabbit), were purchased from Immune Technology Corp. (New York, NY).

All solutions and buffers used in the biosensor study were prepared in de-ionized (DI) water (from Millipore Direct-Q system). Iron (III) oxide (γ-Fe2O3) nanopowder,

aniline monomer, ammonium persulfate, hydrochloric acid (HCl), methanol, diethyl ether, hydrogen tetrachloroaurate (III) trihydrate, sodium citrate dehydrate, glutaraldehyde, Polysorbate-20 (Tween-20), phosphate buffered saline (PBS), trizma base, casein, sodium phosphate (dibasic and monobasic), and streptavidin were purchased from Sigma-Aldrich (St. Louis, MO). Solutions were prepared as follows: PBS buffer (10 mM PBS, pH 7.4), wash buffer (10 mM PBS, pH 7.4, with 0.05% Tween-20), phosphate buffer (100 mM phosphate buffer, pH 7.4), casein blocking buffer (100 mM Tris–HCl buffer, pH 7.6, with 0.1% w/v casein), and glycine blocking buffer (67 μM glycine in 10 mM PBS, pH 7.4). HBS-P buffer, 10 mM glycine pH 2.5, and 50 mM NaOH were purchased from GE Healthcare (Piscataway, NJ). Avidin/Biotin blocking kit was purchased from Vector Laboratories, Inc. (Burlingame, CA). Mouse serum (ICR SCID) was purchased from Bioreclamation, Inc. (Liverpool, NY).

4.3.1.2 Methodology of Supporting SPR Assay

Glycan partners were chosen for the HAs of interest based on widely accepted HA specificities, as previously investigated using glycan microarrays (Blixt *et al.*, 2004; Stevens *et al.*, 2006). Biotinylated glycans were diluted to 1 μM in Biacore HBS-P buffer and 8 μl were injected over a Biacore Streptavidin (SA) chip at 10 μl/min. Glycans were immobilized to saturation at approximately 300 resonance units (RU). H5 HA (Vietnam) at 140 nM was incubated with a serial dilution of anti-H5 monoclonal antibody (shown to be neutralizing for H5 HA in standard hemagglutination inhibition assays) for 10 min at 25 °C and injected over the glycan chip surface to investigate the ability of the antibodies to neutralize the glycan/H5 binding. Binding was assessed by an increase in RU. After 25 min dissociation time, the glycan surface was regenerated with 60 s of 10 mM glycine pH

2.5 and 18 s of 50 mM NaOH at 100 µl/min. Anti-H5 monoclonal antibody binding to the glycan/H5 complex was also investigated. H5 at 140 nM was injected for 10 min at 5 µl/min. After 1 min dissociation and no regeneration, anti-H5 monoclonal antibody was injected over the glycan/H5 complex for 5 min at 5 µl/min.

4.3.1.3 Biosensor Architecture

The platform for electrochemical detection of the HA of interest was a screen printed carbon electrode (SPCE) comprised of three electrodes, including a working, common reference, and counter electrode, screen printed on low-cost polyester backing (Gwent Group, UK). The overall dimension of the sensor chip was 22 x 12 mm, with a 4mm diameter working electrode surrounded by a 1.5 mm wide, partially circular (270°) common reference and counter electrode. The working electrode was composed of carbon and the common reference and counter electrode of silver/silver chloride (Ag/AgCl). Manufacturer's specifications listed the resistance of the carbon as 50 Ohms at 12 microns and the resistance of the silver as 320 mOhms at 25 microns.

4.3.1.4 Gold Nanoparticle Synthesis

Application of the carbon-based glycans directly onto the screen-printed carbon electrode would result in an insulating device. To enhance the electron transducer, thus amplifying response current and improving detection limits, gold nanoparticles (AuNPs) were applied to the SPCEs (Daniel and Astruc, 2004; Lin *et al.*, 2008; Willner *et al.*, 2007). AuNPs were synthesized according to a published procedure and their size, spectroscopic properties, and magnetic profiles have been previously characterized (Hill and Mirkin, 2006; Zhang *et al.*, 2009). The referenced synthesis procedure required hydrogen tetrachloroaurate (III) trihydrate aqueous solution (1mM, 50 mL) to be stirred

while heated. Vigorous reflux was achieved, followed by titration with 5 mL of 38.8 mM sodium citrate. The solution shifted from yellow to the deep red characteristic of the AuNPs.

4.3.2 Electrically Active Polyaniline Coated Magnetic Nanoparticles

4.3.2.1 EAM Synthesis

Aniline monomer was polymerized around gamma iron (III) oxide (γ-Fe2O3) cores to obtain magnetic/polyaniline core/shell (c/s) nanoparticles (Sharma *et al.*, 2005). Commercially manufactured γ-Fe2O3 nanoparticles were sonicated and dispersed in 50 ml of 1 M HCl, 10 ml deionized (DI) water, and 0.4 ml aniline monomer at 0 °C for 1 h. The γ-Fe2O3 : monomer weight ratio was fixed at 1:0.6. 1 g ammonium persulfate in 20 ml DI water was added as oxidant while the mixture was stirred at 0 °C. As electrically-active polyaniline, typically green, was formed over the γ-Fe2O3 nanoparticles, typically brown, the color of the solution visibly transitioned from rust brown to dark green. The reaction proceeded for 4 h with continuous stirring at 0 °C. The solution was filtered, washed with 1 M HCl, 10% methanol, and diethyl ether, and dried for 18 h. The resulting green solid was ground into fine powder and stored in a vacuum desiccator.

4.3.2.2 EAM Nanoparticle Characterization

The electrically-active magnetic/polyaniline c/s NPs have been previously characterized in terms of structure, size, magnetization, and conductivity (Pal *et al.*, 2008a; Pal and Alocilja, 2009). Magnetic characterization and room temperature hysteresis measurements of the EAMs were performed by Pal and Alocilja (2009) using a superconducting quantum interference device (Quantum Design MPMS SQUID). A magnetic field cycling range of + 20 kOe to -20 kOe at 300 K constant temperature was

used to measure M-H hysteresis loops. The effect of polyaniline on the saturation magnetization (Ms) values of the EAMs were calculated. Super paramagnetic behavior was investigated by calculating coercivity (Hc) and retentivity (MR) of the EAMs. Blocking temperatures of the EAMs were also investigated using zero field cooled-field cooled (ZFC-FC) measurements from 5 K to 300 K temperature range and 100 Oe applied magnetic field.

The solid form of the EAMs was evaluated for electrical conductivity. A hydraulic press (Fisher Scientific, NJ) applied 10,000 psi to compress approximately 0.25 grams of sample into 1.5-2 mm thick pellets. A Four Point Probe (Lucas/Signaton Corporation, Pro4, CA) then measured room temperature electrical conductivity (Pal and Alocilja, 2009).

4.3.2.3 EAM Immunofunctionalization

EAM nanoparticles were immunofunctionalized with either anti-H5 monoclonal antibody IgG2 or anti-H1 polyclonal antibody. Desiccated EAM polyaniline nanoparticles were dissolved in 100 mM phosphate buffer (pH 7.4) to obtain a concentration of 10 mg/ml, and sonicated for 15 min. The EAM polyaniline nanoparticles were then conjugated with anti-H5 monoclonal antibodies by direct physical adsorption as previously described and confirmed by Pal and Alocilja (2009). Anti-H5 monoclonal antibody IgG2 (mouse ascites fluid) or anti-H1 polyclonal antibody (rabbit) was added to the EAM polyaniline nanoparticles to obtain an antibody:EAM ratio of 1:10 by volume. The solution was incubated for 1 h at 25 °C in a rotational hybridization oven (Amerex Instruments, Inc., Lafayette, CA). Following adsorption of antibody onto the EAM nanoparticles, the immunofunctionalized nanoparticles were magnetically separated using

a FlexiMag Magnetic Separator (Spherotech, Inc., Lake Forest, IL) to remove any unbound antibody in the supernatant. The anti-HA—EAM complexes were washed twice with blocking buffer consisting of 100 mM tris–HCl buffer (pH 7.6) with 0.1% (w/v) casein with magnetically separated supernatant discarded each time. The anti-HA—EAM complexes were then resuspended in 100 mM phosphate buffer (pH 7.4). The anti-HA—EAM complexes were prepared on the day of testing and stored at 4 °C until use.

4.3.2.4 EAM Structural Characterization

The structural morphologies of the EAMs and immunofunctionalized EAMs were analyzed using a transmission electron microscope (TEM, Japan Electron Optics Laboratories, JEOL 100CX II). Selected area electron diffraction performed by the 200kV JEOL 2200 field emission TEM was used to study the crystalline nature of the EAMs.

4.3.2.5 Spectral Analysis

Pal and Alocilja (2009) previously analyzed the UV-visible spectra of the EAMs using a UV-VIS-NIR scanning spectrophotometer (UV-3101PC, Shimadzu, Kyoto, Japan). EAMs at 10 mg/ml were dispersed in de-ionized water by sonication for 10 min. the nanoparticle suspension was transferred to a quartz cuvette and the sample was scanned with a 300 to 1000 nm wavelength range using a step size of 1 nm to determine absorbance.

4.3.3 Biosensor Fabrication

4.3.3.1 SPCE Modification

SPCE chips were prepared by removing the overlaying mesh and foam (Gwent, Inc., UK). Each chip was washed with 2 ml sterile DI water and air dried for 15 min. As

described in Lin *et al.* (2008), 25 µl of 2.5 mM glutaraldehyde solution as crosslinker were applied to the working area and incubated at 4 °C for 1 h. The SPCEs were then washed with 2 ml DI water and air dried at 25 °C for 15 min. 25 µl of AuNP solution were applied to the glutaraldehyde-treated working electrode and incubated at 4 °C for 1 h. The SPCEs were then washed with 2 ml DI water and air dried at 25 °C for 15 min. 20 µl of streptavidin at 1 µg/ml were applied to the working area and dried at 4 °C for 2 h or overnight.

4.3.4 Preconcentration Preparation Technique

4.3.4.1 Sample Preparation

Glycans were prepared at 3x desired concentration in 0.01 M PBS. HAs were prepared at 3x desired concentration in 0.01 M PBS with 10% mouse serum (ICR SCID) by volume. 30 µl each of glycan and HA were incubated for 15 min at 25 degrees C in a rotational hybridization oven. 30 µl of the appropriate anti-HA—EAM complex was then added to the glycan/HA solution and incubated for 20 min at 25 degrees C in a rotational hybridization oven. The glycan/HA/anti-HA—EAM complexes were magnetically separated and washed twice with 0.01 M PBS containing 0.05% Tween-20 for 5 minutes and resuspended in 0.01 M PBS.

4.3.4.2 Capture Experiments

The SPCE chips prepared with glutaraldehyde, AuNPs, and streptavidin were then treated with the biotinylated glycan/HA/anti-HA—EAM complex. 90 µl of the solution was applied to the treated SPCE and incubated at 25 degrees C for 15 min. The SPCE was washed with 2 ml DI water and air dried at 25 degrees C for 15 min (Figure 13).

4.3.5 Stepwise Preparation Technique

4.3.5.1 Sample Preparation and Capture Experiments

25 µl of the desired glycan concentration were added to the working area of the glutaraldehyde, AuNPs, and streptavidin treated electrode and allowed to incubate at 25 degrees C for 30 min. Excess was rinsed with 2 ml DI water and air dried at 25 degrees C for 15 min. Available sites were blocked with sequential additions of 25 µl Avidin D and biotin solutions for 30 min each, with DI water rinse and air dry after each. 25 µl of the desired H5 concentration were added, incubated at 25 degrees C for 30 min, rinsed with 2 ml DI water, and air dried at 25 degrees C for 15 min. 100 µl of anti-HA—EAM complex solution were added to the electrode, incubated at 25 degrees C for 15 min, rinsed with 2 ml DI water, and air dried at 25 degrees C for 15 min (Figure 12).

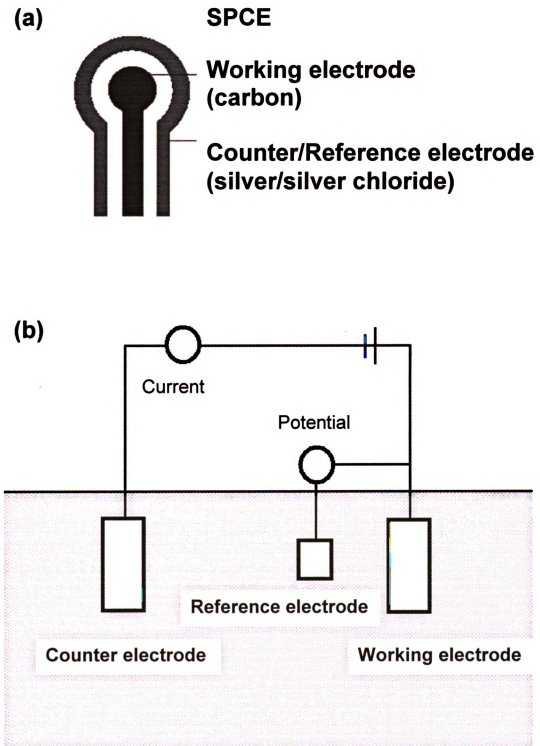

Figure 11. Testing schematic. (a) Screen-printed carbon electrode (SPCE) consisting of two electrodes: carbon working electrode and silver/silver chloride counter/reference electrode, (b) schematic of the three electrode voltammetry system (adapted and modified from Bard and Faulkner, 2000).

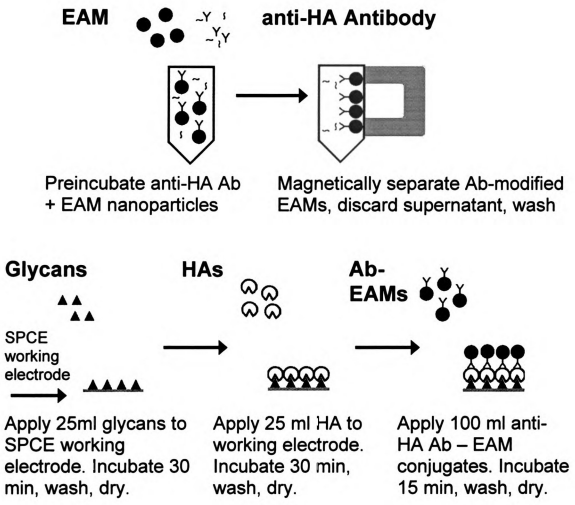

Figure 12. Testing schematic. Stepwise preparation method.

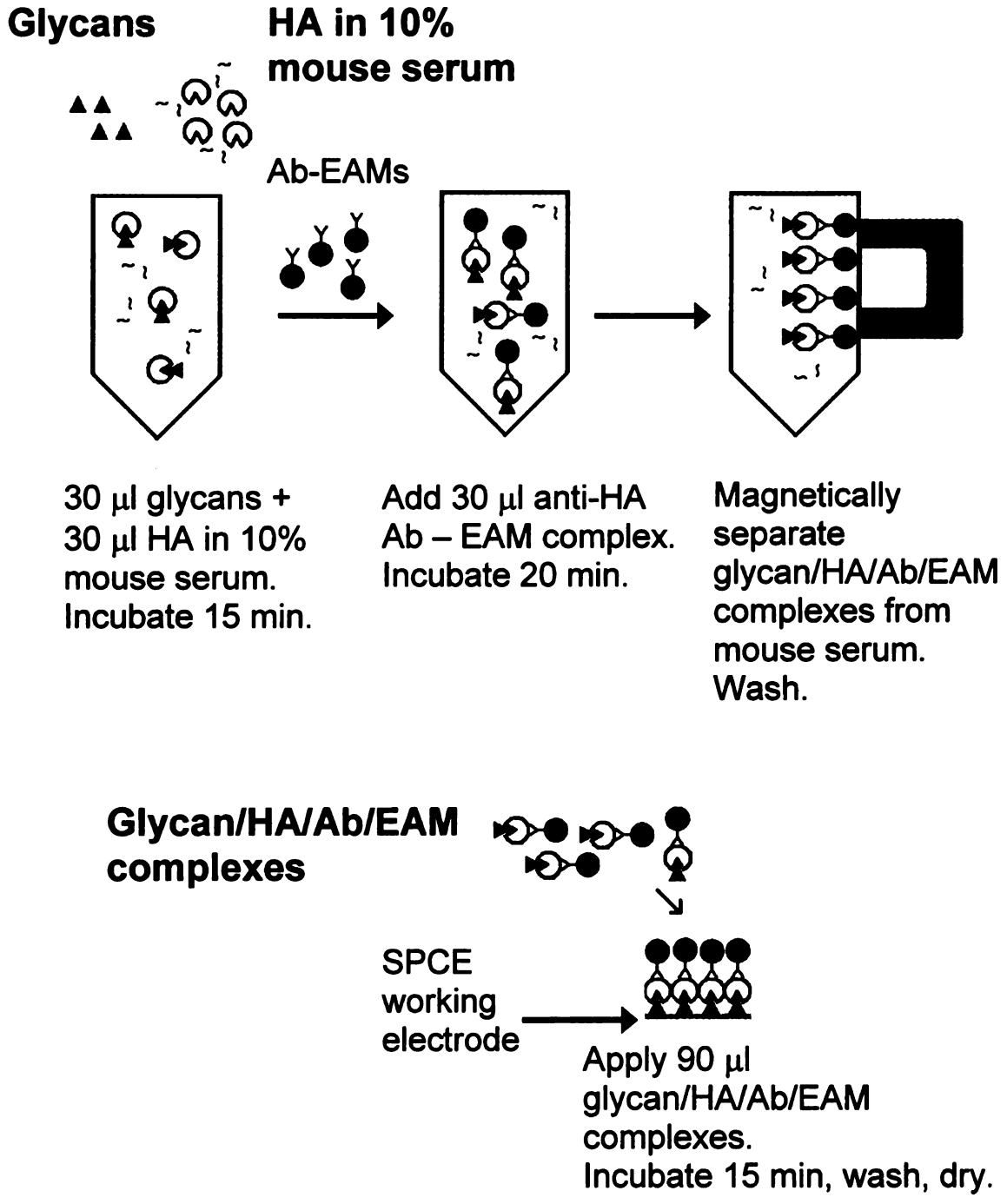

Figure 13. Testing schematic. Preconcentration preparation method.

4.3.6 Biosensor Testing

4.3.6.1 Testing Apparatus

Cyclic voltammetric measurements were performed using a 263A potentiostat/galvanostat (Princeton Applied Research, MA, USA) connected to a personal computer. Data collection and analysis were controlled through the PowerSuite electrochemical software operating system (Princeton Applied Research, Wellesley, MA). SPCE chips purchased from Gwent Inc. (UK) are shown in Figure 11.

4.3.6.2 Detection and Data Analysis

100 µl of 0.1 M HCl solution were applied to cover the entire SPCE electrode area and allowed to incubate for 5 min. The SPCE electrodes were connected to the potentiostat and cyclic voltammetry was performed at a scan rate of 55 mV/sec and a cyclic scan range of -0.4 to 1 V, with four consecutive 2 min scans recorded (Figure 14). Previous experimentation indicated that the third scan produced the most pronounced current flow differences for different samples and was chosen for analysis. For each experiment, including positive and negative controls and blanks, three replications were performed. The samples were calibrated against a negative control, also repeated in triplicate, which consisted of the anti-HA—EAM application step alone. The total charge transferred, ΔQ, was computed from the cyclic voltammogram as the integral of current, according to the relationship

$$I = \Delta Q/\Delta t \qquad (6)$$

where, I = current (A), ΔQ = charge transferred (C), and Δt = time elapsed (s) (Kuznetsov, 1995). The ΔQ values described in this paper were calculated from the current and time interval data generated by the potentiostat. Standard deviations and

mean ΔQ values of the third scans for the triplicate data sets were calculated.

The presence of the target is indicated by an increase in total charge transferred into the SPCE surface. Target HA labeled with the immunofunctionalized EAMs were captured on the SPCE surface, and the EAMs, consisting of conductive polyaniline synthesized around a magnetic γ-Fe2O3 core, were made electrically active by acid doping. An applied external cyclic potential causes polyaniline to switch redox states, transferring charge into the SPCE surface. Higher current recorded by the potentiostat indicates more target in the sample (Figure 14).

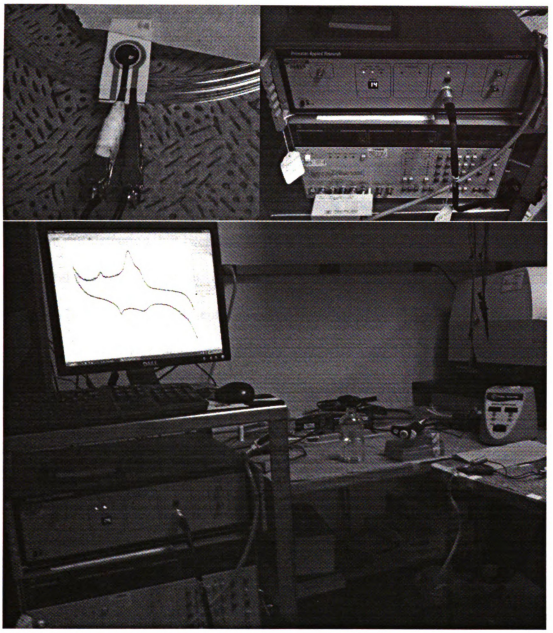

Figure 14. SPCE and potentiostat setup.

4.3.6.3 Sensitivity and Specificity Testing

The lowest detection limit of the biosensor for H5 was investigated. The prepared biosensors were tested using three samples at 1:2 dilution in 0.01 M PBS to obtain H5 at 1.4 μM, 700 nM, and 360 nM. Testing for each dilution was performed in triplicate. Anti-HA—EAM complexes without glycan or HA were tested as the control. The lowest dilution of H5 that produced a signal distinguishable from the control was taken as the sensitivity of detection, but because our H5 dilution series was limited to three samples by reagent availability, this sensitivity is not a conclusive analytical sensitivity, but the detection limit for the experimental concentrations tested here.

The specificity of the biosensor was investigated using H1, anti-H1, and glycans nonspecific for H5, GT3 (α2,8 binder), 6'SLN (α2,6 binder), and 6'S-Di-LN (α2,6 binder). The H1 was prepared at 1.4 μM in 0.01M PBS, the non-H5 binding glycans were prepared at 100 μM, and the EAMs were immunofunctionalized with anti-H1 at 1:10 using the method described in *2.6*.

4.3.6.4 Complex Matrix Testing

The complexity of biological samples was considered, as the ultimate application of the biosensor as an in-field detection system would require testing of blood or sputum samples. In the preconcentration method, the HA samples were prepared to consist of 10% mouse serum. After complexing the glycan/HA/anti-HA—EAM, the magnetic separation and washing technique was investigated for its ability to specifically isolate the target HA from a complex serum matrix.

4.3.6.5 Statistical Analysis

Each sample preparation was tested in triplicate with the biosensors to account for the effect of equipment or user variation. The prepared biosensors were assumed to have the same physical properties. For each experiment, the cyclic voltammetry (CV) data were obtained as a curve of current versus potential (I vs. E), including 1020 points for each scan cycle from -0.4 to 1 V. The mean and standard deviations of the ΔQ values were calculated for each sample preparation, including negative controls and blanks. The differences between the means were calculated and analyzed based on single factor analysis of variance (ANOVA) to a significance of 95% ($\alpha = 0.05$) (Tables A-3-A-5), using SAS software. The effects of different HAs, glycans, anti-HA antibodies, and HA concentration were assessed to calculate the lower detection limit of the biosensor as well as the biosensor specificity. Oxidation (anodic) and reduction (cathodic) peak currents were also determined from the CV data, which consisted of an oxidation reaction (first half) and a reduction reaction (second half). The peak currents were determined at the corresponding peak potentials for each experimental run.

4.4 OBJECTIVE 4

Biosensor to Distinguish α2,3 v. α2,6 Receptor Binding

This objective is aimed towards modification of the previously described electrochemical biosensor (Objective 3) to detect α2,6 receptor specificity as an indicator of pandemic potential. The ability to distinguish between α2,3 and α2,6 linked receptors was also important for application in the event that a historically avian (α2,3) FLUAV strain acquires human (α2,6) transmissibility.

4.4.1 Biosensor Design

4.4.1.1 Reagents and Chemicals

The biotinylated carbohydrate compounds 3'S-Di-LN (B178) and 6'S-Di-LN (B179) were provided by the Carbohydrate Synthesis/Protein Expression Core of The Consortium for Functional Glycomics funded by the National Institute of General Medical Sciences grant GM62116. The following reagent was obtained through the NIH Biodefense and Emerging Infections Research Resources Repository, NIAID, NIH: H5 Hemagglutinin (HA) Protein from Influenza Virus, A/Vietnam/1203/04 (H5N1), Recombinant from baculovirus, NR-10510 (Source A H5, referred to as H5). The following reagent was obtained through the NIH Biodefense and Emerging Infections Research Resources Repository, NIAID, NIH: Monoclonal Anti-Influenza Virus H5 Hemagglutinin (HA) Protein (VN04-2), A/Vietnam/1203/04 (H5N1), (ascites, Mouse), NR-2728. 6xHis tagged H5 hemagglutinin (HA) protein from 293 cell culture, A/Vietnam/1203/04 (H5N1) (Source B H5, referred to as H5*); C-terminal 6xHis tagged H1 hemagglutinin (HA) protein from 293 cell culture, A/South Carolina/1/18 (H1N1); and polyclonal anti-influenza virus H1 hemagglutinin (HA) protein, H1N1/Pan, (rabbit),

were purchased from Immune Technology Corp. (New York, NY). All solutions and buffers used in the biosensor study were obtained and prepared as in *4.3.1.1*.

4.4.1.2 Biosensor Fabrication

The gold nanoparticles were prepared as in *4.3.1.4*. The EAMs were synthesized, immunofunctionalized with anti-H5 or anti-H1 antibodies, and characterized as described in *4.3.2.1-4.3.2.5*. The SPCEs described in 4.3.1.3 were treated as in 4.3.3.1.

4.4.2 Biosensor Testing

4.4.2.1 Sample Preparation

The preconcentration preparation method was followed. Glycans were prepared at 3x desired concentration in 0.01 M PBS. HAs were prepared at 3x desired concentration in 0.01 M PBS with 10% mouse serum (ICR SCID) by volume. 30 µl each of glycan and HA were incubated for 15 min at 25 degrees C in a rotational hybridization oven. 30 µl of the appropriate anti-HA—EAM complex was then added to the glycan/HA solution and incubated for 20 min at 25 degrees C in a rotational hybridization oven. The glycan/HA/anti-HA—EAM complexes were magnetically separated and washed twice with 0.01 M PBS containing 0.05% Tween-20 for 5 minutes and resuspended in 0.01 M PBS.

4.4.2.2 Capture Experiments

The SPCE chips prepared with glutaraldehyde, AuNPs, and streptavidin were then treated with the biotinylated glycan/HA/anti-HA—EAM complex. 90 µl of the solution was applied to the treated SPCE and incubated at 25 degrees C for 15 min. The SPCE was washed with 2 ml DI water and air dried at 25 degrees C for 15 min (Figure 13).

4.4.2.3 Detection and Data Analysis

Cyclic voltammetry was performed on the treated SPCEs using the potentiostat as described in *4.3.6.2*. For each experiment, including positive and negative controls and blanks, three replications were performed. The samples were calibrated against a negative control, also repeated in triplicate, which consisted of the anti-HA—EAM application step alone. The ΔQ values were calculated from the current and time interval data generated by the potentiostat. Standard deviations and mean ΔQ values of the third scans for the triplicate data sets were calculated.

The presence of the target is indicated by an increase in total charge transferred across the electrodes. Target HA labeled with the immunofunctionalized EAMs were captured on the SPCE surface, and the EAMs, consisting of conductive polyaniline synthesized around a magnetic γ-Fe2O3 core, formed an electrical circuit between the silver electrodes, with current recorded by the potentiostat.

4.4.2.4 Sensitivity and Specificity Testing

The lowest detection limit of the biosensor for H5 and H1 was investigated. The prepared biosensors were tested using two samples at 1:2 dilution in 0.01 M PBS to obtain H5 at 1.4 μM and 700 nM. Testing for each dilution was performed in triplicate. Anti-HA—EAM complexes without glycan or HA were tested as the control. The lowest dilution of H5 or H1 that produced a signal distinguishable from the control was taken as the sensitivity of detection. The H5-targeted biosensor required H5 incubation with α2,3-linked glycan 3'S-Di-LN and EAM immunofunctionalization with anti-H5, while the H1-targeted biosensor required H1 incubation with α2,6-linked glycan 6'S-Di-LN and EAM immunofunctionalization with anti-H1.

The specificity of the biosensor for H5 was investigated using H1, anti-H1, and α2,6-linked glycan 6'S-Di-LN. The specificity of the biosensor for H1 was investigated using H5, anti-H5, and α2,3-linked glycan 3'S-Di-LN.

The specificity of the biosensor was investigated using H1, anti-H1, and glycans nonspecific for H5, GT3 (α2,8 binder), 6'SLN (α2,6 binder), and 6'S-Di-LN (α2,6 binder). The H1 was prepared at 1.4 μM in 0.01 M PBS, the non-H5 binding glycans were prepared at 100 μM, and the EAMs were immunofunctionalized with anti-H1 at 1:10 using the method described in *2.6.*

4.4.2.5 Complex Matrix Testing

The complexity of biological samples such as blood or respiratory samples was considered. The HA samples were prepared to consist of 10% mouse serum. After complexing the glycan/HA/anti-HA—EAM, the magnetic separation and washing technique was investigated for its ability to specifically isolate the target HA from a complex serum matrix.

4.4.2.6 Statistical Analysis

Each sample preparation was tested in triplicate with the biosensors to nullify the effect of equipment or user variation. The prepared biosensors were assumed to have the same physical properties. For each experiment, the cyclic voltammetry (CV) data was obtained as a curve of current versus potential (I vs. E), including 1020 points for each scan cycle from -0.4 to 1 V. The mean and standard deviations of the ΔQ values were calculated for each sample preparation, including negative controls and blanks. The differences between the means were calculated and analyzed based on single factor analysis of variance (ANOVA) to a significance of 95% ($\alpha = 0.05$) (Table A-3-A-5),

using SAS software. The effects of different HAs, glycans, anti-HA antibodies, and HA concentration were assessed to calculate the lower detection limit of the biosensor as well as the biosensor specificity. Oxidation (anodic) and reduction (cathodic) peak currents were also determined from the CV data, which consisted of an oxidation reaction (first half) and a reduction reaction (second half). The peak currents were determined at the corresponding peak potentials for each experimental run.

CHAPTER 5: RESULTS AND DISCUSSION

5.1 OBJECTIVE 1

Surface Plasmon Resonance—based Binding Assay

5.1.1 SPR Binding Assay Design

5.1.1.1 Glycan Immobilization and Chip Stability

Glycans were chosen based on their predicted binding to the HAs of interest. On Chip 1, H5 is predicted to bind 3'SLex and 3'SLN but not CT/Sda. On Chip 3, H5 is predicted to bind 3'SLN but not GD2 or 6'SLN. 3'SLN and 6'SLN were chosen for comparison because their sialylated receptors are similar in structure except for the α2,3 versus α2,6 linkage. The samples were double referenced, by subtracting either the blank fc1 or nonbinder CT/Sda from the binder results, as well as subtracting a buffer run to compensate for irrelevant machine fluctuations. Chips 1 and 3, immobilized with glycans to saturation, were found to be stable and reusable over a 3 month period, exhibiting repeatable binding to H5. The regeneration reagents, glycine 10 mM pH 2.5 and 50 mM NaOH, reliably removed bound HA from the surface, without interfering with the streptavidin/biotin linkage or damaging the biological activity of the glycan receptors. The minimum immobilization level on chip 2 did not provide a reliable RU level, with fluctuations indistinguishable from background noise. This low glycan immobilization did not yield repeatable binding with H5.

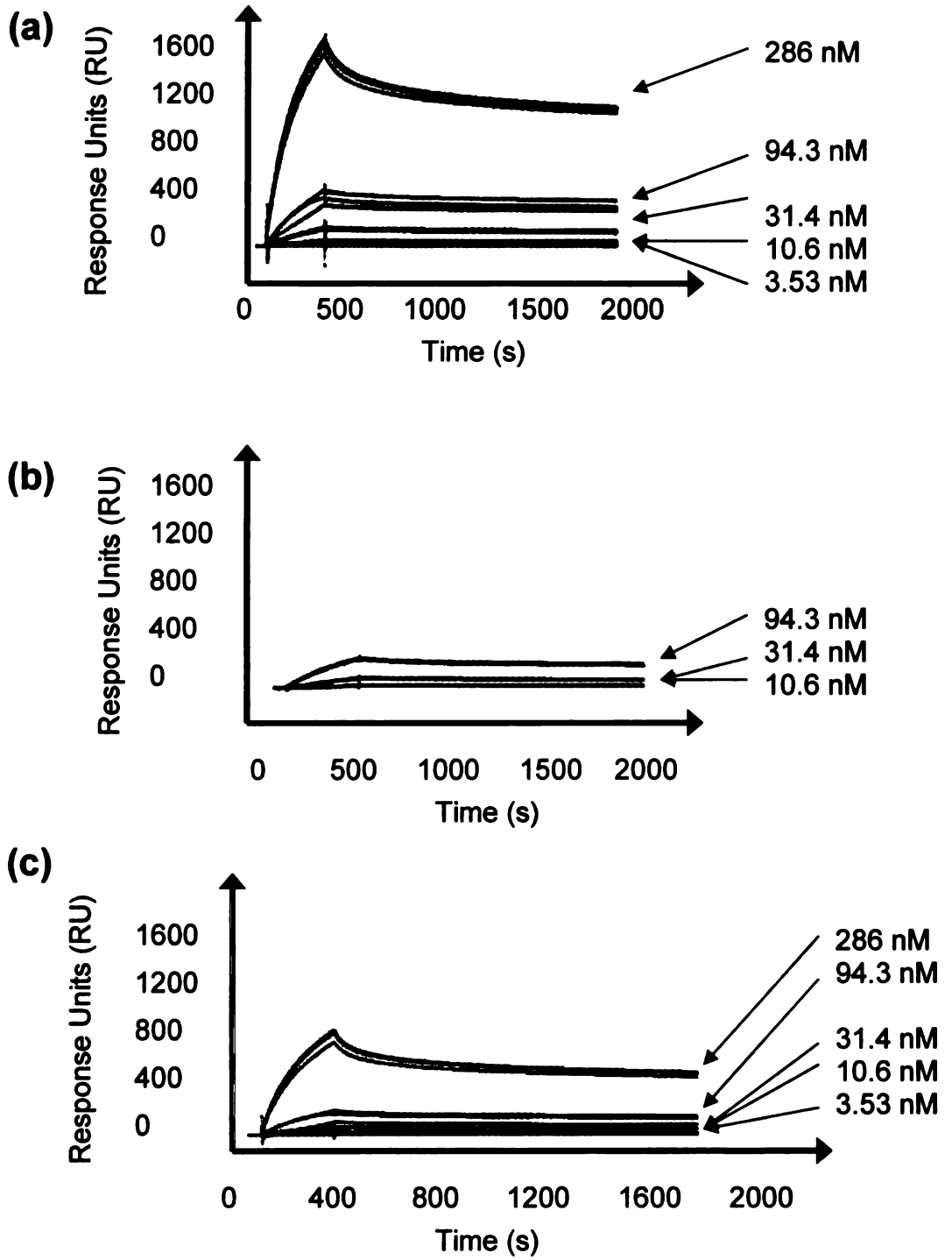

Figure 15. Glycan/H5 binding experiments. Comparing glycans and regenerations. (a) Triplicates of H5 dilutions binding to 3'SLN; Regeneration: 60 s of 10mM glycine pH 2.5 and 30 s of 50mM NaOH at 100 μl/min, (b) triplicates of H5 dilutions binding to 3'SLN; Regeneration: 60 s of 10mM glycine pH 2.5 and 18 s of 50mM NaOH at 100 μl/min, and (c) triplicates of H5 dilutions binding to 3' SLex; Regeneration: 60 s of 10mM glycine pH 2.5 and 30 s of 50mM NaOH at 100 μl/min.

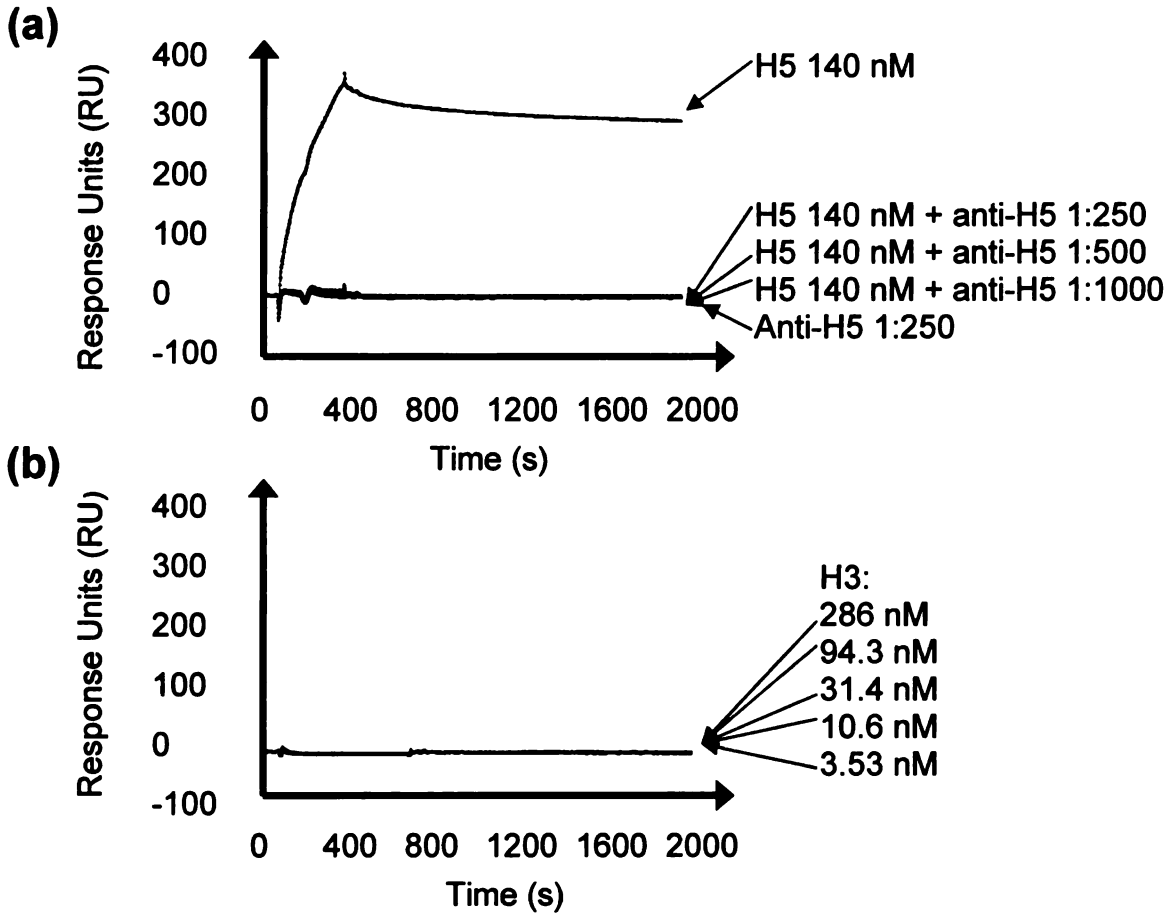

Figure 16. H5 Indonesia and H3 Wyoming binding to 3'SLN. Single replicate shown for clarity. (a) H5 (A/Vietnam/1203/04) 140nM; H5 (A/Indonesia5/05) 140nM; H5 Indonesia 140nM + anti-H5 Indonesia 1:250, 1:500, and 1:1000; anti-H5 Indonesia 1:250 and (b) H3 (A/Wyoming/3/03) at 286nM, 94.3nM, 31.4nM, 10.6nM, and 3.53nM.

5.1.2 SPR Binding Between Glycan Receptors and Hemagglutinin

5.1.2.1 Confirmation of H5 Recognition

SPR analysis demonstrated a high avidity, specific binding between H5-specific α2,3-linked glycan receptors and recombinant H5 HA (A/Vietnam/1203/04). The SPR binding curves were not fit to a model because the binding of the aggregated H5 yielded an interaction that was not 1:1. The glycan/H5 binding also did not reach equilibrium.

The aggregated nature of the H5 would result in many available receptor binding domains on one complex, and could lead to binding and rebinding of the HA to the immobilized glycans as the HA "walks" along the surface. The kinetics and binding constants are thus not explored here, in favor of yes/no binding results. The H5 molarity range from 3.53-286 nM exhibited a dose response in which response level could be correlated with H5 concentration (Figure 15). H5 at 3.53 nM was indistinguishable from the negative controls as well as the blanks, and H5 at 10.6 nM was thus taken as the lower limit of detection and the sensitivity of the system. Although both are H5-specific, H5 showed higher avidity binding to 3'SLN than 3'SLex (Figure 15). Both of these glycans offered the same lower limit of detection.

5.1.2.2 Chip Regeneration

The dilution series using the different regeneration schemes were compared, and triplicates revealed better repeatability when the surface was regenerated with 60 s of 10 mM glycine pH 2.5 and 18 s of 50 mM NaOH at 100 μl/min, as compared to the 30 s NaOH pulse (Figure 15). The 30 s NaOH pulse may have begun to strip the immobilized glycan surface, preventing a repeatable level of HA to be bound.

5.1.2.3 Specificity Testing

The specificity of the H5-targeted system was investigated using H1, anti-H1, H3, anti-H3, and H5-nonspecific glycans. Binding of H1 alone and anti-H1 alone to the glycans GD2, 6'SLN, and 3'SLN revealed negligible binding that was not statistically different from buffer alone. Binding of preincubated H1 and anti-H1 also revealed negligible binding to all glycans, indicating that despite the polyclonal nature of the anti-H1 antibodies, there is little cross-reactivity between the H1-based negative controls and

the H5-targeted SPR assay. Recombinant H3 HA (A/Wyoming/3/03) prepared at the same concentration range showed no cross-reactivity with the H5-specific glycans, indicating that H3 can be used as an appropriate negative control for the H5 detection system (Figure 16). The H5-nonspecific glycans, CT/Sda, GD2, and 6'SLN were assessed for their binding to H5, and this was seen to be within the statistical range of a buffer injection on the H5-specific glycan, or within the range of H5 binding to the blank flow cell. H5 thus was shown to bind α2,3 receptors with higher avidity than α2,6 or α2,8 receptors, and we can thus conclude that the SPR assay offers H5-specificity based on sialic acid receptor preference.

5.1.2.4 Clade Specificity

Recombinant H5 HA (A/Indonesia/5/05) was found to show negligible binding to the H5-specific glycans that was not statistically different from the H3 negative controls or the buffer injections (Figure 16). This may indicate that the immobilized glycans are specific for the Vietnam H5N1 strain from clade 1 but not for the Indonesia H5N1 strain from clade 2.1.3 (WHO, 2009). The H5-specific glycans may be clade-specific. Alternatively, the predicted composition of the Vietnam H5N1 strain as a large aggregate may allow for stronger binding to the glycans, whereas an H5 preparation composed mainly of monomers and trimers may offer lower affinity binding.

5.1.2.5 HA Receptor Binding Domain Binding Assessment

The receptor binding domain on HA is located within the HA1 sequence, and is responsible for binding to the host glycan receptor. We investigated the binding of the HA1 segment of H5 and H3 to glycans 3'SLex, CT/Sda, and 3'SLN. As compared to the binding between glycans and recombinant H5, HA1 H5 showed negligible binding to H5-

specific and nonspecific glycans (Figure 17). HA1 H5 binding was not statistically different from the negative controls or blanks. The HA1 H3 showed slight cross-reactivity with H5-specific 3'SLex and 3'SLN, generating 2-5% of the signal produced by corresponding concentrations of H5 (Figure 17). This may be attributable to slight overlap of glycan specificities. In an attempt to improve glycan/HA1 H5 binding, the binding experiment was repeated with running and sample buffers of HBS-P with 0.1% BSA and 0.5% glycerol. HA1 H5 and HA1 H3 were compared to H5 140 nM and a glycerol concentration curve from 0-1%. Under these conditions, HA1 H5 did not bind any glycans, and the slight binding of HA1 H3 was also reduced to a similar level that is statistically similar to the negative controls and blanks.

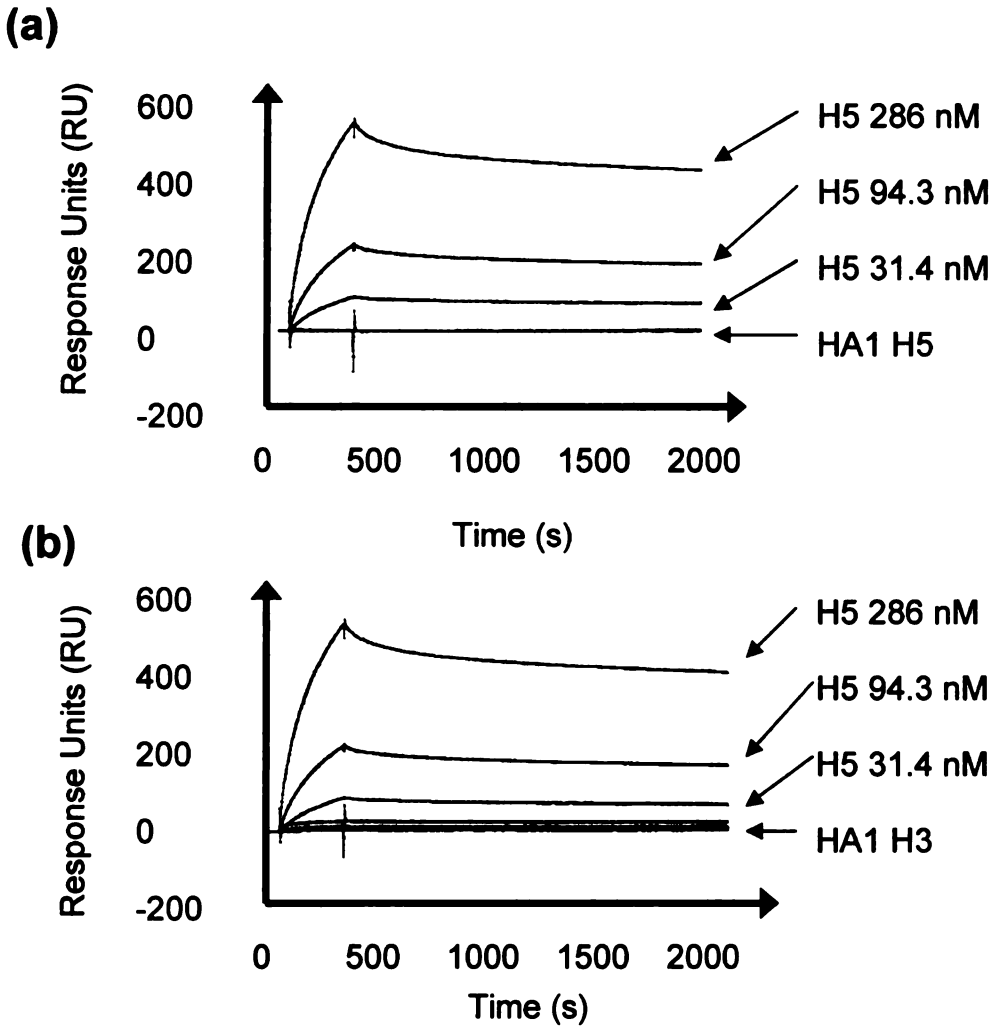

Figure 17. (a) H5 at 286nM, 94.3nM, 31.4nM; HA1 H5 at 286nM, 94.3nM, 31.4nM, and (b) H5 at 286nM, 94.3nM, 31.4nM; HA1 H3 at 286nM, 94.3nM, 31.4nM.

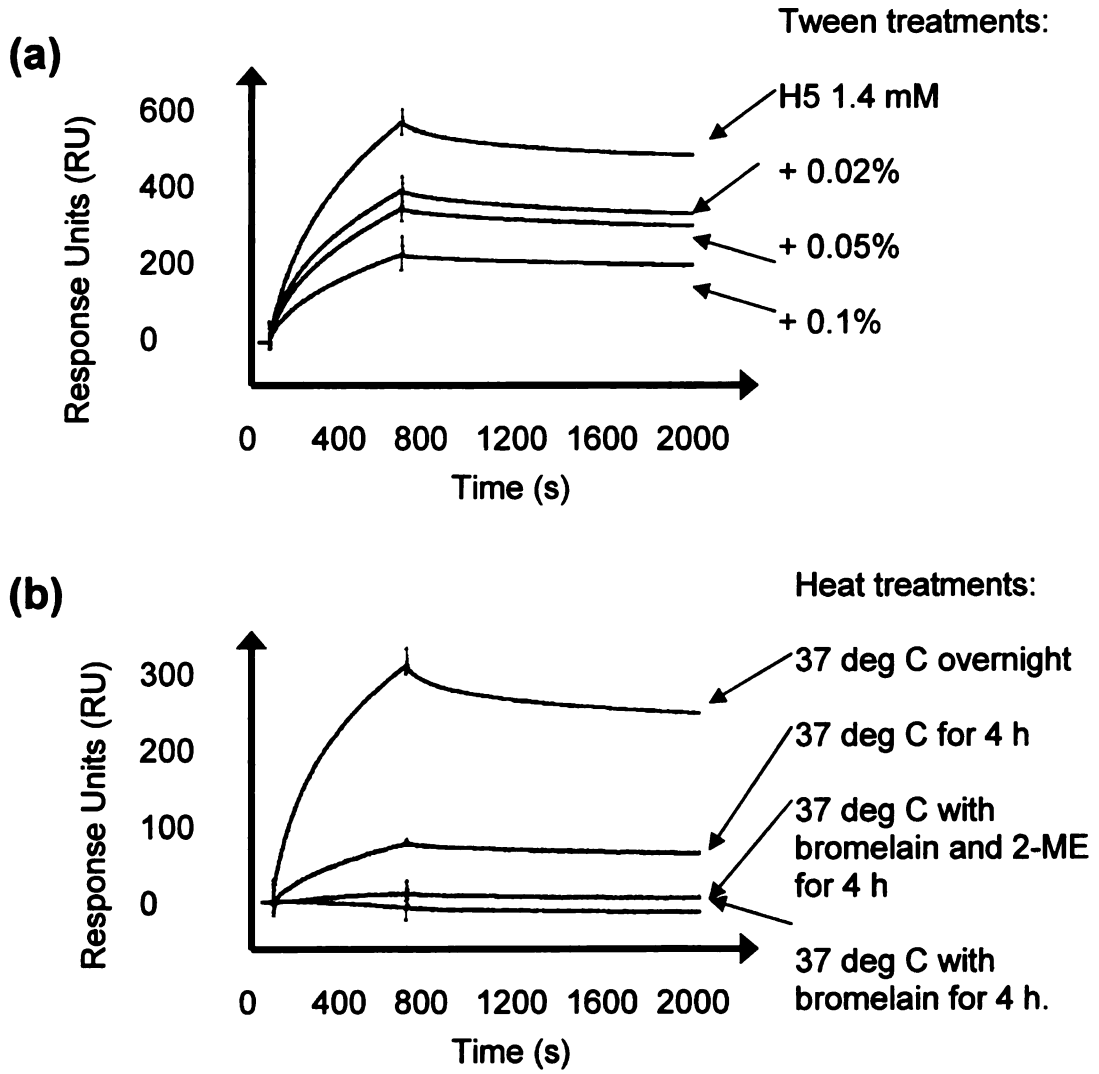

Figure 18. H5 1.4μM pretreatments. (a) Tween-20 (b) heat treatment at 37 degrees C overnight, 37 degrees C for 4 h, 37 degrees C with bromelain and 2-ME for 4 h, and 37 degrees C with bromelain for 4 h.

5.1.2.6 HA Preparation

Because we conclude that the H5 is present as large aggregates, the HA was pretreated in an effort to break down these complexes into more consistent trimer preparations. Increasing Tween-20 from 0.02 to 0.1% resulted in a 50% drop in SPR signal for H5 at 1.4 μM (Figure 18). Bromelain and 2-ME treatment served to completely

destroy H5 biological activity, and no glycan binding was observed with these preparations (Figure 18). Heat treatment at 37 degrees C lowered the binding activity of the H5 at this concentration, although 4 h treatment showed a five-fold reduction of binding as compared to overnight heat treatment (Figure 18). A longer heat treatment may have resulted in more consistent trimers while a short heat treatment only served to shock the sample without generating any viable trimers. Heat treatment at 56 degrees C for 10 min, with or without subsequent 4 degrees C treatment to cease heat effects, completely destroyed binding ability. All pretreatments were thus ineffective in bringing uniformity to the HA aggregates for a more repeatable signal, and all served to depress or destroy the glycan/HA binding.

5.1.2.7 Serum Experiments

The SPR binding assay was also repeated with mouse serum matrix at 1-2% by volume. H5 at 286 nM, 94.3 nM, 31.4 nM, 10.6 nM, and 3.53 nM, both with and without 2% mouse serum (ICR SCID) by volume, were injected over glycans 3'SLex, CT/Sda, and 3'SLN. The presence of 2% serum depressed the SPR signal, but the H5 concentrations retained a dose response, if statistically lower than the H5 dilution series without serum. A comparison of each H5 concentration with 2% serum revealed a 70-85% drop in SPR signal as compared to the corresponding H5 concentration prepared without serum (Figure 22). H3, previously shown to offer negligible binding to the H5-specific glycans, showed slight increase of binding signal with presence of 2% serum, likely due to nonspecific binding effects.

Background binding of serum to the chip or immobilized glycans was investigated by injecting varying concentrations of serum in buffer over the glycan surface with no

HA or antibody added. Serum at 10% showed approximately 10 RU of nonspecific binding to 3'SLN, but lower concentrations were not statistically different from the buffer injections with no serum added. This likely indicates that the addition of 1-2% serum inhibits glycan/HA binding by nonspecifically binding to the HA, but we cannot conclude that the serum binds nonspecifically to the glycans or the chip.

5.1.2.8 Structural Morphology Characterization

The synthetic glycans and recombinant HA were analyzed by a JEOL (Peabody, MA) 100CX II Transmission Electron Microscope (TEM) to obtain their structural morphologies (Figure 19). 1% uranyl acetate was used as stain.

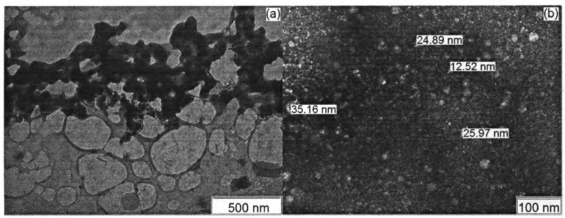

Figure 19. TEM imaging of (a) synthetic glycans and (b) purified recombinant H5 HA.

5.2 OBJECTIVE 2

SPR to Detect Ab-Mediated Binding Inhibition

5.2.1 SPR Neutralization Assay Design

5.2.1.1 Neutralization Ability of Anti-H5 Monoclonal Antibody

Preincubating H5 with neutralizing anti-H5 monoclonal antibody resulted in a neutralization of glycan/H5 binding on the SPR system. Anti-H5 monoclonal antibody IgG2 (mouse ascites fluid) at 1:500 neutralized the binding between H5 at 140 nM and H5-specific glycans 3'SLex and 3'SLN (Figure 20). The glycan/H5 binding was significantly reduced by anti-H5 monoclonal antibody 1:2000, and the antibody concentration range from 1:250 to 1:4000 displayed a reproducible dose response.

Convalescent H5N1 plasma has been reported to have a neutralizing antibody titer when diluted to 1:80, and the range of antibody concentrations tested here can thus be concluded to be within a physiologically relevant range (Zhou *et al.*, 2007). The anti-H5 monoclonal antibody dilution of 1:4000 offered some glycan/H5 binding inhibition, and the most neutralizing dilution tested, 1:250, offered complete neutralization. Even if a patient convalescent plasma contains a lower protein content than the anti-H5 monoclonal preparation, the requirement of a 1:80 plasma dilution falls far lower than the tested monoclonal range of 1:250 to 1:4000, offering evidence that the neutralization experiments described here have physiological relevance.

5.2.1.2 Neutralization Specificity

The glycan/H5 binding showed slight inhibition by anti-H1 polyclonal antibody at 1:250 but the anti-H1 did not cause complete neutralization as observed with anti-H5 at the same concentration (Figure 20). The binding of H5 to glycans 3'SLex and 3'SLN was

also slightly inhibited by anti-H3 polyclonal antibody at 1:500 but this concentration did not cause the complete neutralization observed with the same concentration of anti-H5 monoclonal antibody (Figure 20). These minor inhibitions of glycan/H5 binding by anti-H1 and anti-H3 polyclonals can be attributed to their composition as compared to the anti-H5 monoclonal, as the nature of a polyclonal antibody offers a matrix similar in complexity to a serum matrix, which was also seen to interfere with glycan/HA binding. We conclude that the anti-H1 and anti-H3 polyclonals at high concentrations do interfere with binding but not necessarily by binding within the receptor binding domain of H5 in a cross-protective manner.

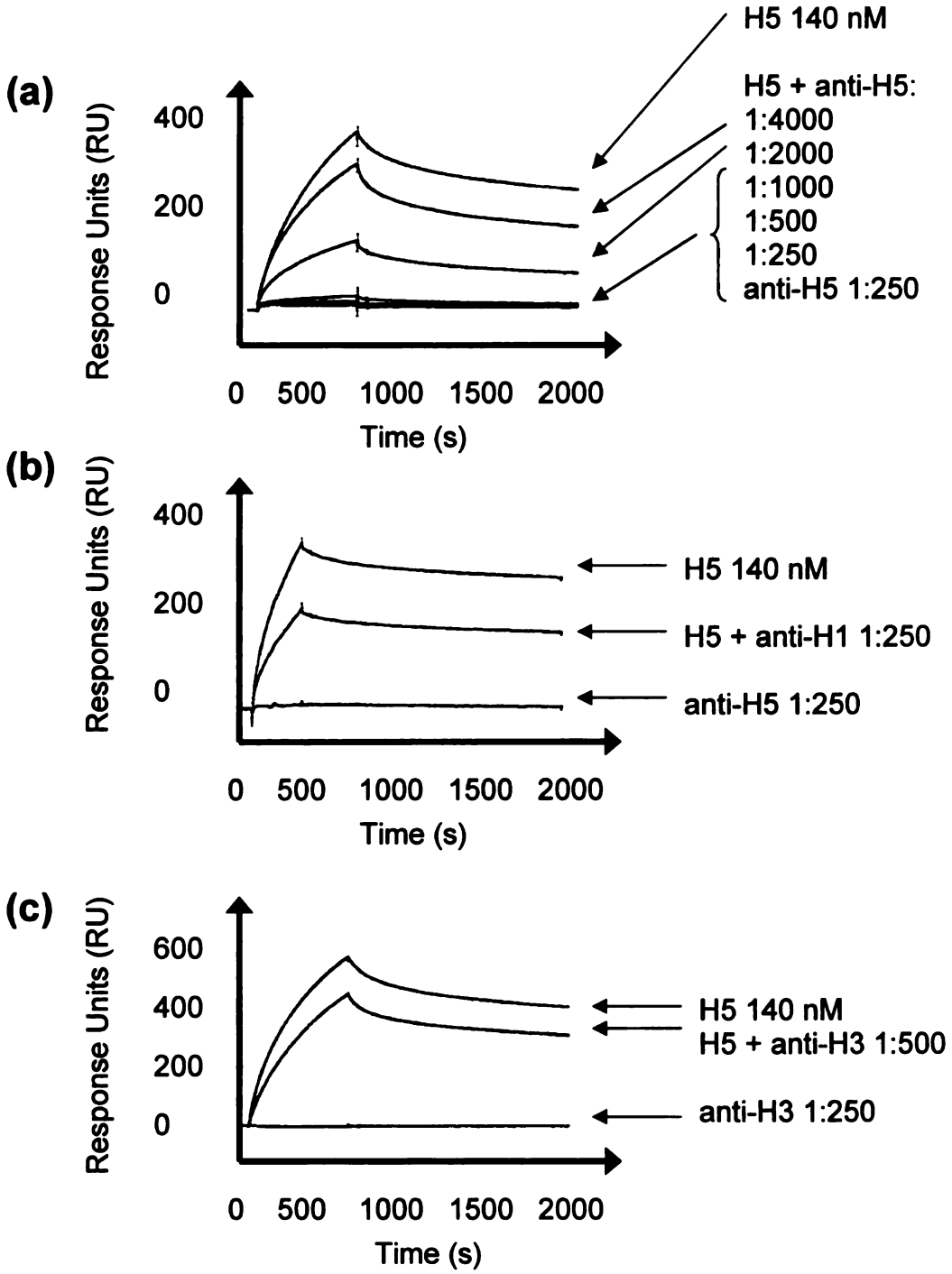

Figure 20. Neutralization experiments. (a) 3'SLN/H5 neutralization by anti-H5 monoclonal antibody: H5 140nM; H5 140nM + anti-H5 1:4000, 1:2000, 1:1000, 1:500, 1:250; anti-H5 1:250 only, (b) 3'SLN/H5 binding inhibition by anti-H1 (H1N1/Pan): H5 140nM; H5 140nM + anti-H1 1:250; anti-H1 1:250 only, and (c) 3'SLN/H5 binding inhibition by anti-H3 (A/Shandong/9/93): H5 140nM; H5 140nM + anti-H3 1:500; anti-H3 1:250 only.

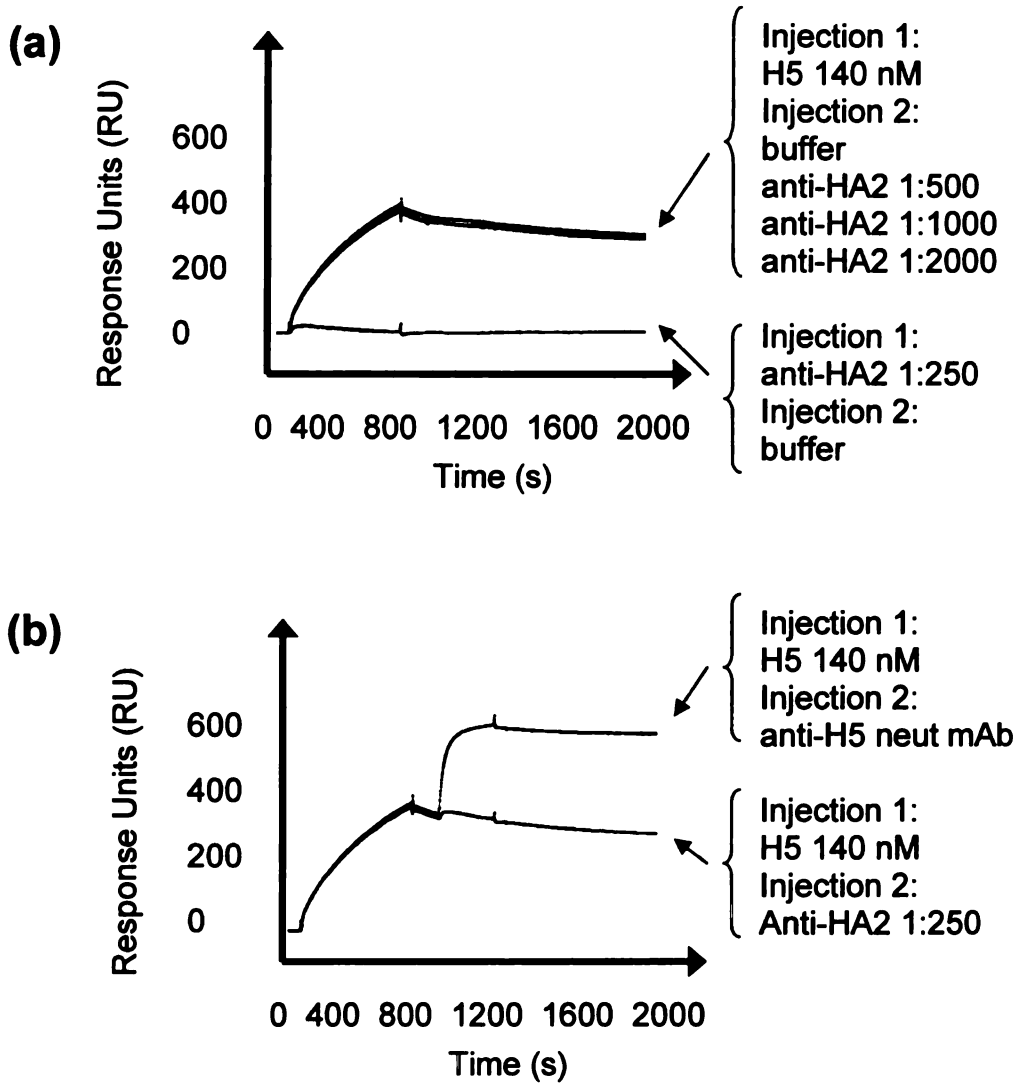

Figure 21. Antibody binding to 3'SLN/H5 precomplex. (a) Injection 1: H5 140nM, Injection 2: buffer, anti-HA2 H5 1:500, 1:1000, or 1:2000; Injection 1: anti-HA2 1:250, Injection 2: buffer, and (b) Injection 1: H5 140nM, Injection 2: anti-H5 neutralizing monoclonal antibody or anti-HA2 H5 1:250.

5.2.1.3 Antibody Testing: Anti-HA versus Anti-HA2

The ability of a polyclonal antibody against the HA2 portion of H5 to bind to the already-formed glycan/HA complex was investigated. This was expected to offer binding because the HA2 segment does not include the receptor binding domain, the area which

is utilized in glycan/HA binding. After an injection of H5 at 140 nM over glycans 3'SLex, CT/Sda, and 3'SLN, the anti-HA2 H5 polyclonal antibody at 1:500, 1:1000, and 1:2000 was injected before regeneration. The anti-HA2 H5 polyclonal antibody did not show a further increase in RU, indicating that the antibody did not bind the glycan/HA complex (Figure 21). This could be due to the aggregated nature of the H5, if the HA2 portion of the H5 was hidden within the aggregate. The sequential binding procedure was repeated with anti-H5 monoclonal antibody, previously shown to be neutralizing due to binding within the glycan/HA receptor binding domain. However, this monoclonal exhibited a further increased SPR signal, which indicated that the second injection of anti-H5 monoclonal antibody also bound to the already formed glycan/H5 complex, thus forming a glycan/H5/ anti-H5 complex (Figure 21). The monoclonal thus did not displace the glycan but instead bound the H5 outside of the receptor binding domain. Alternatively, this may also be a result of the aggregated nature of the H5, as the monoclonal may have bound to an available receptor binding domain exposed on the large aggregate. The anti-H5 monoclonal antibody may thus neutralize glycan/H5 binding when preincubated with H5, and may also additionally bind an already formed glycan/H5 complex without displacing the glycan. This would present the anti-H5 monoclonal antibody as an appropriate reagent in a sandwich-type assay, if reaction sequence is maintained.

5.2.1.4 Serum Experiments

The neutralization experiment described in *2.6* was repeated with H5 at 140 nM prepared in 1% mouse serum. The signal was similarly depressed as seen in the glycan/H5 + 2% serum binding experiment. Comparing H5 at 140 nM preincubated with

anti-H5 monoclonal antibody from 1:250 to 1:4000 both with and without 1% serum, revealed a 20-70% drop in SPR signal for those samples prepared with serum (Figure 22). A depressed dose response was still observed for the serial dilutions of anti-H5 monoclonal antibody.

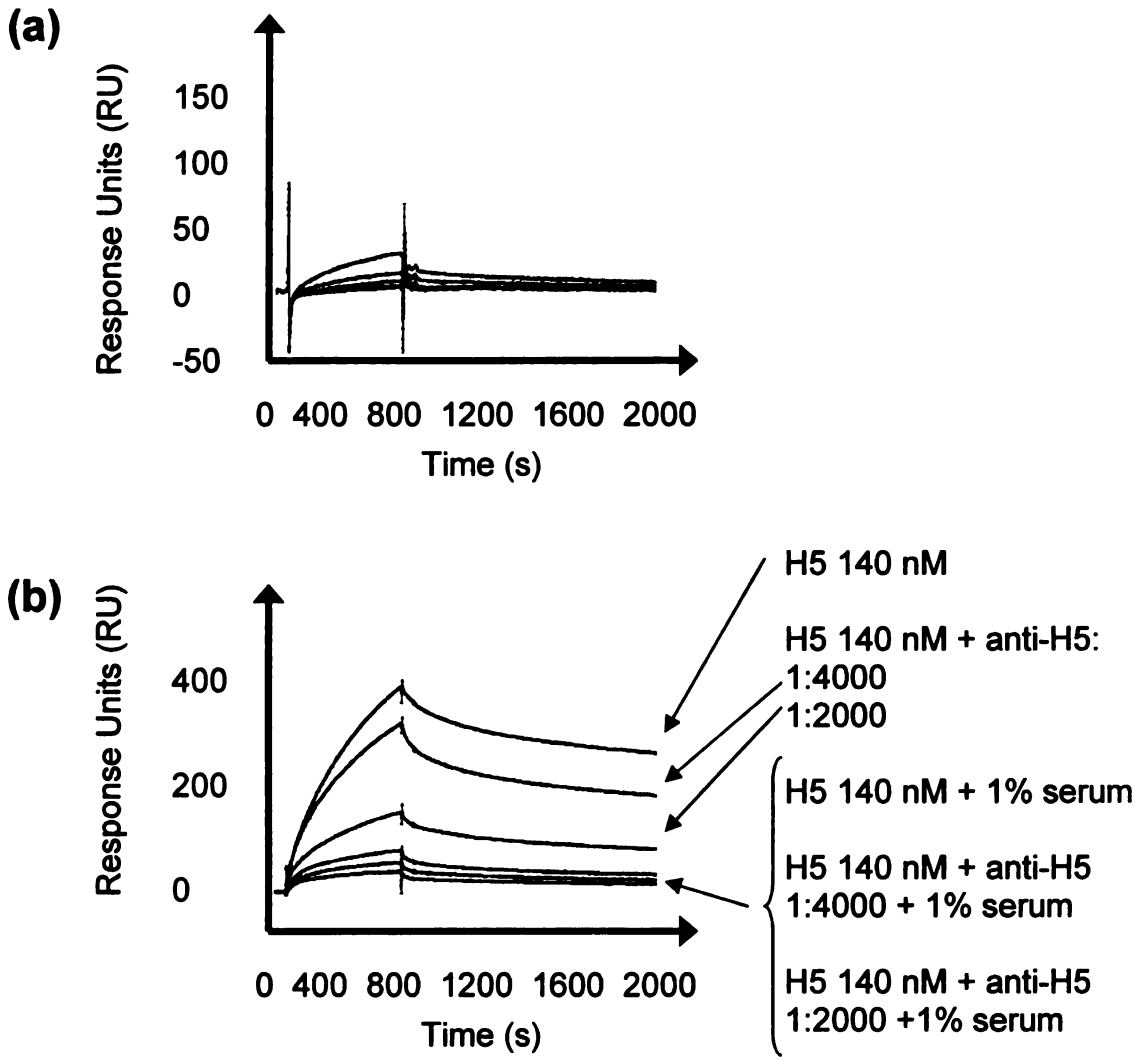

Figure 22. Serum effects. (a) H5 at 286nM, 94.3nM, 31.4nM, 10.6nM, and 3.53nM prepared in 2% mouse serum binding to 3'SLN and (b) H5 140nM, H5 140nM + anti-H5 1:4000, H5 140nM + anti-H5 1:2000, H5 140nM in 1% serum, H5 140nM + anti-H5 1:4000 in 1% serum, H5 140nM + anti-H5 1:2000 in 1% serum.

5.3 OBJECTIVE 3

H5N1—Targeted Biosensor Design

5.3.1 Biosensor Design

5.3.1.1 Supporting SPR data

Biosensor work proceeded on the basis of previous SPR results. As described in 5.1., SPR analysis demonstrated a high avidity, specific binding between H5-specific α2,3-linked glycan receptors and recombinant H5, with concentration series offering an observable dose response. Preincubating H5 with neutralizing anti-H5 monoclonal antibody resulted in neutralization of glycan/H5 binding on the SPR system. Anti-H5 monoclonal antibody IgG2 (mouse ascites fluid) at 1:500 neutralized the binding between H5 at 140 nM and H5-specific α2,3 linked glycans 3'SLex and 3'SLN (Figure 23; Table 4). Again, this antibody dilution falls within the range of physiological relevance, where plasma 1:80 is neutralizing (Zhou *et al.*, 2007). The glycan/H5 binding showed slight inhibition by anti-H1 polyclonal antibody at 1:250 but the anti-H1 did not cause complete neutralization as observed with anti-H5 at the same concentration (Figure 23).

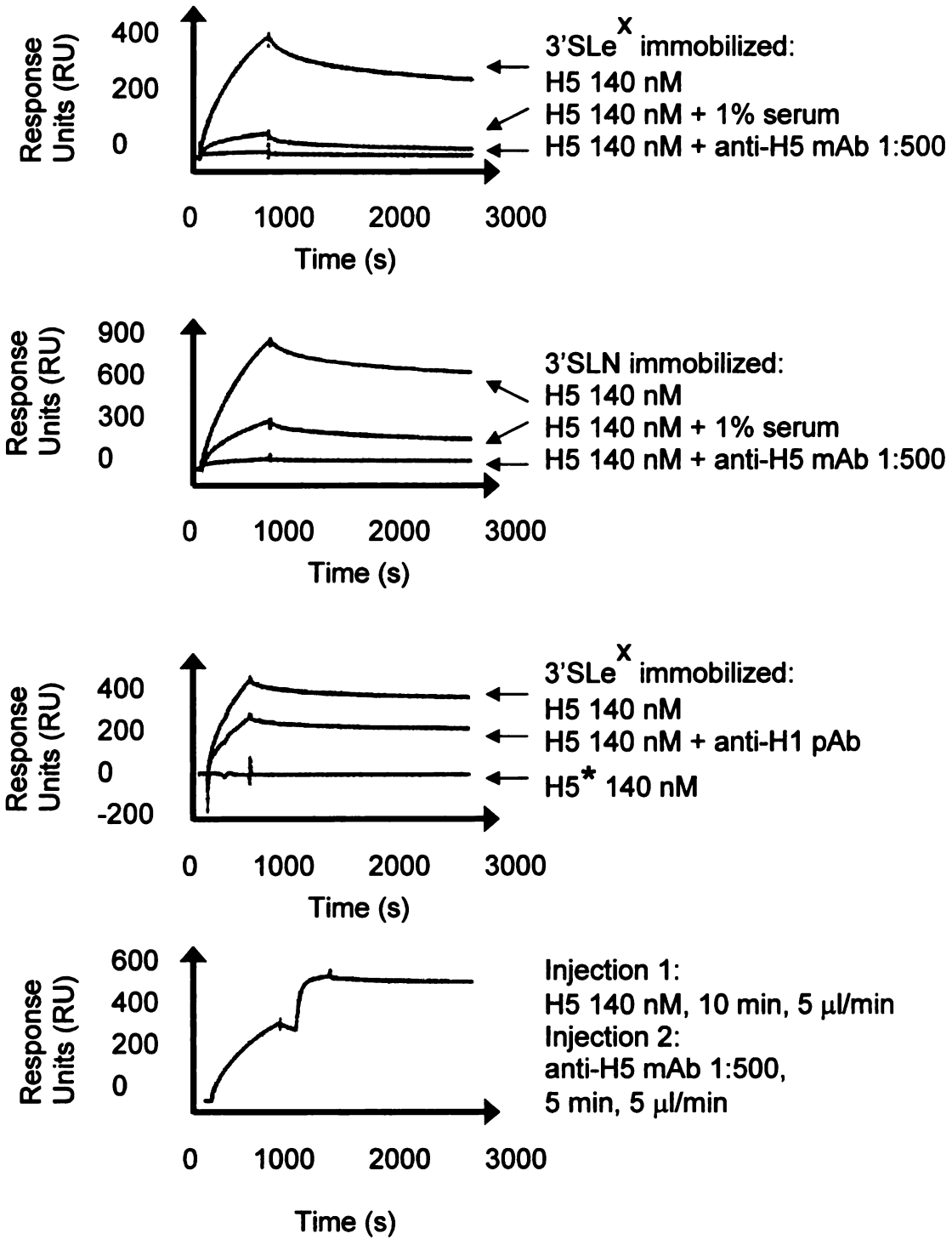

Figure 23. Supporting SPR results. (a) H5 140nM binding to H5-specific glycan 3'SLex, as inhibited by 1% mouse serum and anti-H5 monoclonal antibody 1:500, (b) H5 140nM binding to H5-specific glycan 3'SLN, as inhibited by 1% mouse serum and anti-H5 monoclonal antibody 1:500, (c) H5 140nM binding to H5-specific glycan 3'SLex, as inhibited by cross-reactivity of anti-H1 polyclonal antibody; H5* 140nM binding to 3'SLex, and (d) antibody testing on H5-specific glycan 3'SLN.

The order of interaction was found to be important, as described in *5.2.1.3*. The glycan/H5 binding was not neutralized when the same anti-H5 monoclonal antibody was allowed to react with the already formed glycan/H5 complex. Following typical H5-binding, a further increased SPR signal indicated that the second injection of anti-H5 monoclonal antibody also bound, forming a glycan/H5/ anti-H5 complex (Figure 23). The subsequently added anti-H5 monoclonal antibody thus did not displace the glycan but instead bound the H5 in a region outside of the receptor binding domain or in an available binding domain if the H5 is present as a trimer or larger aggregate. This is in contrast to the neutralization experiment, in which the anti-H5 monoclonal antibody binds within, or otherwise blocks, the glycan receptor binding domain on H5. This anti-H5 monoclonal antibody is thus appropriate for use in both the SPR neutralization assay as well as the biosensor sandwich-type assay.

The SPR assay was also repeated with a 1% mouse serum matrix. Although binding was still observed, the results indicated that the glycan/H5 binding was inhibited by the addition of serum to the sample buffer (Figure 23).

5.3.1.2 Electrochemical Detection

The schematic representation of the detection mechanism of the EAM based electrochemical biosensor illustrates the electrode architecture and sample preparation methods. The detection principles is based on an electrochemical sandwich assay in which a specific glycan functions as a capture probe while an antibody specific for HA serves as a detector probe. The glycan is labeled with biotin, the HA is labeled with EAMs, and the SPCE is modified with streptavidin. The glycans are anchored to the SPCE via high affinity streptavidin-biotin interactions. In the stepwise preparation

method, capture probe, target, and detector probe are applied to the streptavidin modified SPCE sequentially with wash and dry steps between each. In the preconcentration preparation method, capture probe and target are preincubated, followed by incubation with detector probe. Magnetic separation then removes unbound material, including mouse serum, and the glycan/HA/anti-HA—EAM complexes are applied to the SPCE in one step. Excess is washed and target present on the SPCE biosensor surface is detected by cyclic voltammetry measurement of the redox activity of the EAMs.

Cyclic voltammetry was used for the electrochemical characterization of the EAM-modified targets. From the cyclic voltammogram (CV), binding can be quantified by the intensity of redox peaks or by the ΔQ, calculated as the integral of current (Kuznetsov, 1995). The cyclic voltammogram of glycan/HA/anti-HA—EAM complexes in 0.1 M HCl with the scan range of -0.4 to 1.0 V and rate of 20 mV/s exhibited two stable redox peaks which are characteristic of the polyaniline conducting polymer, confirming successful capture of the EAM-captured targets. For the preconcentration preparation method shown in Figure 25, the anodic peak at 0.07 V corresponds to the switching of leucoemeraldine base to emeraldine salt, and the peak at 0.76 V indicates the switch from emeraldine to pernigraniline salt (Arora *et al.*, 2007; Gospodinova *et al.*, 1996). The cathodic peaks occurred at -0.13 and 0.33 V. For the stepwise preparation method, the anodic peaks occurred at 0.09 and 0.77 V, while the corresponding cathodic peaks occurred at -0.14 and 0.37 V. For both methods, the anodic and cathodic peak currents are more defined for the highest H5 concentration, with the lower H5 concentrations and blanks displaying statistically similar peaks. The decrease in redox peak intensity with decreasing H5 concentration is expected since less target means lower concentration of glycan/HA/anti-

HA—EAM complex present on the electrode. The CV of the blanks, which consisted of the immunofunctionalized EAMs with no glycan or HA, also displayed the characteristic redox peaks of the polyaniline, indicating that immunofunctionalization of the EAMs did not alter their native electrochemical behavior (Figures 24-25). Any EAMs present in this case would be due to low levels of nonspecific binding or insufficient washing, and the presence of visible though low intensity redox peaks indicates that the EAMs can generate redox signals even at very low concentrations. Comparison of the blanks to the glycan/HA/anti-HA—EAM complexes showed that while the anodic and cathodic peak potentials did show variation based on HA concentration, the peaks were located within the same voltage range, indicating that complex formation of the immunofunctionalized EAMs with the glycan/HA also did not affect electrochemistry.

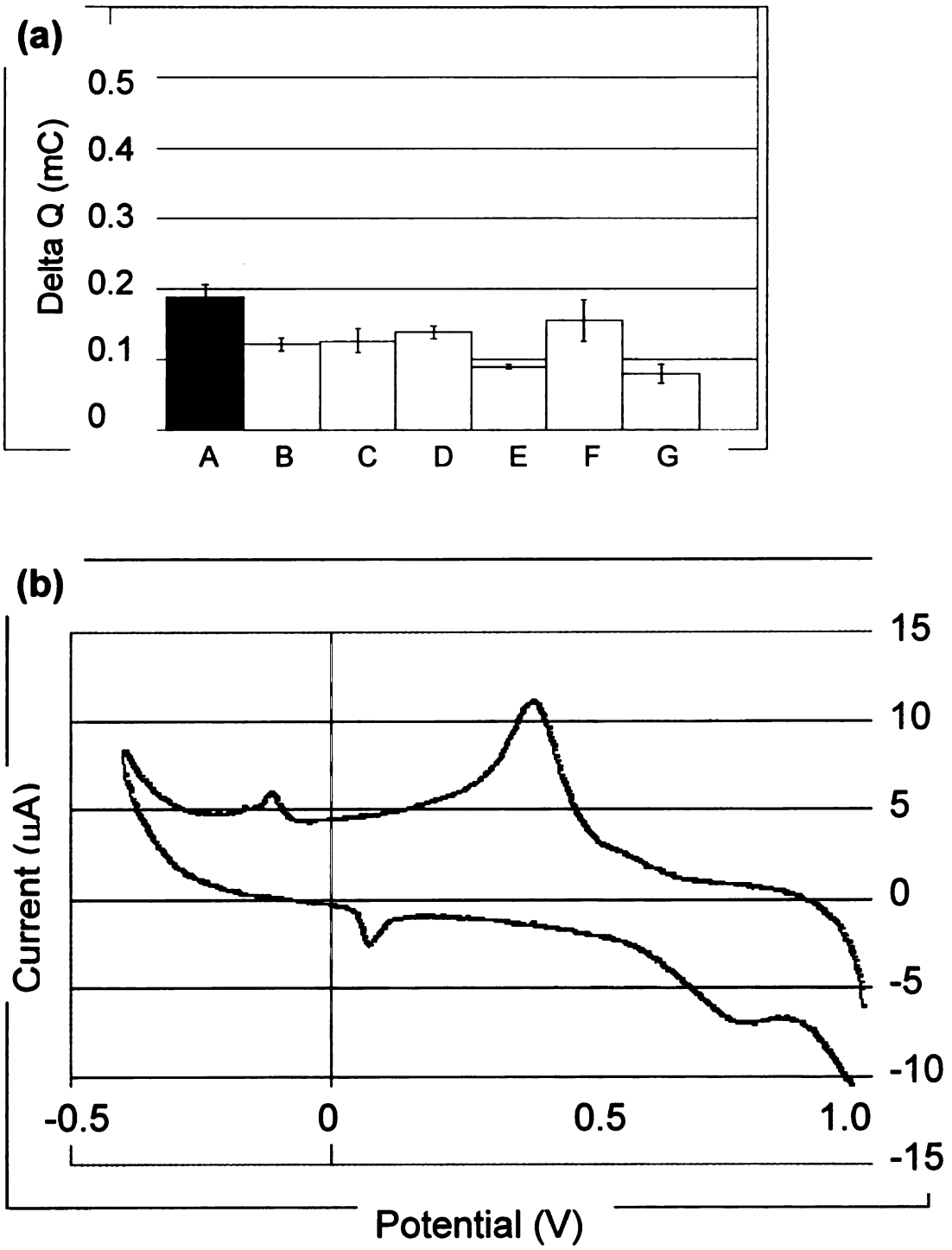

Figure 24. Stepwise preparation method. (a) Delta Q values of (A) 3'SLex 100μM + H5 1.4μM, (B) 3'SLex 100μM + H5 700nM, (C) 3'SLex 100μM + H5 360nM, (D) CT/Sda 500μM + H5 1.4μM, (E) 3'SLN 500μM + no HA, (F) no glycan + H5 1.4μM, and (G) no glycan + no HA, and (b) CV of 3'SLex 100μM + H5 1.4μM.

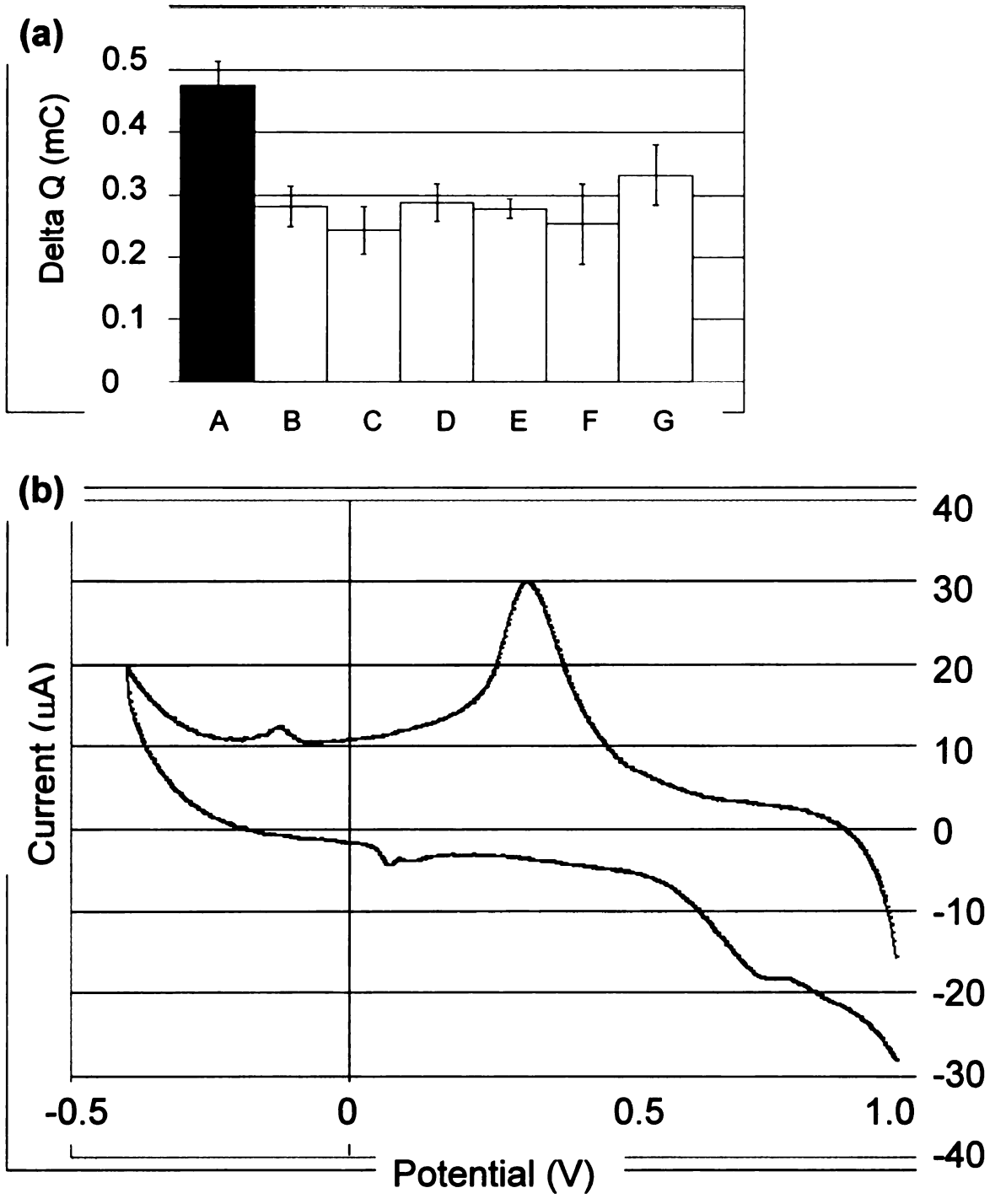

Figure 25. Preconcentration preparation method. (a) Delta Q values of (A) 3'SLex 100μM + H5 1.4μM + 10% mouse serum, (B) 3'SLex 100μM + H5 700nM + 10% mouse serum, (C) 3'SLex 100μM + H5 360nM + 10% mouse serum, (D) GT3 100μM 0+ H5 1.4μM + 10% mouse serum, (E) 3' SLex 100μM + no HA, (F) no glycan + H5 1.4μM + 10% mouse serum, and (G) no glycan + no HA, and (b) CV of 3'SLex 100μM + H5 1.4μM + 10% mouse serum.

5.3.1.3 Biosensor Sensitivity

The biosensor platform showed correlation to the SPR assay results. The sensitivity of the biosensor platform was explored by testing a range of H5 concentrations. The preconcentration preparation method yielded an average ΔQ value of 0.474 mC for the H5 at 1.4 μM binding to 3'SLex. The lower concentrations of 700 nM and 360 nM displayed significantly decreased ΔQ values which were not statistically different from each other or from the blanks (Figure 26a(H-J); Tables A-3, A-5). The stepwise preparation method yielded an average ΔQ value of 0.188 mC for the H5 at 1.4 μM, which was within the range of the preconcentration method blanks and was statistically lower than the preconcentration value for H5 1.4 μM (Tables A-3, A-5). The lower H5 concentrations of the stepwise method were not statistically different from each other but also showed significantly lower ΔQ values than the 1.4 μM stepwise (Figure 26a(A-C); Tables A-3, A-5). The sensitivity of both preconcentration and stepwise preparation methods to detect H5 using biosensors prepared with 3'SLex were thus taken to be 1.4 μM (Figures 24-25). We conclude that the preconcentration method, which includes two magnetic separation and wash steps, is better able to isolate the target HA, thus offering a consistently higher ΔQ value than the equivalent concentrations prepared using the stepwise method.

5.3.1.4 Magnetic Separation by EAMs

The preconcentration HA preparations included 10% mouse serum, which the stepwise HA did not, but the increased signal for the preconcentration method is not likely attributable to nonspecific binding due to the mouse serum. It can be observed that the preconcentration method when performed with the same concentrations of glycan and

H5 with and without 10% mouse serum yielded similar ΔQ values, though still statistically different ($P = 0.0324$) (Figure 26b(B,C); Tables A-3, A-5). It is a likely conclusion then that the magnetic separation technique was able to fully extract the target HA from the 10% mouse serum matrix to yield a similar signal to that obtained when the sample was prepared with no serum. This is an improvement on the SPR assay, in which 1% mouse serum depressed the signal as described in *5.1.2.4* and *5.2.1.4* (Figure 22).

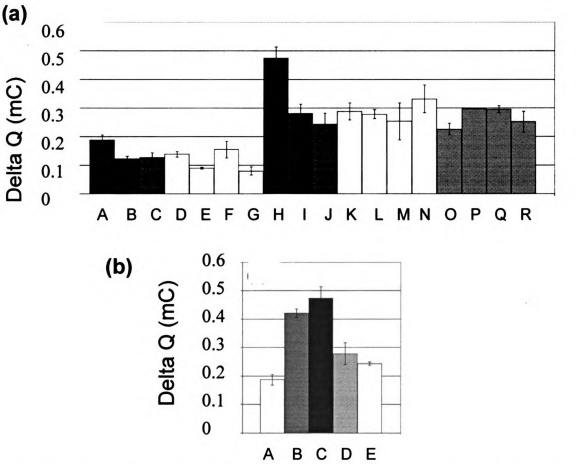

Figure 26. Cyclic voltammetry results. (a) H5 concentration study as a function of preparation method and comparison to negative controls and blanks, as numbered and described in Table A-3. Group (A) 1, (B) 2, (C) 3, (D) 24, (E) 25, (F) 27, (G) 26, (H) 9, (I) 10, (J) 11, (K) 14, (L) 13, (M) 12, (N) 15, (O) 16, (P) 17, (Q) 18, and (R) 19. (b) Response for H5 1.4μM using different preparation methods. (A) 1, (B) 8, (C) 9, (D) 20, and (E) 21. For the respective samples, mean ΔQ ± SD, $n = 3$ (SD = standard deviation, n = no. of replicates).

Table 5. Biotinylated saccharide sequences and predicted binding to H5N1

Common Name	Saccharide Name and Spacer	Predicted to bind H5N1
3'SLex	Neu5Acα2-3Galβ1-4[Fucα1-3]GlcNAcβ-SpNH	Yes
3'SLN	Neu5Acα2-3Galβ1-4GlcNAcβ-SpNH	Yes
3'S-Di-LN	Neu5Acα2-3[Galβ1-4GlcNacβ1-3]$_2$β-SpNH	Yes
6'SLN	Neu5Acα2-6Galβ1-4GlcNAcβ-SpNH	No
GT3	Neu5Acα2-8Neu5Acα2-8Neu5Acα2-3Galβ1-4Glcβ-SpNH	No
6'S-Di-LN	Neu5Acα2-6[Galβ1-4GlcNacβ1-3]$_2$β-SpNH	No

5.3.1.5 Preparation Effects

The signals generated for the same H5 concentration, 1.4 μM, were compared using different preparation methods. The preconcentration method, with or without 10% mouse serum added to the H5, yielded statistically higher ΔQ values than the stepwise method (Figure 27b). The stepwise method did confirm that H5 binds to 3'SLN with statistically higher avidity than it binds to 3'SLex, which is confirmatory to SPR results (Figure 27a,e). However, both of these stepwise values fell far lower than the preconcentration method values. Source A H5 was also shown to be a better binder to 3'SLex than Source B H5*. H5*, while the same FLUAV strain as Source A H5, yielded a far lower ΔQ value when preconcentrated with 3'SLex than for the 3'SLex/H5 (Source A) preconcentration result (Figure 27c,d). However, 3'SLex /H5* preconcentration did yield a higher ΔQ value with statistical significance as compared to the 3'SLex/H5 (Source A) prepared stepwise (Figure 27a,d; Tables A-3, A-5). We can conclude that the

preconcentration method offers a more robust response and that H5 from Source A offers stronger binding to the 3'SLN and 3'SLex than H5*, possibly due to the predicted aggregated nature of Source A H5.

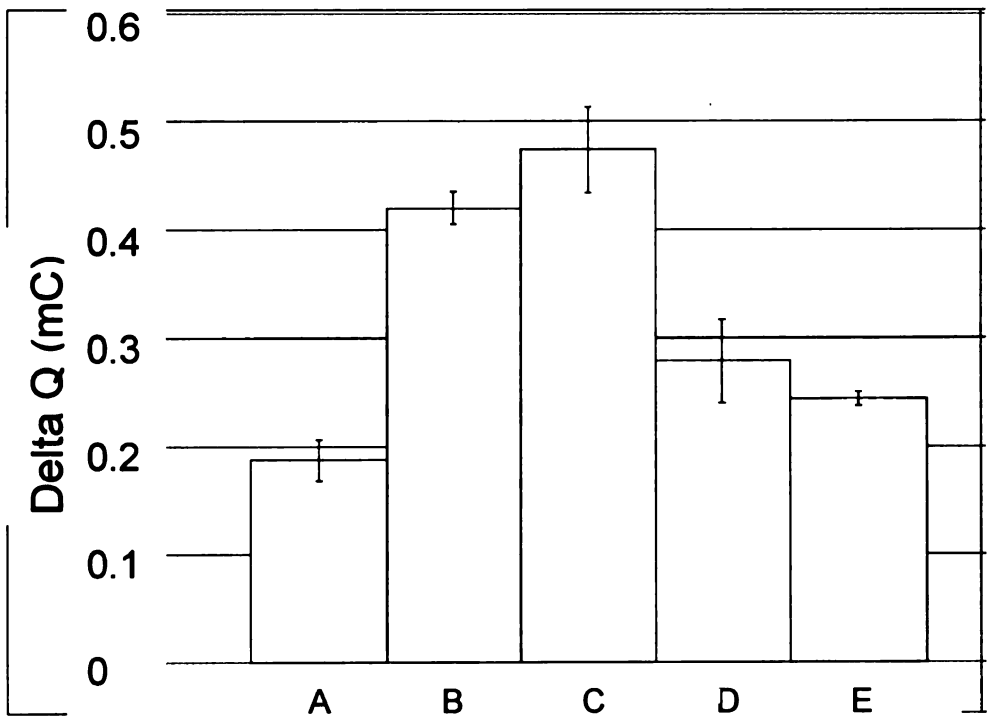

Figure 27. Comparison of different preparation methods. (A) 3'SLex 100μM + H5 1.4μM, stepwise, (B) 3'SLex 100μM + H5 1.4μM, preconcentration, (C) 3'SLex 100μM + H5 1.4μM + 10% mouse serum, preconcentration, (D) 3'SLex 100μM + H5* 1.4μM + 10% mouse serum, preconcentration, and (E) 3'SLN 100μM + H5 1.4μM, stepwise.

5.3.1.6 Nonspecific Binding

In both preparation methods, the blanks yielded ΔQ values that were statistically lower than the reading from the H5-specific glycan/H5 interaction, with H5 at 1.4 μM and glycans 3'SLN or 3'SLex. For the stepwise preparation method, the presence of H5

at 1.4 μM, whether incubated after the nonbinder glycan 6'SLN or after no glycan, resulted in average ΔQ values lower with statistical significance than the 3'SLN/H5 response, but higher with statistical significance than the blanks with no H5 added to either the H5-specific glycan or no glycan (Figure 26a(A, D-G); Tables A-3, A-5). The absence of H5 yielded repeatable blank tests. The presence of H5 in those blanks which resulted in higher ΔQ values than in those blanks without H5 indicates that there may be low levels of nonspecific binding between H5 and the SPCE surface or any of the immobilized partners previously incubated on the SPCE. Further blocking could prove useful to eliminate nonspecific binding.

For the preconcentration method, the blanks both with and without H5 were repeatable and within a statistically similar range (Figure 26a(K-R); Tables A-3, A-5). The blanks, including the GT3/H5 interaction, were also statistically lower than the 3'SLex/H5 interaction. The negative control which included no glycan and no HA but only the anti-H5—EAM antibody complex yielded the highest ΔQ value of the blanks, but this remained below the positive control (Figure 26a(N); Tables A-3, A-5).

The preconcentration method did not include a blocking step, while in the stepwise method the SPCE surface was blocked with avidin and biotin after incubation with the biotinylated glycans or, when no glycan was included in the sample, before addition of HA or anti-HA—EAM complexes. The preconcentration method does not lend itself to blocking with avidin and biotin, since all of the interaction partners, including glycan, HA, and anti-HA—EAM are added simultaneously as an already formed complex. However, the lack of a blocking step does not appear to influence the signal with nonspecific binding effects. The magnetic separation step serves to eliminate irrelevant

material which could interfere with target binding.

5.3.1.7 Biosensor Specificity

The specificity of the system was investigated using a series of H1 samples. In the preconcentration method, the H1, diluted to 1.4 μM with 10% mouse serum, was preincubated with the H5-specific glycan 3'SLex and subsequently incubated with EAMs conjugated with either anti-H5 or anti-H1 antibodies. The samples containing both H1 and anti-H1—EAM complexes showed an increase in ΔQ as compared to the samples with no H1 or with anti-H5—EAM complexes (Figure 26a(O-R)). This may indicate that the H1 and anti-H1 antibodies interact and cause slightly higher levels of nonspecific binding as compared to H1 alone or anti-H1 alone. However, the levels of all H1-based blanks remain within the statistical range of the H5-based blanks (Tables A-3, A-5). This indicates that despite the polyclonal nature of the anti-H1 antibodies, there is little cross-reactivity with the H5-targeted biosensor which improves upon the Biacore system (Figure 23c). Both stepwise and preconcentration methods yielded ΔQ values for the binding to the H5-nonspecific glycans, GT3 or 6'SLN, which were distinguishably lower than their corresponding positive binder, 3'SLex or 3'SLN. We conclude that the biosensor is highly specific for H5.

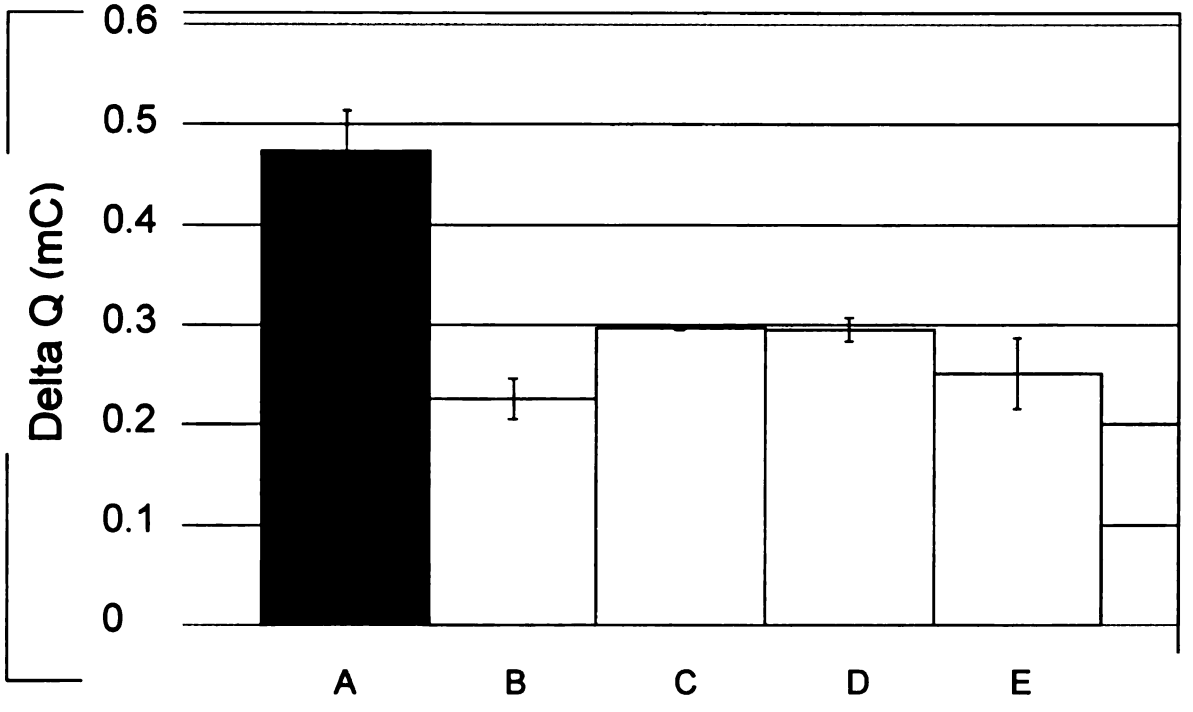

Figure 28. Specificity investigation using H1-based negative controls and preconcentration preparation. (A) 3'SLex 100μM + H5 1.4μM + 10% mouse serum + anti-H5—EAMs, (B) 3'SLex 100μM + H1 1.4μM + 10% mouse serum + anti-H5—EAMs, (C) 3'SLex 100μM + H1 1.4μM + 10% mouse serum + anti-H1—EAMs, (D) no glycan + H1 1.4μM +10% mouse serum + anti-H1—EAMs, and (E) no glycan + no HA + anti-H1—EAMs.

5.3.1.8 Structural Morphology Characterization

The EAM polyaniline nanoparticles, EAMs immunofunctionalized with anti-H5 antibody, and glycan/HA/anti-HA—EAM complex were analyzed by a JEOL (Peabody, MA) 100CX II Transmission Electron Microscope (TEM) to obtain their structural morphologies. 1% uranyl acetate was used to stain anti-H5 antibody, HA, and glycans. The crystalline nature of the EAM nanoparticles was also studied by selected area electron diffraction using the JEOL 2200FS field emission TEM. As shown in Figure 29a, the TEM and electron diffraction micrograph revealed EAM polyaniline

nanoparticle sizes in the 25-100 nm range. As observed in the TEM image, the darkest circular areas correspond to the γ-Fe2O3 cores which are surrounded by the lighter colored polyaniline polymerized around the cores. Immunofunctionalization of the EAM nanoparticles yields a cloudier border as compared to the crisp edge of the EAM nanoparticles alone, indicating that immunofunctionalization was effective (Figure 29b). TEM imaging of the 3'SLex/H5/anti-H5—EAM antibody complex after two magnetic separations and washes resulted in a web-like boundary which could be attributed to the binding of the H5 and glycan, forming a more branched complex than the EAMs or immunofunctionalized EAMs alone. When comparing the 3'SLex/H5/anti-H5—EAM antibody complex prepared with H5 with and without 10% mouse serum, the TEM images reveal similarly shaped aggregates, indicating that there is no nonspecific binding of the serum components to the complex (Figure 29c,d). This is in confirmation of the cyclic voltammetry results (Figure 26b(B,C)). The backgrounds of the images do reveal that the sample prepared with mouse serum has a cloudier supernatant, suggesting the benefit of a more thorough washing, although the ΔQ values are not affected.

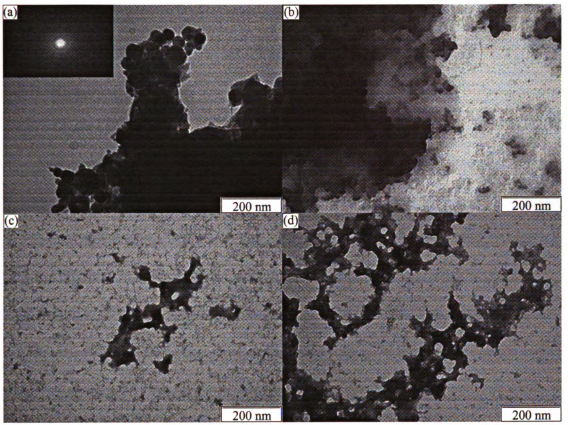

Figure 29. TEM imaging. (a) TEM and electron diffraction micrograph (inset) of EAM polyaniline nanoparticles with gamma iron (III) oxide cores, (b) TEM of EAMs immunofunctionalized with anti-H5 antibody, (c) 3'SLex /H5/anti-H5—EAM complex, magnetically separated and washed, with H5 prepared with 10% mouse serum, and (d) 3'SLex /H5/anti-H5—EAM complex, magnetically separated and washed, with H5 prepared without serum.

5.4 OBJECTIVE 4

Biosensor to Distinguish α2,3 v. α2,6 Receptor Binding

5.4.1 Biosensor Design

5.4.1.1 Glycan Sequences

The preconcentration method was also utilized to compare a α2,3 versus α2,6 linked glycan receptors. 3'S-Di-LN and 6'S-Di-LN were chosen for comparison purposes as their saccharide sequences were identical except for the sialic acid linkage, ensuring that any differences in binding would be the result of this linkage. 3'S-Di-LN was predicted to bind H5 due to the α2,3 preference of avian FLUAV, and 6'S-Di-LN was predicted to bind H1 due to the α2,6 preference of human FLUAV.

5.4.1.2 Avian FLUAV-Targeted Biosensor

The H5-specific glycan 3'S-Di-LN at 100 μM bound H5 at 1.4 μM and 700 nM, prepared to contain 10% mouse serum. The glycan/H5 complex was immunomagnetically separated from the mouse serum and other extraneous unbound material using EAMs immunofunctionalized with anti-H5 monoclonal antibody. The ΔQ values of 3'S-Di-LN binding to H5 at 1.4 μM and 700 nM were not statistically different from each other, but were statistically higher than the ΔQ values of H5 at 1.4 μM binding to the H5-nonspecific glycan 6'S-Di-LN at 100 μM.

5.4.1.3 Human FLUAV-Targeted Biosensor

The glycan with predicted binding to human HA, 6'S-Di-LN, was shown by the preconcentration method to specifically bind H1 (H1N1 A/South Carolina/1/18) while not binding H5. The α2,6 glycan, 6'S-Di-LN, at 100 μM, bound H1 at 1.4 μM and 700 nM, prepared to contain 10% mouse serum. The glycan/H5 complex was immunomagnetically separated from the mouse serum and other extraneous unbound material using EAMs immunofunctionalized with anti-H1 monoclonal antibody. The ΔQ values of 6'S-Di-LN binding to H1 at 1.4 μM and 700 nM were not statistically different from each other, but were statistically higher than the ΔQ values of H1 at 1.4 μM binding to the H5-specific glycan 3'S-Di-LN at 100 μM.

5.4.1.4 Specificity

The ΔQ value of 6'S-Di-LN/H5 was within the statistical range of the negative control, in which only anti-H5—EAMs with no glycan or HA were incubated on the SPCE. Similarly, the ΔQ value of 3'S-Di-LN/H1 was within the statistical range of the negative control, in which only anti-H1—EAMs with no glycan or HA were incubated on the SPCE. From these results, we can conclude that the biosensor is able to distinguish α2,3 versus α2,6 sialic acid linkages with repeatability. Because human transmissibility and thus pandemic potential rely on α2,6 specificity of the FLUAV strain, these results offer proof of concept that the biosensor is able to identify pandemic strains, and to distinguish them from nonpandemic strains.

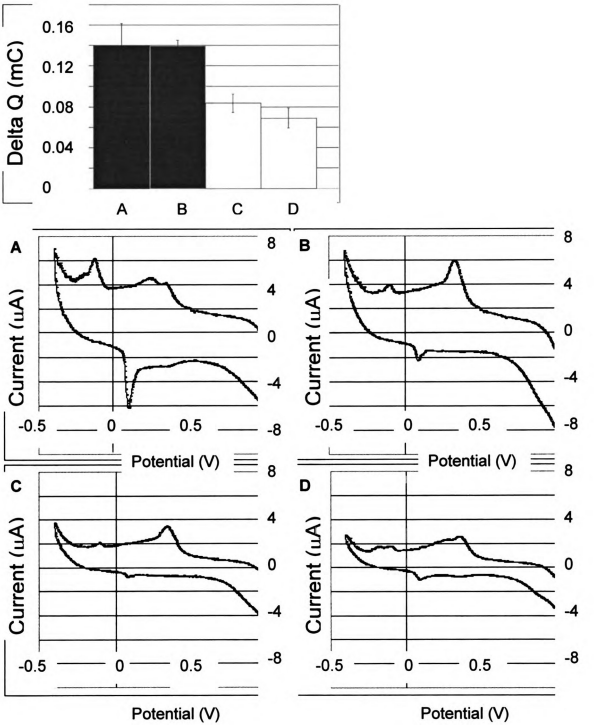

Figure 30. H5 binding to α2,3 versus α2,6-linked glycan receptors using preconcentration method. (A) 3'S-Di-LN 100μM + H5 1.4μM + 10% mouse serum, (B) 3'S-Di-LN 100μM + H5 700nM + 10% mouse serum, (C) 6'S-Di-LN 100μM + H5 1.4μM +10% mouse serum, and (D) αH5—EAMs only.

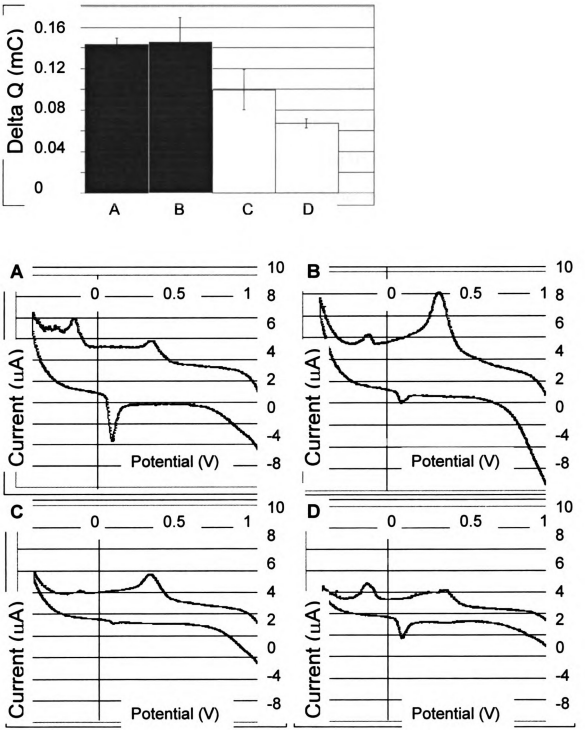

Figure 31. H1 binding to a2,3 versus a2,6-linked glycan receptors using preconcentration method. (a) 6'S-Di-LN 100μM + H1 1.4μM + 10% mouse serum, (b) 6'S-Di-LN 100μM + H1 700nM + 10% mouse serum, (c) 3'S-Di-LN 100μM + H1 1.4μM + 10% mouse serum, and (d) αH1—EAMs only.

CHAPTER 6: CONCLUSION AND FUTURE RESEARCH

In this dissertation, SPR and biosensor assays were explored as tools for pandemic FLUAV detection. A novel SPR assay was designed, which utilized H5-specific sialic acid receptors to specifically and sensitively identify H5 HA protein. The sensitivity of the H5-targeted assay in the detection of recombinant H5 hemagglutinin (H5N1 A/Vietnam/1203/04) was found to be 10.6 nM in buffer and 31.4 nM in 2% mouse serum. The SPR assay demonstrated high avidity of binding between H5 and α2,3-linked glycans 3'SLex and 3'SLN with statistically lower binding between H5 and α2,6-linked 6'SLN, α2,8-linked GD2, and α2,3-linked CT/Sda, which is confirmatory to expected results and demonstrates that the SPR assay can characterize HA by sialic acid receptor preference. The biosensor showed high specificity for H5 as compared to H1 (H1N1 A/South Carolina/1/18) and H3 (H3N2 A/Wyoming/3/03).

Our results indicate that the SPR assay could identify plasma with high neutralizing activity, as inhibitors of glycan/HA binding, for facilitating high potency FLUIGIV manufacture. The SPR neutralization assay has shown a range of anti-H5 monoclonal antibodies from 1:250 to 1:4000 to be neutralizing against glycan/H5 binding. These highly diluted samples ensure physiologically relevant inclusion, as a 1:80 convalescent plasma dilution has previously been shown in patient testing to have a neutralizing antibody titer (Zhou *et al.*, 2007). The assay may facilitate large-scale FLUIGIV screening to reliably identify plasma that is highly neutralizing against pandemic avian influenza viruses with α2,3 specificity.

From these results, we expect that the SPR-based assay can be easily modified to similarly detect HAs with α2,6 specificity, an indicator of human pandemic potential.

The SPR assay may serve as the first line of identification of a historically avian α2,3-specific FLUAV that antigenically shifts to become α2,6 specific and thus transmissible from human-to-human.

Future work will include the development of a pandemic H1N1 targeted assay, in which H1 HA will be identified by H1-specific sialic acids. Screening for H1N1-specific FLUIGIV would produce passive therapies that could be useful in the face of a vaccine shortage as seen with the 2009 novel H1N1 pandemic. Clinical samples of plasma or nasal fluid from animal or human subjects would increase complexity of the system, and the mouse serum matrix tested here is only intended to offer a first step towards a more complex system. Because clinical experimentation indicates that highly diluted samples offer neutralizing activity, any limitations of the SPR system as a plasma screening assay due to matrix interference may be reduced when testing high dilutions. Identification of multimeric recombinant HA, pseudovirus particles, or whole virus in complex matrices such as serum or respiratory secretions is another long-term goal. The development of such an assay which identifies FLUAV HA based on specificity to host sialic acids is a significant initiative with applications in surveillance, serodiagnosis, and homeland security.

Further work is required to optimize the SPR assay in terms of sensitivity to detect HA at concentrations reflecting the viral load in an influenza infected patient. Preconcentration of target analyte is a viable option. Nonspecific binding can be further reduced by improving blocking techniques. The sensitivity, specificity, and repeatability of our novel method are promising. The SPR assay design is easily adaptable to detection of other FLUAV strains, including the current swine-origin H1N1. The Biacore SPR

assay is an appropriate technique for understanding the specificity and avidity of glycan/HA partners and for probing cross-clade protection of anti-HA antibodies, and ultimately could find applicability as a screening assay for highly-neutralizing plasma.

An electrochemical biosensor was developed which utilized electrically active polyaniline coated magnetic nanoparticles (EAMs) both as a magnetic separator and a biosensor transducer.

The sensitivity of the biosensor prepared with 3'SLex or 3'SLN in the detection of recombinant H5 hemagglutinin (H5N1 A/Vietnam/1203/04) was found to be 1.4 μM in 10% mouse serum. The sensitivity of the biosensor prepared with 3'S-Di-LN in the detection of recombinant H5 was found to be 700 nM in 10% mouse serum. The biosensor sensitivity for H1 hemagglutinin (H1N1 A/South Carolina/1/18) as prepared with 6'S-Di-LN was found to be 700 nM. The biosensor demonstrates high avidity of binding between H5 and α2,3-linked glycans 3'SLex, 3'SLN, and 3'S-Di-LN, with statistically lower binding between H5 and α2,6-linked 6'SLN and 6'S-Di-LN, and α2,8-linked GT3, which is confirmatory to expected results and demonstrates that the biosensor can characterize HA by sialic acid receptor preference. The avian FLUAV targeted biosensor showed high specificity for H5 as compared to H1 and the human FLUAV targeted biosensor also offered proof of concept for H1 binding to α2,6 sialic acids, indicating that the biosensor is easily adaptable to an α2,6 targeted biosensor using appropriate α2,6 linked sialic acid receptors. The biosensor architecture and fabrication and testing techniques are easily amenable to the detection of any FLUAV HA subtype.

The biosensor system is rapid to results, with signal detection time at 8 minutes or less. The five-hour SPCE preparation may be performed offline, with SPCE storage for

months prior to testing. Using the preconcentration method, the entire sample preparation time requires 75 minutes, including complex incubation, magnetic separations, washes, and SPCE application.

The biosensor technology is thus able to repeatably distinguish α2,3-specific FLUAV strains from α2,6 specific strains, and could thus offer frontline detection of an emerging human-transmissible strain. Once a highly pathogenic FLUAV strain achieves human transmissibility via antigenic shifting, the strain could cause a human pandemic, and a point-of-care biosensor such as that proposed here, could be used at hospitals, doctors' offices, or borders as the first line in detection, prophylaxis, and mobilizing of treatments. The biosensor technology offers quick and reliable identification of the receptor preference of a FLUAV strain, which is the key characteristic involved in host range and pandemic potential.

This research shows the ability of the EAMs to immunomagnetically separate target HA from serum matrix. This capacity will be exploited in future applications in which whole or pseudotyped virus will be identified in complex matrices such as serum or respiratory secretions. The large size of a whole or pseudotyped virus in comparison to the recombinant HA proteins tested here may introduce stearic hindrance effects. The sandwich biosensor assay is attractive in that while the whole virus may be large, there will be many HA proteins covering the surface, allowing a similarly high number of immunofuntionalized EAMs to cover the surface of any captured virions, and thus leading to no signal loss. This is in comparison to the direct label-free SPR assay, in which stearic hindrance effects could lead to signal loss if fewer virions are captured to the immobilized glycans.

The results indicate that the biosensor technology is valuable as a rapid, specific, and sensitive detection method with applicability at point-of-care for identifying highly pathogenic avian influenza viruses with α2,3 specificity or for identifying human influenza viruses with α2,6 specificity, and for differentiating between pandemic and nonpandemic strains. This is important from an agricultural as well as a biosecurity standpoint. The development of such a biosensor technology which identifies FLUAV HA based on specificity to host sialic acids is a significant initiative with applications in disease monitoring and homeland security.

In summary, this research demonstrates the applicability of both SPR and biosensor platforms for the detection of FLUAV HA using strain-specific glycan receptors, for purposes of prophylaxis, treatment, and early detection.

APPENDIX A: STATISTICAL ANALYSIS RESULTS

A.1 ANOVA ANALYSIS OF SPR RESULTS

Table A-1. SPR Results for Different HA-Glycan Pairs: Least Square Means

Group	Description	Peak Estimate (RU)	Standard Error	DF	t Value	Pr > |t|
1	H5 0.25ug/ml 3'Slex	4.730	1.1847	2	3.99	0.0001
2	H5 0.74ug/ml 3'Slex	19.707	1.8258	2	10.79	<0.0001
3	H5 0.74ug/ml 3'Slex Chip 3	24.410	0.3151	2	77.47	<0.0001
4	H5 2.2ug/ml 3'Slex	59.036	3.3999	2	17.36	<0.0001
5	H5 2.2ug/ml 3'Slex Chip 3	82.855	3.4933	2	23.72	<0.0001
6	H5 6.6ug/ml 3'Slex	145.210	25.1075	2	5.78	<0.0001
7	H5 6.6ug/ml 3'Slex Chip 3	228.900	2.5977	2	88.12	<0.0001
8	H5 V BEI 10ug/ml 3'Slex	397.040	15.9780	2	24.85	<0.0001
9	H5 20ug/ml 3'Slex	745.060	27.1531	2	27.44	<0.0001
10	H5 0.25ug/ml 3'SLN	10.309	1.2086	2	8.53	<0.0001
11	H5 0.74ug/ml 3'SLN	39.811	2.9209	2	13.63	<0.0001
12	H5 2.2ug/ml 3'SLN	131.520	5.3201	2	24.72	<0.0001
13	H5 6.6ug/ml 3'SLN 2	361.500	23.1912	2	15.59	<0.0001
14	H5 10ug only 3'SLN	897.170	13.9810	2	64.17	<0.0001
15	H5 20ug/ml 3'SLN	1493.760	32.0269	2	46.64	<0.0001
16	H1 2.2ug/ml 3'SLN	-4.159	0.5703	2	-7.29	<0.0001
17	H1 6.6ug/ml 3'SLN	-7.628	1.7263	2	-4.42	<0.0001
18	H16.6+aH1 1:500 3'SLN	-3.276	0.7730	2	-4.24	<0.0001
19	H16.6+aH1 1:1000 3'SLN	-4.443	0.8485	2	-5.24	<0.0001
20	anti-H1 1:500 3'SLN	-2.698	16.6168	2	-0.16	0.8712
21	H16.6+aH5 1:500 3'SLN	-0.127	0.3061	2	-0.42	0.6786
22	H16.6+aH5 1:1000 3'SLN	2.050	0.6675	2	3.07	0.0025
23	anti-H5 1:500 3'SLN	1.857	16.6168	2	0.11	0.9112
24	H56.6+anti1:250 3'SLN	41.658	4.6252	2	9.01	<0.0001
25	H56.6+anti1:500 3'SLN	46.624	5.1730	2	9.01	<0.0001
26	H56.6+anti1:1000 3'SLN	14.581	0.4621	2	31.55	<0.0001
27	HA1 H5 2.2ug/ml 3'SLN	-8.397	0.6350	2	-13.22	<0.0001
28	HA1 H5 2.2ug/ml 3'Slex	0.156	16.6168	2	0.01	0.9925
29	HA1 H5 6.6ug/ml 3'SLN	-9.242	1.7890	2	-5.17	<0.0001
30	HA1 H5 6.6ug/ml 3'Slex	1.286	16.6168	2	0.08	0.9384
31	HA1 H5 20ug/ml 3'SLN	-8.921	0.2980	2	-29.94	<0.0001
32	HA1 H5 20ug/ml 3'Slex	1.094	16.6168	2	0.07	0.9476
33	HA1 H3 2.2ug/ml 3'SLN	-9.093	0.5135	2	-17.71	<0.0001

Table A-1. Continued

34	HA1 H3 2.2ug/ml 3'Slex	5.872	16.6168	2	0.35	0.7243
35	HA1 H3 6.6ug/ml 3'SLN	-9.115	0.0545	2	-167.24	<0.0001
36	HA1 H3 6.6ug/ml 3'Slex	15.639	16.6168	2	0.94	0.3482
37	HA1 H3 20ug/ml 3'SLN	-8.384	0.7060	2	-11.88	<0.0001
38	HA1 H3 20ug/ml 3'Slex	30.125	16.6168	2	1.81	0.0719
39	D5 0%	-4.008	3.9640	2	-1.01	0.3136
40	D4 0.25%	-3.870	3.5615	2	-1.09	0.279
41	D3 0.5%	-2.911	5.4010	2	-0.54	0.5907
42	D2 0.75%	4.780	4.2085	2	1.14	0.2579
43	D1 1%	8.779	2.0315	2	4.32	<0.0001
44	HA1 H5 2.2ug/ml - D3	-0.722	1.3285	2	-0.54	0.5879
45	HA1 H5 6.6ug/ml - D3	-2.171	1.5290	2	-1.42	0.1577
46	HA1 H5 20ug/ml - D3	-2.980	0.8140	2	-3.66	0.0004
47	HA1 H3 2.2ug/ml - D3	-1.663	0.4065	2	-4.09	<0.0001
48	HA1 H3 6.6ug/ml - D3	-1.914	0.2190	2	-8.74	<0.0001
49	HA1 H3 20ug/ml - D3	-1.285	0.6345	2	-2.02	0.0447
50	BEI H5 10ug/ml - D3	77.953	16.6168	2	4.69	<0.0001
51	H510ugH5mAb1:250 3'Slex	21.825	4.1990	2	5.20	<0.0001
52	H510ugH5mAb1:500 3'Slex	23.629	3.1844	2	7.42	<0.0001
53	H510ugH5mAb1:1k 3'Slex	26.229	4.6675	2	5.62	<0.0001
54	H510ugH5mAb1:2k 3'Slex	120.000	15.4232	2	7.78	<0.0001
55	H510ugH5mAb1:4k 3'Slex	352.290	40.1883	2	8.77	<0.0001
56	H510ugH5mAb1:8k 3'Slex	546.050	16.6620	2	32.77	<0.0001
57	antiH5mAb 1:250 3'Slex	15.695	2.8137	2	5.58	<0.0001
58	H510ug+1%s 3'Slex	77.637	16.6168	2	4.67	<0.0001
59	H510mAb1:250+1%s 3'Slex	14.951	16.6168	2	0.90	0.3697
60	H510mAb1:500+1%s 3'Slex	17.416	16.6168	2	1.05	0.2963
61	H510mAb1:1k+1%s 3'Slex	18.973	16.6168	2	1.14	0.2554
62	H510mAb1:2k+1% 3'Slex	37.571	16.6168	2	2.26	0.0252
63	H510mAb1:4k+1% 3'Slex	54.793	16.6168	2	3.30	0.0012
64	antiH51:250+1% 3'Slex	7.813	16.6168	2	0.47	0.6389
65	H510ugH5mAb1:250 3'SLN	58.851	5.2785	2	11.15	<0.0001
66	H510ugH5mAb1:500 3'SLN	75.372	6.6805	2	11.28	<0.0001
67	H510ugH5mAb1:1k 3'SLN	75.357	23.7535	2	3.17	0.0018
68	H510ugH5mAb1:2k 3'SLN	358.640	9.4680	2	37.88	<0.0001
69	H510ugH5mAb1:4k 3'SLN	824.760	15.7440	2	52.39	<0.0001
70	H510ugH5mAb1:8k 3'SLN	1129.820	10.9750	2	102.94	<0.0001
71	antiH5mAb 1:250 3'SLN	46.071	5.1215	2	9.00	<0.0001
72	H510ug+1%s 3'SLN	334.670	16.6168	2	20.14	<0.0001

Table A-1. Continued

73	H510mAb1:250+1%s 3'SLN	47.372	16.6168	2	2.85	0.005
74	H510mAb1:500+1%s 3'SLN	55.637	16.6168	2	3.35	0.001
75	H510mAb1:1k+1%s 3'SLN	50.081	16.6168	2	3.01	0.003
76	H510mAb1:2k+1% 3'SLN	148.240	16.6168	2	8.92	<0.0001
77	H510mAb1:4k+1% 3'SLN	229.790	16.6168	2	13.83	<0.0001
78	antiH51:250+1% 3'SLN	21.135	16.6168	2	1.27	0.2054
79	H5VBEI10+aI1:250 3'Slex	283.670	16.6168	2	17.07	<0.0001
80	H5VBEI10+aH1250 3'Slex	213.410	16.6168	2	12.84	<0.0001
81	H5 V IT 10ug/ml 3'Slex	-3.759	16.6168	2	-0.23	0.8213
82	H5VIT10+aV1:250 3'Slex	322.860	16.6168	2	19.43	<0.0001
83	H5VIT10+aV1:500 3'Slex	13.606	16.6168	2	0.82	0.4142
84	H5VIT10+aV1:1000 3'Slex	5.772	16.6168	2	0.35	0.7288
85	H5 Indo IT 10ug/ml 3'Slex	3.032	16.6168	2	0.18	0.8555
86	H5IIT10+aI1:250 3'Slex	9.693	16.6168	2	0.58	0.5606
87	H5IIT10+aI1:500 3'Slex	9.933	16.6168	2	0.60	0.5509
88	H5IIT10+aI1:1000 3'Slex	6.612	16.6168	2	0.40	0.6913
89	a-Indo 1:250 3'Slex	-0.893	16.6168	2	-0.05	0.9572
90	H5IIT10+aV1:250 3'Slex	107.880	16.6168	2	6.49	<0.0001
91	H5IIT10+aH11:250 3'Slex	27.783	16.6168	2	1.67	0.0966
92	H1SC 10ug/ml 3'Slex	-2.407	16.6168	2	-0.14	0.885
93	H1SC10+a-H11:250 3'Slex	10.842	16.6168	2	0.65	0.5151
94	H1SC10+a-H11:500 3'Slex	2.822	16.6168	2	0.17	0.8654
95	H1SC10+a-H11000 3'Slex	-1.585	16.6168	2	-0.10	0.9241
96	a-H1 Pan 1:250 3'Slex	8.872	16.6168	2	0.53	0.5942
97	H1SC10+a-V1:250 3'Slex	47.264	16.6168	2	2.84	0.0051
98	H1SC10+a-I1:250 3'Slex	-0.973	16.6168	2	-0.06	0.9534
99	H5VBEI10+aI1:250 3'SLN	282.010	16.6168	2	16.97	<0.0001
100	H5VBEI10+aH1250 3'SLN	211.990	16.6168	2	12.76	<0.0001
101	H5 V IT 10ug/ml 3'SLN	-5.064	16.6168	2	-0.30	0.761
102	H5VIT10+aV1:250 3'SLN	321.350	16.6168	2	19.34	<0.0001
103	H5VIT10+aV1:500 3'SLN	12.589	16.6168	2	0.76	0.4499
104	H5VIT10+aV1:1000 3'SLN	4.572	16.6168	2	0.28	0.7836
105	H5 Indo IT 10ug/ml 3'SLN	1.951	16.6168	2	0.12	0.9067
106	H5IIT10+aI1:250 3'SLN	8.287	16.6168	2	0.50	0.6187
107	H5IIT10+aI1:500 3'SLN	8.820	16.6168	2	0.53	0.5964
108	H5IIT10+aI1:1000 3'SLN	5.219	16.6168	2	0.31	0.7539
109	a-Indo 1:250 3'SLN	-2.001	16.6168	2	-0.12	0.9043
110	H5IIT10+aV1:250 3'SLN	106.560	16.6168	2	6.41	<0.0001
111	H5IIT10+aH11:250 3'SLN	26.665	16.6168	2	1.60	0.1107
112	H1SC 10ug/ml 3'SLN	-3.413	16.6168	2	-0.21	0.8375
113	H1SC10+a-H11:250 3'SLN	9.177	16.6168	2	0.55	0.5816
114	H1SC10+a-H11:500 3'SLN	1.816	16.6168	2	0.11	0.9131

Table A-1. Continued

115	H1SC10+a-H11000 3'SLN	-2.806	16.6168	2	-0.17	0.8661
116	a-H1 Pan 1:250 3'SLN	7.629	16.6168	2	0.46	0.6468
117	H1SC10+a-V1:250 3'SLN	45.888	16.6168	2	2.76	0.0065
118	H1SC10+a-I1:250 3'SLN	-2.140	16.6168	2	-0.13	0.8977
119	H5 6.6ug + 1%s 3'Slex	65.617	16.6168	2	3.95	0.0001
120	H5 20ug + 1%s 3'Slex	443.440	16.6168	2	26.69	<0.0001
121	H5 6.6ug + 1%s 3'SLN	238.340	16.6168	2	14.34	<0.0001
122	H5 20ug + 1%s 3'SLN	999.190	16.6168	2	60.13	<0.0001
123	H3 2.2ug 3'Slex	-3.137	16.6168	2	-0.19	0.8505
124	H3 6.6ug 3'Slex	-2.666	16.6168	2	-0.16	0.8728
125	H3 11.9ug 3'Slex	-3.233	16.6168	2	-0.19	0.846
126	H5 0.24ug + 2%s 3'Slex	-5.936	16.6168	2	-0.36	0.7214
127	H5 0.73ug + 2%s 3'Slex	-6.668	16.6168	2	-0.40	0.6888
128	H5 2.2ug + 2%s 3'Slex	-7.298	16.6168	2	-0.44	0.6612
129	H5 6.6ug + 2%s 3'Slex	-4.873	16.6168	2	-0.29	0.7697
130	H5 20ug + 2%s 3'Slex	14.021	16.6168	2	0.84	0.4002
131	H3 0.24ug + 2%s 3'Slex	26.359	16.6168	2	1.59	0.1148
132	H3 0.73ug + 2%s 3'Slex	-1.701	16.6168	2	-0.10	0.9186
133	H3 2.2ug + 2%s 3'Slex	26.717	16.6168	2	1.61	0.11
134	H3 6.6ug + 2%s 3'Slex	-1.709	16.6168	2	-0.10	0.9182
135	H3 11.9ug + 2%s 3'Slex	10.403	16.6168	2	0.63	0.5322
136	H3 2.2ug 3'SLN	-5.191	16.6168	2	-0.31	0.7552
137	H3 6.6ug 3'SLN	-5.334	16.6168	2	-0.32	0.7487
138	H3 11.9ug 3'SLN	-5.593	16.6168	2	-0.34	0.7369
139	H5 0.24ug + 2%s 3'SLN	3.197	16.6168	2	0.19	0.8477
140	H5 0.73ug + 2%s 3'SLN	2.306	16.6168	2	0.14	0.8898
141	H5 2.2ug + 2%s 3'SLN	7.072	16.6168	2	0.43	0.671
142	H5 6.6ug + 2%s 3'SLN	13.290	16.6168	2	0.80	0.4251
143	H5 20ug + 2%s 3'SLN	28.034	16.6168	2	1.69	0.0937
144	H3 0.24ug + 2%s 3'SLN	41.077	16.6168	2	2.47	0.0146
145	H3 0.73ug + 2%s 3'SLN	-4.963	16.6168	2	-0.30	0.7656
146	H3 2.2ug + 2%s 3'SLN	41.955	16.6168	2	2.52	0.0126
147	H3 6.6ug + 2%s 3'SLN	-4.804	16.6168	2	-0.29	0.7729
148	H3 11.9ug + 2%s 3'SLN	3.519	16.6168	2	0.21	0.8326
149	H5 HBSEP 4hr 37 3'Slex	76.432	16.6168	2	4.60	<0.0001
150	H5 Brom 4hr 37 3'Slex	10.813	16.6168	2	0.65	0.5162
151	H5 Brom2ME 4hr37 3'Slex	-6.798	16.6168	2	-0.41	0.6831
152	H5 HBSEP o/n 37 3'Slex	309.130	16.6168	2	18.60	<0.0001
153	H5 Brom o/n 37 3'Slex	4.153	16.6168	2	0.25	0.803
154	H5 Brom2ME o/n37 3'Slex	-3.114	16.6168	2	-0.19	0.8516
155	H5 0.02%tween 3'Slex	578.480	16.6168	2	34.81	<0.0001

Table A-1. Continued

156	H5 0.05%tween 3'Slex	398.980	16.6168	2	24.01	<0.0001
157	H5 0.08%tween 3'Slex	351.030	16.6168	2	21.13	<0.0001
158	H5 0.1%tween 3'Slex	230.320	16.6168	2	13.86	<0.0001
159	H5 10min56 +4deg 3'Slex	0.514	16.6168	2	0.03	0.9754
160	H5 10min 56 only 3'Slex	4.732	16.6168	2	0.28	0.7762
161	H5 HBSEP 4hr 37 3'SLN	121.000	16.6168	2	7.28	<0.0001
162	H5 Brom 4hr 37 3'SLN	-21.223	16.6168	2	-1.28	0.2035
163	H5 Brom2ME 4hr37 3'SLN	-62.782	16.6168	2	-3.78	0.0002
164	H5 HBSEP o/n 37 3'SLN	548.840	16.6168	2	33.03	<0.0001
165	H5 Brom o/n 37 3'SLN	-2.915	16.6168	2	-0.18	0.861
166	H5 Brom2ME o/n37 3'SLN	-19.331	16.6168	2	-1.16	0.2466
167	H5 0.02%tween 3'SLN	959.430	16.6168	2	57.74	<0.0001
168	H5 0.05%tween 3'SLN	754.050	16.6168	2	45.38	<0.0001
169	H5 0.08%tween 3'SLN	668.130	16.6168	2	40.21	<0.0001
170	H5 0.1%tween 3'SLN	464.360	16.6168	2	27.95	<0.0001
171	H5 10min56 +4deg 3'SLN	-0.257	16.6168	2	-0.02	0.9877
172	H5 10min 56 only 3'SLN	4.547	16.6168	2	0.27	0.7847
173	HA5 10ug 3'Slex	102.180	16.6168	2	6.15	<0.0001
174	HA5 10ug + anti-HA2 1:250 3'Slex	107.140	16.6168	2	6.45	<0.0001
175	HA5 10ug + anti-HA2 1:500 3'Slex	101.050	16.6168	2	6.08	<0.0001
176	HA5 10ug + anti-HA2 1:1000 3'Slex	98.152	16.6168	2	5.91	<0.0001
177	HA5 10ug + anti-HA2 1:2000 3'Slex	98.072	16.6168	2	5.90	<0.0001
178	anti-HA2 1:250 3'Slex	0.878	16.6168	2	0.05	0.9579
179	HA5 10ug + anti-H5 mAb 1:1000 3'Slex	185.930	16.6168	2	11.19	<0.0001
180	HA5 10ug 3'SLN	347.810	16.6168	2	20.93	<0.0001
181	HA5 10ug + anti-HA2 1:250 3'SLN	350.130	16.6168	2	21.07	<0.0001
182	HA5 10ug + anti-HA2 1:500 3'SLN	334.310	16.6168	2	20.12	<0.0001
183	HA5 10ug + anti-HA2 1:1000 3'SLN	331.490	16.6168	2	19.95	<0.0001
184	HA5 10ug + anti-HA2 1:2000 3'SLN	332.750	16.6168	2	20.02	<0.0001
185	anti-HA2 1:250 3'SLN	0.834	16.6168	2	0.05	0.96
186	HA5 10ug + anti-H5 mAb 1:1000 3'SLN	640.140	16.6168	2	38.52	<0.0001
187	buffer	-1.827	0.4462	2	-4.10	<0.0001

Table A-1. Continued

188	buffer different regen 7mMNaOH 2.5MNaCl	-4.892	0.2458	2	-19.90	<0.0001
189	buffer 1%mouse serum 3'Slex	6.327	0.2388	2	26.50	<0.0001
190	buffer 1%mouse serum 3'SLN	0.412	0.2103	2	1.96	0.0523
191	buffer 10%serum 3'Slex	19.465	2.8250	2	6.89	<0.0001
192	buffer 5%serum 3'Slex	29.515	0.4850	2	60.86	<0.0001
193	buffer 2%serum 3'Slex	15.315	0.6550	2	23.38	<.0001
194	buffer 1%serum 3'Slex	5.865	0.4550	2	12.89	<.0001
195	buffer 10%serum 3'SLN	37.400	5.8000	2	6.45	<.0001
196	buffer 5%serum 3'SLN	35.050	0.5500	2	63.73	<.0001
197	buffer 2%serum 3'SLN	13.750	0.3500	2	39.29	<.0001
198	buffer 1%serum 3'SLN	3.130	0.0500	2	62.60	<.0001
199	buffer 10%serum 3'Slex after 3 min dissoc	1.920	0.7400	2	2.59	0.0104
200	buffer 5%serum 3'Slex after 3 min dissoc	-1.009	0.0715	2	-14.10	<.0001
201	buffer 2%serum 3'Slex after 3 min dissoc	-1.018	0.6445	2	-1.58	0.1165
202	buffer 1%serum 3'Slex after 3 min dissoc	-0.993	0.4830	2	-2.06	0.0415
203	buffer 10%serum 3'SLN after 3 min dissoc	10.095	3.2050	2	3.15	0.002
204	buffer 5%serum 3'SLN after 3 min dissoc	0.706	0.0730	2	9.67	<.0001
205	buffer 2%serum 3'SLN after 3 min dissoc	-0.769	0.4310	2	-1.78	0.0764
206	buffer 1%serum 3'SLN after 3 min dissoc	-0.839	0.4110	2	-2.04	0.043

Table A-2. SPR Group Comparisons: Estimates

Label	Peak Estimate (RU)	Standard Error	DF	t Value	Pr > |t|
Group 1 vs. 2	-14.977	2.1764	2	-6.88	<0.0001
Group 1 vs. 4	-54.306	3.6004	2	-15.08	<0.0001
Group 1 vs. 6	-140.480	25.1354	2	-5.59	<0.0001
Group 1 vs. 8	-392.310	16.0218	2	-24.49	<0.0001
Group 1 vs. 9	-740.330	27.1790	2	-27.24	<0.0001
Group 2 vs. 4	-39.330	3.8591	2	-10.19	<0.0001
Group 2 vs. 6	-125.500	25.1738	2	-4.99	<0.0001
Group 2 vs. 8	-377.330	16.0820	2	-23.46	<0.0001
Group 2 vs. 9	-725.360	27.2144	2	-26.65	<0.0001
Group 4 vs. 6	-86.170	25.3366	2	-3.40	0.0009
Group 4 vs. 8	-338.000	16.3357	2	-20.69	<0.0001
Group 4 vs. 9	-686.030	27.3651	2	-25.07	<0.0001
Group 6 vs. 8	-251.830	29.7604	2	-8.46	<0.0001
Group 6 vs. 9	-599.860	36.9821	2	-16.22	<0.0001
Group 8 vs. 9	-348.020	31.5054	2	-11.05	<0.0001
Group 2 vs. 3	-4.703	1.8528	2	-2.54	0.0122
Group 4 vs. 5	-23.818	4.8746	2	-4.89	<0.0001
Group 6 vs. 7	-83.691	25.2415	2	-3.32	0.0012
Group 10 vs. 11	-29.502	3.1611	2	-9.33	<0.0001
Group 10 vs. 12	-121.210	5.4557	2	-22.22	<0.0001
Group 10 vs. 13	-351.190	23.2227	2	-15.12	<0.0001
Group 10 vs. 14	-886.870	14.0332	2	-63.20	<0.0001
Group 10 vs. 15	-1483.450	32.0497	2	-46.29	<0.0001
Group 11 vs. 12	-91.705	6.0692	2	-15.11	<0.0001
Group 11 vs. 13	-321.690	23.3744	2	-13.76	<0.0001
Group 11 vs. 14	-857.360	14.2829	2	-60.03	<0.0001
Group 11 vs. 15	-1453.950	32.1598	2	-45.21	<0.0001
Group 12 vs. 13	-229.980	23.7936	2	-9.67	<0.0001
Group 12 vs. 14	-765.660	14.9590	2	-51.18	<0.0001
Group 12 vs. 15	-1362.250	32.4657	2	-41.96	<0.0001
Group 13 vs. 14	-535.670	27.0796	2	-19.78	<0.0001
Group 13 vs. 15	-1132.260	39.5418	2	-28.63	<0.0001
Group 14 vs. 15	-596.590	34.9455	2	-17.07	<0.0001
Group 1 vs. 10	-5.579	1.6924	2	-3.30	0.0012
Group 2 vs. 11	-20.104	3.4446	2	-5.84	<0.0001
Group 4 vs. 12	-72.479	6.3137	2	-11.48	<0.0001
Group 6 vs. 13	-216.290	34.1792	2	-6.33	<0.0001
Group 8 vs. 14	-500.140	21.2312	2	-23.56	<0.0001
Group 9 vs. 15	-748.700	41.9882	2	-17.83	<0.0001

Table A-2. Continued

Group 12 vs. 16	135.670	5.3506	2	25.36	<0.0001
Group 13 vs. 17	369.130	23.2554	2	15.87	<0.0001
Group 16 vs. 17	3.469	1.8181	2	1.91	0.0583
Group 18 vs. 19	1.167	1.1478	2	1.02	0.3112
Group 17 vs. 18	-4.352	1.8915	2	-2.30	0.0228
Group 17 vs. 19	-3.186	1.9235	2	-1.66	0.0998
Group 21 vs. 22	-2.177	0.7343	2	-2.96	0.0035
Group 18 vs. 21	-3.149	0.8314	2	-3.79	0.0002
Group 19 vs. 22	-6.492	1.0796	2	-6.01	<0.0001
Group 24 vs. 25	-4.965	6.9392	2	-0.72	0.4754
Group 24 vs. 26	27.078	4.6482	2	5.83	<0.0001
Group 25 vs. 26	32.043	5.1936	2	6.17	<0.0001
Group 12 vs. 27	139.910	5.3579	2	26.11	<0.0001
Group 53 vs. 57	10.534	5.4500	2	1.93	0.0552
Group 54 vs. 55	-232.290	43.0462	2	-5.40	<0.0001
Group 54 vs. 56	-426.050	22.7045	2	-18.77	<0.0001
Group 54 vs. 57	104.310	15.6777	2	6.65	<0.0001
Group 55 vs. 56	-193.760	43.5054	2	-4.45	<0.0001
Group 55 vs. 57	336.590	40.2867	2	8.35	<0.0001
Group 56 vs. 57	530.360	16.8979	2	31.39	<0.0001
Group 8 vs. 51	375.210	16.5205	2	22.71	<0.0001
Group 8 vs. 52	373.410	16.2922	2	22.92	<0.0001
Group 8 vs. 53	370.810	16.6457	2	22.28	<0.0001
Group 8 vs. 54	277.040	22.2074	2	12.48	<0.0001
Group 8 vs. 55	44.751	43.2481	2	1.03	0.3025
Group 8 vs. 56	-149.010	23.0850	2	-6.45	<0.0001
Group 8 vs. 57	381.340	16.2238	2	23.51	<0.0001
Group 65 vs. 66	-16.521	8.5142	2	-1.94	0.0542
Group 65 vs. 67	-16.506	24.3329	2	-0.68	0.4986
Group 65 vs. 68	-299.790	10.8400	2	-27.66	<0.0001
Group 65 vs. 69	-765.910	16.6053	2	-46.12	<0.0001
Group 65 vs. 70	-1070.960	12.1784	2	-87.94	<0.0001
Group 65 vs. 71	12.780	7.3547	2	1.74	0.0844
Group 66 vs. 67	0.015	24.6750	2	0.00	0.9995
Group 66 vs. 68	-283.270	11.5876	2	-24.45	<0.0001
Group 66 vs. 69	-749.390	17.1027	2	-43.82	<0.0001
Group 66 vs. 70	-1054.440	12.8483	2	-82.07	<0.0001
Group 66 vs. 71	29.301	8.4178	2	3.48	0.0007
Group 67 vs. 68	-283.280	25.5709	2	-11.08	<0.0001
Group 67 vs. 69	-749.400	28.4974	2	-26.30	<0.0001

Table A-2. Continued

Group 67 vs. 70	-1054.460	26.1664	2	-40.30	<0.0001
Group 67 vs. 71	29.286	24.2994	2	1.21	0.23
Group 68 vs. 69	-466.120	18.3716	2	-25.37	<0.0001
Group 68 vs. 70	-771.180	14.4946	2	-53.20	<0.0001
Group 68 vs. 71	312.570	10.7644	2	29.04	<0.0001
Group 69 vs. 70	-305.060	19.1918	2	-15.90	<0.0001
Group 69 vs. 71	778.690	16.5561	2	47.03	<0.0001
Group 70 vs. 71	1083.740	12.1112	2	89.48	<0.0001
Group 14 vs. 65	838.320	14.9443	2	56.10	<0.0001
Group 14 vs. 66	821.800	15.4951	2	53.04	<0.0001
Group 14 vs. 67	821.820	27.5626	2	29.82	<0.0001
Group 14 vs. 68	538.530	16.8853	2	31.89	<0.0001
Group 14 vs. 69	72.416	21.0557	2	3.44	0.0008
Group 14 vs. 70	-232.640	17.7741	2	-13.09	<0.0001
Group 14 vs. 71	851.100	14.8896	2	57.16	<0.0001
Group 187 vs. 188	3.064	0.5095	2	6.01	<0.0001
Group 187 vs. 190	-2.239	0.4933	2	-4.54	<0.0001
Group 188 vs. 190	-5.303	0.3235	2	-16.39	<0.0001
Group 189 vs. 190	5.915	0.3182	2	18.59	<0.0001
Group 191 vs. 192	-10.050	2.8663	2	-3.51	0.0006
Group 191 vs. 193	4.150	2.8999	2	1.43	0.1545
Group 191 vs. 194	13.600	2.8614	2	4.75	<0.0001
Group 192 vs. 193	14.200	0.8150	2	17.42	<0.0001
Group 192 vs. 194	23.650	0.6650	2	35.56	<0.0001
Group 193 vs. 194	9.450	0.7975	2	11.85	<0.0001
Group 191-194 vs. 195-198	-4.793	1.6378	2	-2.93	0.004
Group 191 vs. 199	17.545	2.9203	2	6.01	<0.0001
Group 192 vs. 200	30.524	0.4902	2	62.26	<0.0001
Group 193 vs. 201	16.333	0.9189	2	17.77	<0.0001
Group 194 vs. 202	6.858	0.6636	2	10.34	<0.0001
Group 195 vs. 203	27.305	6.6266	2	4.12	<0.0001
Group 196 vs. 204	34.344	0.5548	2	61.90	<0.0001
Group 197 vs. 205	14.519	0.5552	2	26.15	<0.0001
Group 198 vs. 206	3.969	0.4140	2	9.59	<0.0001
Group 187 vs. 199-206	-2.839	0.6197	2	-4.58	<0.0001
Group 187 vs. 16-21	1.894	2.8290	2	0.67	0.5041
Group 187 vs. 51-53	-25.724	2.3893	2	-10.77	<0.0001
Group 187 vs. 65-67	-71.687	8.4243	2	-8.51	<0.0001
Group 187 vs. 71	-47.898	5.1409	2	-9.32	<0.0001

A.2 ANOVA ANALYSIS OF BIOSENSOR RESULTS

Table A-3. Biosensor Results for Different HA-Glycan Pairs: Average ΔQ and Standard Deviation

Grp	Prep	Description	ave ΔQ ± SD (n=3) (mC)
1	Stepwise	H5-specific glycan 3'SLex 100μM - H5 1.4μM - anti-H5--EAM	0.18782 ± 0.0108
2	Stepwise	H5-specific glycan 3'SLex 100μM - H5 700nM - anti-H5--EAM	0.12188 ± 0.0053
3	Stepwise	H5-specific glycan 3'SLex 100μM - H5 360nM - anti-H5--EAM	0.12657 ± 0.0100
4	Stepwise	H5-specific glycan 3'SLex 100μM - H1 1.4μM - anti-H5--EAM	0.08906 ± 0.0045
5	Stepwise	H5-specific glycan 3'SLex 100μM - H1 1.4μM - anti-H1--EAM	0.11863 ± 0.0180
6	Stepwise	no glycan - H1 1.4μM - anti-H1—EAM	0.11747 ± 0.0227
7	Stepwise	no glycan - no HA - anti-H1—EAM	0.13402 ± 0.0073
8	Preconc	(H5-spec glycan 3'SLex 100μM + H5 1.4μM) + anti-H5--EAM	0.42050 ± 0.0087
9	Preconc	[H5-spec glycan 3'SLex 100μM + (H5 1.4μM + 10% mouse serum)] + anti-H5--EAM	0.47444 ± 0.0230
10	Preconc	[H5-spec glycan 3'SLex 100μM + (H5 700nM + 10% mouse serum)] + anti-H5--EAM	0.28153 ± 0.0188
11	Preconc	[H5-spec glycan 3'SLex 100μM + (H5 360nM + 10% mouse serum)]+ anti-H5--EAM	0.24322 ± 0.0226
12	Preconc	[no glycan + (H5 1.4μM + 10% mouse serum)] + anti-H5--EAM	0.25331 ± 0.0373
13	Preconc	(H5-spec glycan 3'SLex 100μM + no H5) + anti-H5--EAM	0.27839 ± 0.0089
14	Preconc	[H5-nonspec glycan GT3 100μM + (H5 1.4μM + 10% mouse serum)] + anti-H5--EAM	0.28812 ± 0.0172
15	Preconc	no glycan + no HA + anti-H5—EAM	0.33222 ± 0.0281
16	Preconc	[H5-spec glycan 3'SLex 100μM + (H1 1.4μM + 10% mouse serum)] + anti-H5--EAM	0.22594 ± 0.0115
17	Preconc	[H5-spec glycan 3'SLex 100μM + (H1 1.4μM + 10% mouse serum)] + anti-H1--EAM	0.29739 ± 0.0001
18	Preconc	[no glycan + (H1 1.4μM + 10% mouse serum)] + anti-H1--EAM	0.29573 ± 0.0068
19	Preconc	no glycan + no HA + anti-H1--EAM	0.25182 ± 0.0207
20	Preconc	[H5-spec glycan 3'SLex 100μM + (H5* 1.4μM + 10% mouse serum)] + anti-H5--EAM	0.27883 ± 0.0222
21	Stepwise	H5-specific glycan 3'SLN 100μM - H5 1.4μM - anti-H5--EAM	0.24382 ± 0.0037
22	Stepwise	H5-specific glycan 3'SLN 500μM - H5 1.4μM - anti-H5--EAM	0.28515 ± 0.0479

Table A-3. Continued

23	Stepwise	H5-specific glycan 3'SLN 500μM - H5 290nM - anti-H5--EAM	0.24340 ± 0.0810
24	Stepwise	H5-nonspecific glycan 6'SLN 500μM – H5 1.4μM - anti-H5--EAM	0.13880 ± 0.0056
25	Stepwise	H5-specific glycan 3'SLN 500μM – noHA - anti-H5--EAM	0.08950 ± 0.0014
26	Stepwise	no glycan - noHA - anti-H5—EAM	0.07957 ± 0.0080
27	Stepwise	no glycan - H5 1.4μM - anti-H5—EAM	0.15473 ± 0.0167
28	Preconc	[H5-spec glycan 3'S-Di-LN 100μM + (H5 1.4μM + 10% mouse serum)] + anti-H5--EAM	0.14014 ± 0.0216
29	Preconc	[H5-nonspec glycan 6'S-Di-LN 100μM + (H1 1.4μM + 10% mouse serum)] + anti-H1--EAM	0.14331 ± 0.0059
30	Preconc	[H5-spec glycan 3'S-Di-LN 100μM + (H1 1.4μM + 10% mouse serum)] + anti-H1--EAM	0.09957 ± 0.0194
31	Preconc	[H5-nonspec glycan 6'S-Di-LN 100μM + (H5 1.4μM + 10% mouse serum)] + anti-H5--EAM	0.08351 ± 0.0092
32	Preconc	[H5-nonspec glycan 6'S-Di-LN 100μM + (H1 700nM + 10% mouse serum)] + anti-H1--EAM	0.14614 ± 0.0233
33	Preconc	no glycan - no HA - anti-H5—EAMs	0.06879 ± 0.0098
34	Preconc	no glycan - no HA - anti-H1—EAMs	0.06698 ± 0.0044
35	Preconc	[H5-spec glycan 3'S-Di-LN 100μM + (H5 700nM + 10% mouse serum)] + anti-H5--EAM	0.13926 ± 0.0059

Table A-4. Biosensor Results for Different HA-Glycan Pairs: Least Squares Means

Group	ΔQ Estimate (mC)	Standard Error	DF	t Value	Pr > |t|
1	0.1878	0.010840	2	17.33	<.0001
2	0.1219	0.005348	2	22.79	<.0001
3	0.1266	0.009954	2	12.72	<.0001
4	0.0891	0.004502	2	19.78	<.0001
5	0.1186	0.017980	2	6.6	<.0001
6	0.1175	0.022740	2	5.16	<.0001
7	0.1340	0.007329	2	18.29	<.0001
8	0.4205	0.008652	2	48.6	<.0001
9	0.4744	0.022980	2	20.64	<.0001
10	0.2815	0.018840	2	14.94	<.0001
11	0.2432	0.022580	2	10.77	<.0001
12	0.2533	0.037310	2	6.79	<.0001
13	0.2784	0.008902	2	31.27	<.0001
14	0.2881	0.017220	2	16.74	<.0001
15	0.3322	0.028100	2	11.82	<.0001
16	0.2259	0.011470	2	19.7	<.0001
17	0.2974	0.000146	2	2040.9	<.0001
18	0.2957	0.006815	2	43.4	<.0001
19	0.2518	0.020700	2	12.17	<.0001
20	0.2788	0.022170	2	12.58	<.0001
21	0.2438	0.003730	2	65.37	<.0001
22	0.2852	0.047880	2	5.96	<.0001
23	0.2434	0.080990	2	3.01	0.0037
24	0.1388	0.005600	2	24.78	<.0001
25	0.0895	0.001457	2	61.42	<.0001
26	0.0796	0.008042	2	9.89	<.0001
27	0.1547	0.016660	2	9.29	<.0001
28	0.1401	0.012480	2	11.23	<.0001
29	0.1433	0.003428	2	41.81	<.0001
30	0.0996	0.011210	2	8.88	<.0001
31	0.0835	0.006500	2	12.85	<.0001
32	0.1461	0.016450	2	8.89	<.0001
33	0.0688	0.005662	2	12.15	<.0001
34	0.0670	0.002516	2	26.63	<.0001
35	0.1390	0.004000	2	34.75	<.0001

Table A-5. Biosensor Group Comparisons: Estimates

Comparison	ΔQ Estimate (mC)	Standard Error	DF	t Value	Pr > |t|
Group 1 vs. 9	-0.2866	0.02541	2	-11.28	<.0001
Group 1 vs. 21	-0.056	0.01146	2	-4.89	<.0001
Group 1 vs. 28	0.0477	0.01652	2	2.89	0.0053
Group 9 vs. 21	0.2306	0.02329	2	9.9	<.0001
Group 9 vs. 28	0.3343	0.02615	2	12.78	<.0001
Group 21 vs. 28	0.1037	0.01302	2	7.96	<.0001
Group 28 vs. 29	-0.0032	0.01294	2	-0.24	0.8074
Group 28 vs. 30	0.0406	0.01677	2	2.42	0.0183
Group 28 vs. 31	0.0566	0.01407	2	4.03	0.0001
Group 28 vs. 33	0.0714	0.0137	2	5.21	<.0001
Group 28 vs. 35	0.0011	0.0131	2	0.09	0.9309
Group 29 vs. 30	0.0437	0.01172	2	3.73	0.0004
Group 29 vs. 31	0.0598	0.00735	2	8.14	<.0001
Group 29 vs. 32	-0.0028	0.0168	2	-0.17	0.8668
Group 29 vs. 34	0.0763	0.00425	2	17.95	<.0001
Group 10 vs. 35	0.1425	0.01926	2	7.4	<.0001
Group 2 vs. 35	-0.0171	0.00668	2	-2.56	0.0126
Group 4 vs. 30	-0.0105	0.01208	2	-0.87	0.3875
Group 24 vs. 31	0.0553	0.00858	2	6.45	<.0001
Group 26 vs. 33	0.0108	0.00984	2	1.1	0.2773
Group 33 vs. 34	0.0018	0.0062	2	0.29	0.7731
Group 30 vs. 34	0.0326	0.01149	2	2.83	0.0061
Group 31 vs. 33	0.0147	0.00862	2	1.71	0.0926
Group 32 vs. 34	0.0791	0.01664	2	4.76	<.0001
Group 35 vs. 33	-0.0702	0.00693	2	-10.13	<.0001
Group 2 vs. 28	-0.0183	0.01357	2	-1.35	0.1831
Group 3 vs. 28	-0.0136	0.01596	2	-0.85	0.3982
Group 4 vs. 28	-0.0511	0.01326	2	-3.85	0.0003
Group 5 vs. 28	-0.0215	0.02188	2	-0.98	0.3292
Group 28 vs. 10-18	-0.1372	0.01415	2	-9.7	<.0001
Group 29 vs. 10-18	-0.134	0.0075	2	-17.88	<.0001
Group 15 vs. 33	0.2634	0.02867	2	9.19	<.0001

Table A-5. Continued

Group 7 vs. 34	0.067	0.00775	2	8.65	<.0001
Group 1 vs. 29	0.0445	0.01136	2	3.92	0.0002
Group 14 vs. 31	0.2046	0.0184	2	11.12	<.0001
Group 1 vs 2	0.06594	0.01208	2	5.46	<.0001
Group 1 vs. 3	0.06125	0.01471	2	4.16	0.0001
Group 2 vs. 3	-0.0047	0.0113	2	-0.42	0.6798
Group 9 vs. 10	0.1929	0.02972	2	6.49	<.0001
Group 9 vs. 11	0.139	0.02074	2	6.7	<.0001
Group 10 vs. 11	0.03831	0.02941	2	1.3	0.1983
Group 1,2,3 vs. 4,5,6,7	0.03063	0.00919	2	3.33	0.0016
Group 9-11 vs. 12-19	0.05519	0.01429	2	3.86	0.0003
Group 8 vs. 9	-0.0539	0.02456	2	-2.2	0.0324
Group 1 vs. 9	-0.2866	0.02541	2	-11.28	<.0001
Group 1 vs. 8	-0.2327	0.01387	2	-16.78	<.0001
Group 1 vs. 20	-0.091	0.02468	2	-3.69	0.0005
Group 1 vs. 21	-0.056	0.01146	2	-4.89	<.0001
Group 20 vs. 21	0.03501	0.02248	2	1.56	0.1253
Group 21-23 vs. 24-27	0.1418	0.03176	2	4.46	<.0001
Group 1,2,3 vs. 9,10,11	-0.1876	0.01349	2	-13.91	<.0001
Group 1,2,3 vs. 21,22,23	-0.112	0.03182	2	-3.52	0.0009
Group 9,10,11 vs. 21,22,23	0.0756	0.03377	2	2.24	0.0293
Group 9 vs. 20	0.1956	0.03194	2	6.13	<.0001
Group 2,3 vs. 4,5,6,7	0.00943	0.00944	2	1	0.3222
Group 10,11 vs. 12-19	-0.0155	0.0163	2	-0.95	0.3461
Group 12 vs. 13	-0.0251	0.03836	2	-0.65	0.516
Group 12 vs. 14	-0.0348	0.04109	2	-0.85	0.4006
Group 12 vs. 15	-0.0789	0.04671	2	-1.69	0.0969
Group 12 vs. 16	0.02737	0.03903	2	0.7	0.4862
Group 12 vs. 17	-0.0441	0.03731	2	-1.18	0.2426
Group 12 vs. 18	-0.0424	0.03793	2	-1.12	0.2684
Group 12 vs. 19	0.00149	0.04266	2	0.03	0.9723
Group 13 vs. 14	-0.0097	0.01938	2	-0.5	0.6174
Group 13 vs. 15	-0.0538	0.02948	2	-1.83	0.0733
Group 13 vs. 16	0.05245	0.01452	2	3.61	0.0007
Group 13 vs. 17	-0.019	0.0089	2	-2.13	0.0374

Table A-5. Continued

Group 13 vs. 18	-0.0173	0.01121	2	-1.55	0.1278
Group 13 vs. 19	0.02656	0.02253	2	1.18	0.2435
Group 14 vs. 15	-0.0441	0.03296	2	-1.34	0.1865
Group 14 vs. 16	0.06218	0.02069	2	3.01	0.004
Group 14 vs. 17	-0.0093	0.01722	2	-0.54	0.5926
Group 14 vs. 18	-0.0076	0.01852	2	-0.41	0.683
Group 14 vs. 19	0.0363	0.02692	2	1.35	0.1831
Group 15 vs. 16	0.1063	0.03035	2	3.5	0.0009
Group 15 vs. 17	0.03483	0.0281	2	1.24	0.2205
Group 15 vs. 18	0.0365	0.02892	2	1.26	0.2123
Group 15 vs. 19	0.0804	0.0349	2	2.3	0.0251
Group 16 vs. 17	-0.0715	0.01147	2	-6.23	<.0001
Group 16 vs. 18	-0.0698	0.01334	2	-5.23	<.0001
Group 16 vs. 19	-0.0259	0.02366	2	-1.09	0.2789
Group 17 vs. 18	0.00166	0.00682	2	0.24	0.8081
Group 17 vs. 19	0.04557	0.0207	2	2.2	0.032
Group 18 vs. 19	0.0439	0.02179	2	2.01	0.0489
Group 8 vs. 15	0.08828	0.0294	2	3	0.0041
Group 24,27 vs. 25,26	0.06223	0.00969	2	6.42	<.0001
Group 21 vs. 24,27	0.09706	0.00955	2	10.17	<.0001
Group 17,18 vs. 16,19	0.05768	0.01231	2	4.68	<.0001
Group 12-15 vs. 16-19	0.02029	0.01406	2	1.44	0.1548
Group 9 vs. 12-15	0.1864	0.02623	2	7.11	<.0001
Group 9 vs. 16-19	0.2067	0.02379	2	8.69	<.0001

REFERENCES

Ahuja T., Mir I.A., Kumar D., and Rajesh (2007). Biomolecular immobilization on conducting polymers for biosensing applications. *Biomaterials* 28(5): 791-805.

Air G.M., Ghate A.A., and Stray S.J. (1999). Influenza neuraminidase as target for antivirals. Adv. Virus Res. 54: 375-402.

Alexander H.E. (1943a). Treatment of *Haemophilus influenzae* infections and of meningococcic and pneumococcic meningitis. Am. J. Dis. Child. 66: 172-187.

Alexander H.E. (1943b). Experimental basis for treatment of *Haemophilus influenzae* infections. Am. J. Dis. Child. 66: 160-171.

Amano Y. and Cheng Q. (2005). Detection of influenza virus: traditional approaches and development of biosensors. Anal. Bioanal. Chem. 381: 156-164.

Amico C. (2009). How much will the H1N1 flu cost the U.S.? [WWW article]. URL, http://www.pbs.org/newshour/updates/health/july-dec09/flu-costs_10-08.html, Accessed February 16, 2010.

Arora, K., Prabhakar, N., Chand, S., and Malhotra, B.D. (2007). Escherichia coli genosensor based on polyaniline. Anal. Chem. 79(16): 6152-6158.

Atmar R.L., Baxter B.D., Dominguez E.A., and Taber L.H. (1996). Comparison of Reverse Transcription-PCR with Tissue Culture and Other Rapid Diagnostic Assays for Detection of Type A Influenza Virus. J. Clin. Microbiol. 34: 2604–2606.

Aulitzky W.E., Schulz T.F., Tilg H., Niederwieser D., Larcher K., Otberg L., Scriba M., Martindale J., Stern A.C., Grass P., Mach M., Dierich M.P., and Huber C. (1991). Human monoclonal antibodies neutralizing cytomegalovirus (CMV) for prophylaxis of CMV disease: report of a phase I trial in bone marrow transplant recipients. J. Infect. Dis. 163: 1344-7.

Austrian R. (1994). Confronting drug-resistant pneumococci [editorial]. Ann. Intern. Med. 121: 807-9.

Ayesh A.S. (2009). Dielectric Properties of Polyethylene Oxide Doped with NH_4I Salt. Polym. J. 41: 616-621.

Babes L., Denzoit B., Tanguy G., Le Jeune J.J., and Jallet P. (1999). Synthesis of iron oxide nanoparticles used as MRI contrast agents: a parametric study. J. Colloids Interface Sci. 212: 474–82.

Barbas C.F. III, Crowe J.E., Cababa D., Jones T.M., Zebedee S.L., Murphy B.R., Chanock R.M., and Burton D.R. (1992). Human monoclonal Fab fragments derived from a combinatorial library bind to respiratory syncytial virus F glycoprotein and neutralize infectivity. Proc. Natl. Acad. Sci. USA 89:10164-10168.

Barandun S., Kistler P., Jennet F., and Isliker H. (1962). Intravenous administration of human gamma-globulin. Vox Sang. 7: 157.

Bard A.J. and Faulkner L.R. Electrochemical Methods: Fundamentals and Applications. New York: John Wiley & Sons, Inc., 2000.

Barnes G.L., Doyle L.W., Hewson P.H., Knoches A.M., McLellan J.A., Kitchen W.H., and Bishop R.F. (1982). A randomised trial of oral gammaglobulin in low-birth-weight infants infected with rotavirus. Lancet. 1(8286): 1371-1373.

Barry W., Hudgins L., Donta S.T., and Pesanti E.L. (1992). Intravenous immunoglobulin therapy for toxic shock syndrome. J. Amer. Med. Assoc. 267: 3315-6.

Bartlett P.N. and Whitaker R.G. (1988). Strategies for the development of amperometric enzyme electrodes. Biosensors. 3(6): 359-379.

Behring E.A. and Kitasato S. (1890). Uber das Zustandekommen der Diphtherie-Immunitat und der tetanus-immunitat bei thieren. Deutsch Med. Wochenschr. 49: 1113.

Bender S. and Sadik O.A. (1998). Direct electrochemical immunosensor for polychlorinated biphenyls (PCBs). Environ. Sci. Technol. 32: 788-797.

Berggren M., Nilsson D., and Robinson N.D. (2007). Organic materials for printed electronics. Nat. Mater. 6: 3-5.

Berry C.C., Wells S., Charles S., and Curtis A.S.G. (2003). Dextran and albumin derivatised iron oxide nanoparticles: influence on fibroblasts in vitro. Biomaterials. 24: 4551-4557.

Blixt O., Head S., Mondala T., Scanlan C., Huflejt M.E., Alvarez R., Bryan M.C., Fazio F., Calarese D., Stevens J., Razi N., Stevens D.J., Skehel J.J., van Die I., Burton D.R., Wilson I.A., Cummings R., Bovin N., Wong C.-H., and Paulson J.C. (2004). Printed covalent glycan array for ligand profiling of diverse glycan binding proteins. Proc. Nat. Acad. Sci. 101(49): 17033-17038.

Blum L.J. and Coulet P.R. (Eds.), 1991. Biosensor Principles and Applications. Marcel Dekker, New York.

Bodensteiner J.B., Morris H.H., Howell J.T., and Schochet S.S. (1979). Chronic ECHO type 5 virus meningoencephalitis in X-linked hypogammaglobulinemia: treatment with immune plasma. Neurology 29: 815-9.

Boon A.C., French A.M., Fleming D.M., and Zambon M.C. (2001). Detection of Influenza A Subtypes in Community-Based Surveillance. J. Med. Virol. 65: 163–170.

Brand C.M. and Skehel J.J. (1972). Crystalline antigen from the influenza virus envelope. Nature. 238: 467-474.

Branham S.E. (1935). Protection of mice against meningococcus infection by polyvalent antimeningococcic serum. Public Health Rep. 50: 768-778.

Branham S.E. (1937). Sulphanilamide, serum, and combined drug and serum therapy in experimental meningococcus and pneumococcus infections in mice. Public Health Rep. 52: 685-695.

Brunell P.A., Gershon A.A., Hughes W.T., Riley H.D. Jr., and Smith J. (1972). Prevention of varicella in high risk children: a collaborative study. Pediatrics 50: 718-22.

Burnet F. and Clark E. Influenza: a survey of the last 50 years in the light of modern work on the virus of epidemic influenza. Melbourne: MacMillan, 1942.

Burroughes J.H., Jones C.A., and Friend R.H. (1988). New semiconductor device physics in polymer diodes and transistors. Nature. 335: 137-141.

Bussel J.B. and Cunningham-Rundles C. (1985). Intravenous usage of gammaglobulin: humoral immunodeficiency, immune thrombocytopenic purpura, and newer indications. Cancer Invest. 3: 361-6.

Cameron M.L., Schell W.A., Bruch S., Bartlett J.A., Waskin H.A., and Perfect J.R. (1993). Correlation of in vitro fluconazole resistance of Candida isolates in relation to therapy and symptoms of individuals seropositive for human immunodeficiency virus type I. Antimicrob. Agents. Chemother. 37: 2449-53.

Centers for Disease Control and Prevention (CDC). (Aug. 10, 2009). Interim Guidance for the Detection of Novel Influenza A Virus Using Rapid Influenza Diagnostic Tests [WWW document]. URL, http://www.cdc.gov/h1n1flu/guidance/rapid_testing.htm. Accessed December 10, 2009.

Casadevall A. (1996). Antibody-Based Therapies for Emerging Infectious Diseases. Emerg. Infect. Dis. 2(3): 200-208.

Casadevall A. and Scharff M.D. (1994). "Serum therapy" revisited: animal models of infection and the development of passive antibody therapy. Antimicrob. Agents Chemother. 38: 1695-1702.

Casadevall A. and Scharff M.D. (1995). Return to the past: the case for antibody-based therapies in infectious diseases. Clin. Infect. Dis. 21: 150-61.

Grennan K., Killard A.J., Hanson C.J., Cafolla A.A., and Smyth M.R. (2006). Optimisation and characterization of biosensors based on polyaniline. Talanta. 68(5): 1591-1600.

Centers for Disease Control and Prevention (CDC). (2009). Novel H1N1 Flu: Background on the Situation [WWW document]. URL, http://www.cdc.gov/h1n1flu/background.htm, Accessed June 10, 2010.

Charych D.H., Nagy J.O., Spevak W., and Bednarski M.D. (1993). Direct Colorimetric Detection of a Receptor-Ligand Interaction by a Polymerized Bilayer Assembly. Science. 261: 585–588.

Chaudhuri D. and Sarma D.D. (2006). Blue emitting polyaniline. Chem. Commun. 2681-2683.

Cho C.T., Feng K.K., and Brahmacupta N. (1976). Synergistic antiviral effects of adenine arabinoside and humoral antibodies in experimental encephalitis due to Herpesvirus hominis. J. Infect. Dis. 133: 157-167.

Class E.C., Osterhaus A.D., van Beek R., De Jong J.C., Rimmelzwaan G.F., Senne D.A., Krauss S., Shortridge K.F., and Webster R.G. (1998). Human influenza A H5N1 virus related to a highly pathogenic avian influenza virus. Lancet. 351: 472-477.

Cohn E.J., Oncley J.L., Strong L.E., Hughes W.L., and Armstrong S.H. (1944). Chemical, clinical and immunological studies on the products of human plasma fractionation: I. The characterization of protein fractions of human plasma. J. Clin. Invest. 23: 417-432.

Conti D.J., Freed B.M., Gruber S.A., and Lempert N. (1994). Prophylaxis of primary cytomegalovirus disease in renal transplant recipients: a trial of ganciclovir vs. immunoglobulin. Arch. Surg. 129: 443-7.

Cooper M.A. (2003). Label-free screening of bio-molecular interactions. Anal. Bioanal. Chem. 377: 834-842.

Cooper M.A., Dultsev F.N., Minson T., Ostanin V.P., Abell C., and Klenerman K. (2001). Direct and sensitive detection of a human virus by rupture event scanning. Nat Biotechnol. 19: 833–837.

Correa A.G., Baker C.J., Schutze G.E., and Edwards M.S. (1994). Immunoglobulin G enhances C3 degradation on coagulase-negative staphylococci. Infect. Immun. 62: 2362-6.

Cosnier S. and Lepellec A. (1999). Poly (pyrrole-biotin): a new polymer for biomolecule grafting on electrode surfaces. Electrochim. Acta. 44: 1833-1836.

Cross A. (1995). Intravenous immunoglobulins to prevent and treat infectious diseases. In: Atassi M.Z. and Bixler G.S.J., Eds. Immunobiology of Proteins and Peptides VIII. New York: Plenum Press, 1995.

Dallas P., Moutis N., Devlin E., Niarchos D., and Petridis D. (2006). Characterization, electrical and magnetic properties of polyaniline/maghemite nanocomposites. Nanotechnology. 17(19): 5019-5026.

Davis S.S. (1997). Biomedical applications of nanotechnology—implications for drug targeting and gene therapy. Trends Biotechnol. 15(6): 217–224.

Diaz A.F., Kanazawa K.K., and Gardini G.P. (1979). Electrochemical polymerization of pyrrole. J. Chem. Soc., Chem. Commun. 635-636.

Drummond T.G., Hill M.G., and Barton J.K. (2003). Electrochemical DNA sensors. Nat. Biotechnol. 21:1192-1199.

D'Souza S.F. (2001). Review: Microbial Biosensors. Biosens. Bioelectron. 16: 337-353.

Dubowski J.J. (2006, Oct 3). Research opportunity for MSc and PhD students in physics, material engineering, bio-physics and nanomedicine. Laboratory for Quantum Semiconductors and Laser-based Nanotechnology [WWW document]. URL, http://www.gel.usherbrooke.ca/cegi/documents/Epitaxial_QD_Device_v2.pdf. Accessed June 2, 2010.

Dultsev F.N., Ostanin V.P., and Klenerman D. (2000). "Hearing" Bond Breakage. Measurement of Bond Rupture Forces Using a Quartz Crystal Microbalance. Langmuir. 16: 5036-5040.

Dultsev F.N., Speight R.E., Fiorini M.T., Blackburn J.M., Abell C., Ostanin V.P., and Klenerman D. (2001). Direct and Quantitative Detection of Bacteriophage by "Hearing" Surface Detachment Using a Quartz Crystal Microbalance. Anal Chem. 73: 3935-3939.

Ellis J.S. and Zambon M.C. (2002). Molecular diagnosis of influenza. Rev. Med. Virol. 12: 375–389.

Eun A.J., Huang L., Chew F.T., Li S.F., and Wong S.M. (2002). Detection of two orchid viruses using quartz crystal microbalance (QCM) immunosensors. J. Virol. Methods. 99: 71–79.

Expert Committee on Influenza, WHO Tech. Rep. Ser. No. 64. (1953).

Feinberg S.M. The therapy of (horse) serum reactions. General rules in the administration of therapeutic serums. J. Amer. Med. Assoc. 107: 1717-1719.

Felton L.D. (1928). The units of protective antibody in antipneumococcus serum and antibody solution. J. Infect. Dis. 43: 531-42.

Fisher M.W. (1957). Synergism between human gamma globulin and chloroamphenicol in the treatment of experimental bacterial infections. Antibiot. Chemother. 7: 315-321.

Flexner S. (1913). The results of the serum treatment in thirteen hundred cases of epidemic meningitis. J. Exp. Med. 17: 553-576.

Focke W.W., Wnek G.E., and Wei Y. (1987). Influence of oxidation state, pH, and counterion on the conductivity of polyaniline. J. Phys. Chem. 91(22): 5813-5818.

Fodor E., Devenish L., Engelhardt O.G., Palese P., Brownlee G.G., and Garcia-Sastre A. (1999). Rescue of influenza A virus from recombinant DNA. J. Virol. 73: 9679-9682.

Fothergill L.R.D. (1937). Haemophilus influenzae (Pfeiffer bacillus) meningitis and its specific treatment. New Engl. J. Med. 216: 587-590.

Frickhofen N., Abkowitz J.L., Safford M., Berry J.M., Antunez-de-Mayolo J., Astrow A., Cohen R., Halperin I., King L., Mintzer D., Cohen B., and Young N.S. (1990). Persistent B19 parvovirus infection in patients infected with human immunodeficiency virus type 1 (HIV-1): a treatable cause of anemia in AIDS. Ann. Intern. Med. 113: 926-33.

Gajendran P. and Saraswathi R. (2008). Polyaniline—carbon nanotube composites. Pure Appl. Chem. 80(11): 2377-2395.

Gambhir A., Gerard M., Mulchandani A., and Malhotra B.D. (2001). Coimmobilization of urease and glutamate dehydrogenase in electrochemically prepared polypyrole-polyvinyl sulfonate films. Appl. Biochem. Biotechnol. 96: 249-258.

Garjonyte R. and Malinauskas A. (2000). Amperometric glucose biosensors based on Prussian Blue—and polyaniline—glucose oxidase modified electrodes. Biosens. Bioelectron. 15(9-10): 445-451.

GE Healthcare. (2010). About Biacore Systems [WWW document]. URL, http://www.biacore.com/lifesciences/technology/introduction/data_interaction/index.html Accessed July 10, 2010.

Gerard M., Chaubey A., and Malhotra B.D. (2002). Application of Conducting Polymers to Biosensors. Biosens. Bioelectron. 17: 345-359.

Glarum S.H. and Marshall J.H. (1986). In situ potential dependence of poly(aniline) paramagnetism. J. Phys. Chem. 90(23): 6076.

Gorman C.B. and Grubbs R.H. (1991). Conjugated Polymers: The Interplay Between Synthesis, Structure, and Properties. In Conjugated Polymers. Bredas, J.L., and Silbey, R. (eds). Kluwer Academic Publishers, pp. 1-48.

Gospodinova, N., Mokreva, P., and Terlemezyan, L. (1996). Concomitant processes in the redox switching of polyaniline. *Polymer International* 41(1): 79-84.

Gref R., Minamitake Y., Peracchia M.T., Trubetskoy V., Torchilin V., and Langer R. (1994). Biodegradable long-circulating polymeric nanospheres. Science 18(263): 1600–1603.

Grzeszczuk M. and Poks P. (1995). Analysis of charge transport impedance in the reduction of thin films of conducting polyaniline in aqueous trichloroacetic acid solutions. J. Electroanal. Chem. 387(1-2): 79-85.

Grzeszczuk M. and Szostak R. (2003). Electrochemical and Raman studies on the redox switching hysteresis of polyaniline. *Solid State Ionics* 157(1-4): 257-262.

Grzeszczuk M. and Zabinska-Olszak G. (1993). Ionic transport in polyaniline film electrodes: an impedance study. J. Electroanal. Chem. 359(1-2): 161-174.

Hamad-Schifferli K., Schwartz J.J., Santos A.T., Zhang S., and Jacobson J.M. (2002). Remote electronic control of DNA hybridization through inductive coupling to an attached metal nanocrystal antenna. Nature. 415: 152-155.

Hatta M., Gao P., Halfmann P., and Kawaoka Y. (2001a). Molecular basis for high virulence of Hong Kong H5N1 influenza A viruses. Science. 293: 1840-1842.

Hatta M., Neumann G., and Kawaoka Y. (2001b). Reverse genetics approach towards understanding pathogenesis of H5N1 Hong Kong influenza A virus infection. Philos. Trans. R. Soc. Lond. B. Biol. Sci. 356: 1841-1843.

Hay A.J., Wolstenholme A.J., Skehel J.J., and Smith M.H. (1985). The molecular basis of the specific anti-influenza action of amantadine. EMBO J. 4: 3021-3024.

Heeger A. and Smith P. (1991). Solution Processing of Conducting Polymers: Opportunities for Science and Technology. In Conjugated Polymers. Bredas, J.L., and Silbey, R. (eds). Kluwer Academic Publishers, pp. 141-210.

Hindiyeh M., Goulding C., Morgan H., Kenyon B., Langer J., Fox L., Dean G., Woolstenhulme D., Turnbow A., Billetdeaux E., Shakib S., Gordon C., Powers A., Vardeny G., Johnson M., Skodack-Jones L., and Carroll K. (2000). Evaluation of BioStar FLU OIA assay for rapid detection of influenza A and B viruses in respiratory specimens. J. Clin. Virol. 17: 119–126.

Homeland Security Council (HSC). (2005, Nov 1). National Strategy for Pandemic Influenza [WWW document]. URL, http://www.whitehouse.gov/homeland/nspi.pdf. Accessed March 24, 2007.

Homola J. (2003). Present and future of surface plasmon resonance biosensors. Anal. Bioanal. Chem. 377: 528–539.

Hong S.Y. and Park S.M. (2005) Electrochemistry of conductive polymers 36. pH dependence of polyaniline conductivities studied by current-sensing atomic force microscopy. *Journal of Physical Chemistry B* 109(19): 9305-9310.

Huang W., Taylor S., Fu K.F., Zhang D.H., Hanks T.W., Rao A.M., and Sun Y.P. (2002). Attaching proteins to carbon nanotubes via diimide-activated amidation. Nano Lett. 2: 311-314.

Hurt A.C., Baas C., Deng Y.M., Roberts S., Kelso A., and Barr I.G. (2009). Performance of influenza rapid point-of-care tests in the detection of swine lineage A(H1N1) influenza viruses. Influenza Other Respi. Viruses. 3: 171-176.

Ivnitski D., Ihab A.H., Plamen A., and Ebtisam W. (1999). Biosensors for detection of pathogenic bacteria. Biosens. Bioelectron. 14: 599-624.

Ivory D.M., Miller G.G., Sowa J.M., Shacklett L.W., Chance R.R., and Baughman R.H. (1979). Highly conducting charge-transfer complexes of poly(p-phenylene). J. Chem. Phys. 71: 1506.

Jahrling P.B., Peters C.J., and Stephen E.L. (1984). Enhanced treatment of Lassa fever by immune plasma combined with ribavirin in cynomolgus monkeys. J. Infect. Dis. 149: 420-427.

Jager E.W.H., Smela E., and Inganas O. (2000). Microfabricating conjugated polymer actuators. Science. 290(5496): 1540-1545.

Jason-Moller L., Murphy M., and Bruno J. (2006). Overview of Biacore systems and their applications. Curr. Protoc. Protein Sci. S45: 19.13.

Jennes L., Conn P.M., and Stumpf W.E. (1986). Synthesis and use of colloidal gold-coupled receptor ligands. In: Methods in Enzymology, Vol. 124. Conn P.M., Ed. Academic Press, New York, pp. 36-47.

Jiang J., Li L.C., and Xu F. (2006). Preparation, characterization and magnetic properties of PANI/La-substituted LiNi ferrite nanocomposites. Chinese J. Chem. 24(12): 1804-1809.

Jin, J.H., Zhang, D., Alocilja, E.C., and Grooms, D. (2008). Label-free DNA sensor on nano-porous silicon-polypyrrole chip for monitoring Salmonella species. IEEE Sensors Journal. 8(6): 891-895.

Johnson R.C. (2005, Nov 28). EE Times: CMOS chip slashes time needed to ID flu strains [WWW document]. URL, http://www.eetimes.com/showArticle.jhtml?articleID=174401018. Accessed June 27, 2007.

Kahn R.L. (1921). Studies on Complement Fixation: I. The Rate of Fixation of Complement at Different Temperatures. The Journal of Experimental Medicine. 34: 217-230.

Kawai T., Kuwabara T., and Yoshino K. (1991). Electrochemical Preparation of an Insulating Thin Film and Its Characterization. Jpn. J. Appl. Phys. 30: L1192-L1194.

Khurana S., Chearwae W., Castellino F., Manischewitz J., King L.R., Honorkiewicz A., Rock M.T., Edwards K.M., Del Giudice G., Rappuoli R., and Golding H. (2010). Vaccines with MF59 adjuvant expand the antibody repertoire to target protective sites of pandemic avian H5N1 influenza virus. Sci. Transl. Med. 2(15): 15ra5.

Kim H.-S. and Wamser C.C. (2006). Photoelectropolymerization of aniline in a dye-sensitized solar cell. Photochem. Photobio. Sci. 5: 955-960.

Kim J.-H., Cho J.-H., Cha G.-S., Lee C.-W., Kim H.-B., and Paek S.-H. (2000). Conductimetric membrane strip immunosensor with polyaniline-bound gold colloids as signal generator. Biosens. Bioelectron. 14(12): 907-915.

Kim S.W., Cho H.G., and Park C.R. (2009). Fabrication of Unagglomerated Polypyrrole Nanospheres with Controlled Sizes from a Surfactant-Free Emulsion System. Langmuir. 25(16): 9030-9036.

King D. (2006). Development of Rapid Field-Based Diagnostics to Improve the Control of Exotic Livestock Diseases. Speech from Agricultural Biotechnology International Conference 2006 [WWW document]. URL, www.abic2006.org/pdf/speakers/DonaldKing.pdf. Accessed April 20, 2007.

Kistler P. and Nitschmann H. (1962). Large scale production of human plasma fractions. Vox. Sang. 7: 414-424.

Kohler G. and Milstein C. (1975). Continuous cultures of fused cells secreting antibody of predefined specificity. Nature. 256: 495-497.

Kim K.S. (1987). Efficacy of human immunoglobulin and penicillin G in treatment of experimental group B streptococcal infection. Pediatr. Res. 21: 289-92.

Krug R.M. (2003). The potential use of influenza virus as an agent for bioterrorism. Antiviral Research. 57: 147-150.

Kuno A., Uchiyama N., Koseki-Kuno S., Ebe Y., Takashima S., Yamada M., and Hirabayashi J. (2005). Evanescent-field fluorescence-assisted lectin microarray: a new strategy for glycan profiling. Nature Methods. 2: 851-856.

Lacava L.M., Lacava Z.G.M., Da Silva M.F., Silva O., Chaves S.B., Azevedo R.B., Pelegrini F., Gansau C., Buske N., Sabolovic D., and Morais P.C. (2001). Magnetic resonance of a dextran-coated magnetic fluid intravenously administered in mice. Biophys. J. 80: 2483–2486.

Laitinen M.P.A. and Vuento M. (1996). Affinity immunosensor for milk progesterone: identification of critical parameters. Biosens. Bioelectron. 11(12): 1207-1214.

Laitinen O.H., Nordlund H.R., Hytonen V.P., and Kulomaa M.S. (2007). Brave new (strept)avidins in biotechnology. Trends Biotechnol. 25(6): 269-277.

Lang A.B., Cryz S.J., Schurch U., Ganss M.T., and Bruderer U. (1993). Immunotherapy with human monoclonal antibodies. J. Immunol. 151: 466-72.

Leca-Bouvier B. and Blum L.J. (2005). Biosensors for Protein Detection: A Review. Analytical Letters. 38:1491-1517.

Lee C.-W. and Suarez D.L. (2004). Application of real-time RT-PCR for the quantitation and competitive replication study of H5 and H7 subtype avian influenza virus. J. Virol. Meth. 119: 151-158.

Lee M.S., Tzeng J.S., Chen Y.C., and Shiramatsu T. (1989). Stability of Electrical and Photovoltaic Characteristics of HBr Solution-Doped Polyacetylene. Jpn. J. Appl. Phys. 28: 1008-1012.

Li, G., Jiang, L., and Peng, H. (2007a) One-dimensional polyaniline nanostructures with controllable surfaces and diameters using vanadic acid as the oxidant. *Macromolecules* 40(22): 7890-7894.

Li, X., Shen, J.Y., Wan, M.X., Chen, Z.J., and Wei, Y. (2007b) Core-shell structured and electro-magnetic functionalized polyaniline composites. *Synthetic Metals* 157(13-15): 575-579.

Liu Y., Matsumura T., Imanishi N., Hirano A., Ichikawa T., and Takeda Y. (2005). Electrochem. Solid State Lett. 8(2): A599-A602.

Luke T.C., Kilbane E.M., Jackson J.L., and Hoffman S.L. (2006). Meta-Analysis: Convalescent Blood Products for Spanish Influenza Pneumonia: A Future H5N1 Pandemic? Ann. Int. Med. 145(8): 599-609.

Lyons, M.E.G. (1994) Chapter 1, Electroactive Polymer Electrochemistry, Part I: Fundamentals. Plenum Press: New York, NY.

MacBeath G. and Schreiber S.L. (2000). Printing proteins as microarrays for high-throughput function determination. Science. 8: 1760-1763.

MacDiarmid A.G. (2001). Synthetic metals: A novel role for organic polymers (Nobel Lecture). Angew. Chem. Int. Ed. 40: 2581-2590.

MacDiarmid A.G., Chiang J.C., Richter A.F., and Epstein A.J. (1987). Polyaniline: a new concept in conducting polymers. Synthetic Metals. 18(1-3): 285-290.

Magnard C., Valette M., Aymard M., and Lina B. (1999). Comparison of Two Nested PCR, Cell Culture, and Antigen Detection for the Diagnosis of Upper Respiratory Tract Infections due to Influenza Viruses. J. Med. Virol. 59: 215–220.

Malhotra B.D., Chaubey A., and Singh S.P. (2006). Prospects of conducting polymers in biosensors. Anal. Chim. Acta 578: 59-74.

Malinauskas A., Malinauskiene J., and Ramanavicius A. (2005). Topical Review: Conducting polymer-based nanostructurized materials: electrochemical aspects. Nanotechnology. 16: R51-62.

Mann S. (2000). The Chemistry of Form. Angew. Chem. Int. Edit. 39(19): 3392-3406.

Marinakos S.M., Brousseau L.C. III, Jones A., and Feldheim D.I. (1998). Template synthesis of one-dimensional Au, Au-poly(pyrrole), and poly(pyrrole) nanoparticle arrays. Chem. Mater. 10: 1214-1219.

Marks G and Beatty W.K. Epidemics. New York: Scribners, 1976.

Masihi K.N. and Lange W. (1980). J. Immunol. Methods 36: 173–179.

Matrosovich M.N., Matrosovich T.Y., Gray T., Roberts N.A., and Klenk H.-D. (2004). Human and avian influenza viruses target different cell types in cultures of human airway epithelium. Proc. Natl. Acad. Sci. USA. 101: 4620-4624.

McCloskey R.V. (1985). Corynebacterium diphtheriae (diphtheria). In: Mandell G.L., Douglas R.G. Jr., Bennett J.E., Eds. Principles and practice of infectious diseases. 2nd ed. New York: John Wiley and Sons, 1171-1174.

Michaelis M., Doerr H.W., and Cinatl J. Jr. (2009). Novel swine-origin influenza A virus in humans: another pandemic knocking at the door. Med. Microbiol. Immunol. 198: 175-183.

McKimm-Breschkin J.L., Colman P.M., Jin B., Krippner G.Y., McDonald M., Reece P.A., Tucker S.P., Waddington L., Watson K.G., and Wu W.Y. (2003). Angew. Chem. Int. Ed. Engl. 42: 3118–3121.

Meeusen, C., Alocilja, E.C., and Osburn, W. (2005). Detection of E. coli O157:H7 Using a Miniaturized Surface Plasmon Resonance Biosensor. Transactions of the ASAE. 48(6):2409-2416.

Mofenson L.M., Moye J. Jr., Korelitz J., Bethel J., Hirschhorn R., and Nugent R. (1994). Crossover of placebo patients to intravenous immunoglobulin confirms efficacy for prophylaxis of bacterial infections and reduction of hospitalizations in human immunodeficiency virus-infected children. Pediatr. Infect. Dis. J. 13: 477-84.

Moghimi S.M., Hunter A.C., and Murray J.C. (2001). Long-circulating and target-specific nanoparticles: theory to practice. Pharm. Rev. 53: 283–318.

Montalto N.J. (2003). An Office-Based Approach to Influenza: Clinical Diagnosis and Laboratory Testing. Am. Fam. Physician 67: 111–118.

Muhammad-Tahir, Z., Alocilja, E.C., and Grooms, D.L. (2005a). Polyaniline synthesis and its biosensor application. Biosens. Bioelectron. 20(8): 1690-1695.

Muhammad-Tahir, Z., Alocilja, E.C., and Grooms, D.L. (2005b). Rapid detection of bovine viral diarrhea virus as surrogate of bioterrorism agents. IEEE Sensors Journal. 5(4):757-762.

Muhammad-Tahir, Z., Alocilja, E.C., and Grooms, D.L. (2007). Indium Tin Oxide-Polyaniline Biosensor: Fabrication and Characterization. Sensors Journal. 7:1123-1140.

National Institute of Allergy and Infectious Disease (NIAID). (2005). Focus on the Flu: Antigenic Drift vs. Antigenic Shift [WWW document]. URL, http://www3.niaid.nih.gov/news/focuson/flu/illustrations/antigenic/antigenicdrift.htm. Accessed April 18, 2007.

National Institute of Allergy and Infectious Disease (NIAID). (2006). Flu (Influenza): Improving the Gold (Bead) Standard for Flu Tests [WWW document]. URL, http://www3.niaid.nih.gov/healthscience/healthtopics/Flu/Research/ongoingResearch/Archive/GoldBeadStandardforFluTests.htm. Accessed June 27, 2007.

Neumann G. and Kawaoka Y. (2006). Host Range Restriction and Pathogenicity in the Context of Influenza Pandemic. Emerg. Infect. Dis. 12(6): 881-886.

Neumann G., Watanabe T., Ito H., Watanabe S., Goto H., Gao P., Hughes M., Perez D.R., Donis R., Hoffmann E., Hobom G., and Kawaoka Y. (1999). Generation of influenza A viruses entirely from cloned cDNAs. Proc. Natl. Acad. Sci. U.S.A. 96:9345-9350.

Newborg, H. (2009). Swine Flu Scare: It's All About the Adjuvant! [WWW document]. URL, http://www.infowars.com/swine-flu-scare-its-all-about-the-adjuvant/. Accessed May 6, 2010.

Ohlson S., Jungar C., Strandh M., and Mandenius C.-F. (2000). Continuous weak-affinity immunosensing. Trends Biotechnol. 18(2): 49-52.

Paek S.-H., Lee C.-W., Yook S.-H., Kwon O.-H., and Park Y.-N. (1999). Performance control strategies of one-step immuno-chromatographic assay system for Salmonella typhimurium. Anal. Lett. 32(2): 335–360.

Pal, S. and Alocilja, E.C. (2009). Electrically active polyaniline coated Magnetic (EAPM) Nanoparticle as Novel Transducer in Biosensor for Detection of *Bacillus anthracis* Spores in Food Samples. Biosens. Bioelectron. 24(5): 1437-1444.

Pal, S., Alocilja,E.C., and Downes, F.P. (2007). Nanowire Labeled Direct-Charge Transfer Biosensor for Detecting Bacillus species. Biosensors & Bioelectronics Journal. 22:2329-2336.

Pal, S., Setterington, E., and Alocilja, E.C. (2008). Electrically-Active Magnetic Nanoparticles for Concentrating and Detecting Bacillus anthracis Spores in a Direct-Charge Transfer Biosensor. IEEE Sensors Journal. 8(6): 647-654.

Pal, S., Ying, W., Alocilja,E.C., and Downes, F.P. (2008). Sensitivity and Specificity Performance of a Direct-Charge Transfer Biosensor for Detecting Bacillus cereus in Selected Food Matrices. Biosystems Engineering Journal. 99(4): 461-468.

Park S. and Hamad-Schifferli K. (2010). Enhancement of In Vitro Translation by Gold Nanoparticle—DNA Conjugates. ACS Nano. [Epub online].

Paul E.W., Ricco A.J., and Wrighton M.S. (1985). Resistance of Polyaniline Films as a Function of Electrochemical Potential and the Fabrication of Polyaniline-Based Microelectronic Devices. J. Phys. Chem. 89: 1441.

Pennington J.E. (1990). Newer uses of intravenous immunoglobulins as anti- infective agents. Antimicrob. Agents Chemother. 34: 1463-6.

Pier G.B., Thomas D., Small G., Siadak A., and Zweerink H. In vitro and in vivo activity of polyclonal and monoclonal human immunoglobulins G, M, and A against *Pseudomonas aeroginosa* lipopolysaccharide. Infect. Immun. 57: 174-9.

Pinto L.H., Holsinger L.J., and Lamb R.A. (1992). Influenza virus M2 protein has ion channel activity. Cell. 69: 517-528.

Poddar P., Wilson J.L., Srikanth H., Morrison S.A., and Carpenter E.E. (2004). Magnetic properties of conducting polymer doped with manganese-zinc ferrite nanoparticles. Nanotechnology. 15(10): S570-574.

Poks P. and Grzeszczuk M. (1997). Temperature effects in thin film polyaniline electrodes. Pol. J. Chem. 71(8): 1140-1150.

Portet D., Denoit B., Rump E., Lejeunne J.J., and Jallet P. (2001). Nonpolymeric coatings of iron oxide colloids for biological use as magnetic resonance imaging contrast agents. J. Colloids Interface Sci. 238: 37–42.

Potyrailo R.A. (2006). Polymeric sensor materials: Toward an alliance of combinatorial and rational design tools? Angew. Chem. Int. Ed. 45: 702-723.

Pouget J.P., Jozefowicz M.E., Epstein A.J., Tang X., and Macdiarmid A.G. (1991). XRay Structure of Polyaniline. *Macromolecules* 24(3): 779-789.

Powell H.M. and Jamieson W.A. (1939). Combined therapy of pneumococcic rat infections with rabbit antipneumococcic serum and sulfapyridine (2-sulfanilyl aminopyridine). J. Immunol. 36:459-465.

Prince A.M., Reesink H., Pascual D., Horowitz B., Hewlett I., Murthy K.K., Cobb K.E., and Eichberg J.W. (1991). Prevention of HIV Infection by Passive Immunization with HIV Immunoglobulin. AIDS Res. Hum. Retroviruses 7(12): 971-973.

Prince G., Hemming V., and Chanock R. (1986). The use of purified immunoglobulin in the therapy of respiratory syncytial virus infection. Pediatr. Infect. Dis. 5: S201-S203.

Prince H.E. and Leber A.L. (2003). Comparison of Complement Fixation and Hemagglutinin Inhibition Assays for Detecting Antibody Responses following Influenza Virus Vaccination. Clin. Diagn. Lab. Immunol. 10: 481–482.

Rabolt J.F., Clarke T.C., Kanazawa K.K., Reynolds J.R., and Street G.B. (1980). Organic Metals: Polyparaphenylene Sulfide Hexafluoroarsenate. J. Chem. Soc., Chem. Commun. 347-348.

Rackemann F.M. (1942). Allergy: serum reactions, with particular reference to the prevention and treatment of tetanus. J. Amer. Med. Assoc. 226: 726-733.

Radke, S. and Alocilja, E.C. (2005). A Microfabricated Biosensor for Detecting Foodborne Bioterrorism Agents. IEEE Sensors Journal. 5(4): 744-750.

Ramge P., Unger R.E., Oltrogge J.B., Zenker D., Begley D., Kreuer J., von Briesen H. (2000). Polysorbate-80 coating enhances uptake of polybutylcyanoacrylate (PBCA)-nanoparticles by human and bovine primary brain capillary endothelial cells. Eur. J. Neurol. 12: 1931–2934.

Ramisse F., Szatanik M., Binder P., and Alonso J.-M. (1993). Passive local immunotherapy of experimental staphylococcal pneumonia with human intrave- nous immunoglobulin. J. Infect. Dis. 168: 1030-3.

Ray A., Asturias G.E., Kershner D.L., Richter A.F., Macdiarmid A.G., and Epstein A.J. (1989). Polyaniline - Doping, Structure and Derivatives. *Synthetic Metals* 29(1): E141-E150.

Reed E.C., Bowden R.A., Dandliker P.S., Lilleby K.E., and Meyers J.D. (1988). Treatment of cytomegalovirus pneumonia with ganciclovir and intravenous cytomegalovirus immunoglobulin in patients with bone marrow transplants. Ann. Intern. Med. 109: 783-8.

Reid A.H., Taubenberger J.K., and Fanning T.G. (2001). The 1918 Spanish influenza: integrating history and biology. Microbes Infect. 3:81-87.

Reina J., Padilla E., Alonso F., Ruiz De Gopegui E., Munar M., and Mari M. (2002). Evaluation of a New Dot Blot Enzyme Immunoassay (Directigen Flu A + B) for Simultaneous and Differential Detection of Influenza A and B Virus Antigens from Respiratory Samples. J. Clin. Microbiol. 40: 3515–3517.

Sadik O.A., Gheorghiu E., Xu H., Andreescu D., Balut C., Gheorghiu M., and Bratu D. (2002). Differential Impedance Spectroscopy for Monitoring Protein Immobilization and Antibody-Antigen Reactions. Anal. Chem. 74: 3142-3150.

Sato T., Serizawa T., and Okahata Y. (1996). Binding of influenza A virus to monosialoganglioside (GM3) reconstituted in glucosylceramide and sphingomyelin membranes. Biochim. Biophys. Acta. 1285: 14–20.

Schlaes D.M., Binczewski B., and Rice L.B. (1993). Emerging antimicrobial resistance and the immunocompromised host. Clin. Infect. Dis. 17(suppl 2): S527-36.

Schofield D.J. and Dimmock N.J. (1996). Determination of affinities of a panel of IgGs and Fabs for whole enveloped (influenza A) virions using surface Plasmon resonance. J. Virol. Methods. 62: 33–42.

Scott M.T., Spinks G.M., and Wallace G. (2005). Micro-humidity sensors based on a processable polyaniline blend. Sens. Actuators B: Chem. 107(2): 657-665.

Schuhmann W., Lammert R., Uhe B., and Schemidt H.L. (1990). Polypyrrole, a new possibility for covalent binding of oxido-reductases to electrode surfaces as a base for stable biosensors. Sensor Actuator B. 1: 537-541.

Schultze D., Thomas Y., and Wunderli W. (2001). Evaluation of an Optical Immunoassay for the Rapid Detection of Influenza A and B Viral Antigens. Eur. J. Clin. Microbiol. Infect. Dis. 20: 280–283.

See R.H. and Chow A.W. (1989). Microbiology of toxic shock syndrome: overview. Rev. Infect. Dis. 11(suppl 1): S55-60.

Shaw M.W., Arden N.H., and Maassab H.F. (1992). New Aspects of Influenza Viruses. Clinical Microbiology Reviews. 5(1): 74-92.

Shimasaki C.D., Achyuthan K.E., Hansjergen J.A., and Appleman J.R. (2001). Rapid diagnostics: the detection of neuraminidase activity as a technology for high-specificity targets. Philos. Trans. R. Soc. Lond. B. Biol. Sci. 356: 1925–1931.

Shinya K., Ebina M., Yamada S., Ono M., Kasai N., and Kawaoka Y. (2006). Avian flu: influenza virus receptors in the human airway. Nature. 440: 435-6.

Smela E. (2003). Conjugated polymer actuators for biomedical applications. Adv. Mater. 15: 481-494.

Solvay (2010). Cost of Influenza [WWW document]. URL, http://www.solvay-influenza.com/aboutinfluenza/costofinfluenza/0,,2655-2-0,00.htm, Accessed May 4, 2010.

Sonea S., Barduas A., and Frapier A. (1958). Combined protective action of human gamma globulin and antibiotics when administered simultaneously in experimental staphylococcal infections. Rev. Can. Biol. 17: 110-115.

Spackman E., Senne D.A., Myers T.J., Bulaga L.L., Garber L.P., Perdue M.L., Lohman K., Daum L.T., and Suarez D.L. (2002). Development of a Real-Time Reverse Transcriptase PCR Assay for Type A Influenza Virus and the Avian H5 and H7 Hemagglutinin Subtypes. J. Clin. Microbiol. 40(9): 3256-3260.

Stafstrom S., Bredas J.L., Epstein A.J., Woo H.S., Tanner D.B., Huang W.S., and MacDiarmid A.G. (1987). Polaron lattice in highly conducting polyaniline: Theoretical and optical studies. Phys. Rev. Lett. 59(13): 1464-1467.

Stejskal J. and Gilbert R.G. (2002). Polyaniline. Preparation of a conducting polymer (IUPAC Technical Report). Pur Appl. Chem. 74(5): 857-867.

Stejskal J., Kratochvil P., and Jenkins A.D. (1996). The formation of polyaniline and the nature of its structures. Polymer. 37(2): 367-369.

Stevens J., Blixt O., Glaser L., Taubenberger J.K., Palese P., Paulson J.C., and Wilson I.A. (2006a). Glycan Microarray Analysis of the Hemagglutinins from Modern and Pandemic Influenza Viruses Reveals Different Receptor Specificities. J. Mol. Biol. 355: 1143-1155.

Stevens J., Blixt O., Paulson J.C., and Wilson I.A. (2006b). Glycan microarray technologies: tools to survey host specificity of influenza viruses. Nature Reviews: Microbiol. 4: 857-864.

Stevens J., Blixt O., Tumpey T.M., Taubenberger J.K., Paulson J.C., and Wilson I.A. (2006c). Structure and Receptor Specificity of the Hemagglutinin from an H5N1 Influenza Virus. Science. 312: 404-410.

Stratta R.J., Shaefer M.S., Cushing K.A., Markin R.S., Reed E.C., Langnas A.N., Pillen T.J., and Shaw B.W. Jr. (1992). A randomized prospective trial of acyclovir and immune globulin prophylaxis in liver transplant recipients receiving OKT3 therapy. Arch. Surg. 127: 55-64.

Su C.C., Wu T.Z., Chenb L.K., Yang H.H., and Tai D.F. (2003). Development of immunochips for the detection of dengue viral antigens. Anal. Chim. Acta. 479: 117–123.

Suarez D.L., Perdue M.L., Cox N., Rowe T., Bender C., Huang J., and Swayne D.E. (1998). Comparisons of highly virulent H5N1 influenza A viruses isolated from humans and chickens from Hong Kong. J. Virol. 72: 6678-6688.

Subbarao K., Klimov A., Katz J. Regnery H., Lim W., Hall H., Perdue M., Swayne D., Bender C., Huang J., Hemphill M., Rowe T., Shaw M., Xu X., Fukuda K., and Cox N. (1998). Characterization of an avian influenza A (H5N1) virus isolated from a child with a fatal respiratory illness. Science. 279: 393-396.

Suman S., Singhal R., Sharma A.L., Malhotra B.D., and Pundir C.S. (2005). Development of a lactate biosensor based on conducting copolymer bound lactate oxidase. Sensor Actuator B. 107: 768-772.

Sung K.-M., Mosley D.W., Peelle B.R., Zhang S., and Jacobson J.M. (2004). Synthesis of Monofunctionalized Gold Nanoparticles by Fmoc Solid-Phase Reactions. J. Am. Chem. Soc. 126: 5064-5065.

Svorc J., Miertus S., Katrlik J., and Stred'ansky M. (1997). Composite Transducers for Amperometric Biosensors. The Glucose Sensor. Anal. Chem. 69: 2086-2090.

Syritski V., Gyurcsanyi R.E., Opik A., and Toth K. (2005). Synthesis and characterization of inherently conducting polymers by using Scanning Electrochemical Microscopy and Electrochemical Quartz Crystal Microbalance. Synth. Met. 152 (1-3): 133-136.

Tacket C.O., Shandera W.X., Mann J.M., Hargrett N.T., and Blake P.A. (1984). Equine antitoxin use and other factors that predict outcome in type A food- borne botulism. Am. J. Med. 76: 794-8.

Takemoto D.K., Skehel J.J., and Wiley D.C. (1996). A Surface Plasmon Resonance Assay for the Binding of Influenza Virus Hemagglutinin to Its Sialic Acid Receptor. Virology. 217: 452–458.

Talkington D.F., Schwartz B., Black C.M., Todd J.K., Elliott J., Breiman R.F., and Facklam R.R. (1993). Association of phenotypic and genotypic characteristics of invasive Streptococcus pyogenes isolates with clinical components of streptococcal toxic shock syndrome. Infect. Immun. 61: 3369-74.

Taubenberger J.K., Reid A.H., Lourens R.M., Wang R., Jin G., and Fanning T.G. (2005). Characterization of the 1918 influenza virus polymerase genes. Nature. 437: 889-893.

Tumpey T.M., Maines T.R., Van Hoeven N., Glaser L., Solorzano A., Pappas C., Cox N.J., Swayne D.E., Palese P., Katz J.M., and Garcia-Sastre A. (2007). Science. 315: 655-659.

Turner A.P.F., Karube I., and Wilson G.S. (Eds.), 1987. Biosensors Fundamentals and Applications. Oxford University Press, Oxford, UK.

Uttenthaler E., Schraml M., and Mandel J., Drost S. (2001). Ultrasensitive quartz crystal microbalance sensors for detection of M13-Phages in liquids. Biosens. Bioelectron. 16: 735–743.

Vyas R.N. and Wang B. (2010). Electrochemical analysis of conducting polymer thin films. Int. J. Mol. Sci. 11: 1956-1972.

Ward M.D. and Buttry D.A. (1990). In Situ Interfacial Mass Detection with Piezoelectric Transducers. Science. 249: 1000-1007.

Watt C.H. Jr. (1978). Poisonous snakebite treatment in the United States. J. Amer. Med. Assoc. 240: 654-6.

Webby R.J. and Webster R.G. (2003). Are We Ready for Pandemic Influenza? Science. 302(5650): 1519-1522.

Webster R.G., Guan Y., Peiris M., Walker D., Krauss S., Zhou N.N., Govorkova E.A., Ellis T.M., Dyrting K.C., Sit T., Perez D.R., and Shortridge K.F. (2002). Characterization of H5N1 influenza viruses that continue to circulate in geese in southeaster China. J. Virol. 76: 118-126.

Weisman L.E., Cruess D.F., and Fischer G.W. (1993). Standard versus hyper immune intravenous immunoglobulin in preventing or treating neonatal bacterial infections. Clin. Perinatol. 20: 211-224.

Weisman L.E., Cruess D.F., and Fischer G.W. (1994). Opsonic activity of commercially available standard intravenous immunoglobulin preparations. Pediatr. Infect. Dis. J. 13: 1122-5.

Weltzin R. and Monath T.P. (1999). Intranasal antibody prophylaxis for protection against viral disease. Clin. Micr. Rev. 12(3): 383-393.

Wijaya A. and Hamad-Schifferli K. (2007). High-Density Encapsulation of Fe_3O_4 Nanoparticles in Lipid Vesicles. Langmuir. 23: 9546-9550.

Wiley D.C. and Skehel J.J. (1987). The Structure and Function of the Hemagglutinin Membrane Glycoprotein of Influenza Virus. Ann. Rev. Biochem. 56: 365-94.

Wilfert C.M., Buckley R.H., Mohanakumar T., Griffith J.F., Katz S.L., Whisnant J.K., Eggleston P.A., Moore M., Treadwell E., Oxman M.N., and Rosen F.S. (1977). Persistent and fatal central-nervous system echovirus infections in patients with agamma-globulinemia. New Engl. J. Med. 296: 1485-9.

Williams A.E., PhD. (2007). Measures To Maximize Blood and Blood Component Availability during a Pandemic. Office of Blood Research and Review (OBRR) Guidance Concept Paper.

Wilson E.J., Medearis D.N. Jr., Hansen L.A., and Rubin R.H. 9-(1-3-Dihydroxy-2-Propoxymethyl) guanine prevents death but not immunity in murine cytomegalovirus-infected normal and immunosuppressed BALB/c mice. Antimicrob. Agents Chemother. 31: 1017-1020.

World Health Organization (WHO). (2004, March 2). Avian influenza A(H5N1)- update 31: Situation (poultry) in Asia: need for a long-term response, comparison with previous outbreaks [WWW document]. URL, http://www.who.int/csr/don/2004_03_02/en/. Accessed March 24, 2007.

World Health Organization (WHO). (2006, Feb). Avian influenza ("bird flu") – Fact sheet [WWW document]. URL, http://www.who.int/mediacentre/factsheets/avian_influenza/en/. Accessed March 23, 2006.

World Health Organization (WHO) Regional Office for South-East Asia. (2007). Guidelines on Laboratory Diagnosis of Avian Influenza [WWW document]. URL, http://www.searo.who.int/LinkFiles/CDS_CDS-Guidelines-Laboratory.pdf. Accessed December 10, 2009.

World Health Organization (WHO). (2008, June 19). Cumulative Number of Confirmed Human Cases of Avian Influenza A/(H5N1) Reported to WHO [WWW document]. URL, http://www.who.int/csr/disease/avian_influenza/country/cases_table_2008_06_19/en/index.html. Accessed June 26, 2008.

World Health Organization (WHO). (2009). Pandemic (H1N1) 2009 – update 69 [WWW document]. URL, http://www.who.int/csr/don/2009_10_09/en/index.html, Accessed June 3, 2010.

Wright A., Shin S.-U., and Morrison S.L. (1992). Genetically engineering antibodies: progress and prospects. Crit. Rev. Immunol. 12: 125-168.

Wright P.F. and Webster R.G. (2001). Orthomyxoviruses. In: Knipe D.M. and Howley P.M. (Eds.). Fields Virology, 4th ed. Lippincott Williams & Wilkins, Philadelphia: pp. 1533-1579.

Xu X. and Asher S.A. (2004). Synthesis and Utilization of Monodisperse Hollow Polymeric Particles in Photonic Crystals. J. Am. Chem. Soc. 126: 7940-7945.

Xue W.Y., Qiu H., Fang K., Li J., Zhao J.W., and Li M. (2006). Electrical and magnetic properties of the composite pellets containing DBSA-doped polyaniline and Fe nanoparticles. Synth. Met. 156(11-13): 833-837.

Yang G., Cho N.-H., and Kim G.-Y. (2006). Sensing of the Insecticide Carbamate Pesticides by Surface Plasmon Resonance. Published by the American Society of Agricultural and Biological Engineers. 2006 ASAE Annual Meeting. Paper number 067125.

Yap P.L. (1994). Does intravenous immune globulin have a role in HIV-infected patients? Clin. Exp. Immunol. 97(suppl 1): 59-67.

Ybarra G., Moina C., Florit M.I., and Posadas D. (2000). Proton exchange during the redox switching of polyaniline film electrodes. Electrochem. Solid-State Lett. 3(7): 330-332.

Yoshino K., Kyokane J., Ozaki M., Yun M.S., and Inuishi Y. (1983). Effect of Double Doping on Electrical Conductivity of Poly-p-Phenylenesulfide. Jpn. J. Appl. Phys. 22: L289-L290.

Yuen K.Y., Chan P.K., Peiris M., Tsang D.N., Que T.L., Shortridge K.F., Cheung P.T., To W.K., Ho E.T., Sung R., and Cheng A.F. (1998). Clinical features and rapid viral diagnosis of human disease associated with avian influenza A H5N1 virus. Lancet. 351: 467-471.

Yuk J.S., Jin J.-H, Alocilja E.C., and Rose J.B. (2009). Performance enhancement of polyaniline-based polymeric wire biosensor. Biosens. Bioelectron. 24(5): 1348-1352.

Yun Z., Zhengtao D., Jiachang Y., Fangqiong T., and Qun W. (2007). Using cadmium telluride quantum dots as a proton flux sensor and applying to detect H9 avian influenza virus. Analytical Biochem. 364(2): 122-7.

Zhang, D. and Alocilja, E.C. (2008). Characterization of nano-porous silicon-based DNA biosensor for the detection of Salmonella Enteritidis. IEEE Sensors Journal. 8(6): 775-780.

Zhang W.D. and Evans D.H. (1991). J. Virol. Methods. 33:165-189.

Zhang Z., Wan M., and Wei Y. (2005). Electromagnetic functionalized polyaniline nanostructures. Nanotechnology. 16(12): 2827-2832.

Zhou B., Zhong N., and Guan Y. (2007). Treatment with Convalescent Plasma for Influenza A (H5N1) Infection. N. Engl. J. Med. 357(14): 1450-1451.

Zhuang X. (2009). Visualizing Individual Influenza Particles in Living Cells [WWW document]. URL, http://zhuang.harvard.edu/cellentry.html#Figure1. Accessed February 20, 2010.

Ziegler T., Katz J.M., Cox N.J., and Regnery H.L. (1997). Influenza viruses, p. 673-678. *In* N.R. Rose, E.C. de Macario, J.D. Folds, H.C. Lane, and R.M. Nakamura (ed.), Manual of clinical laboratory immunology. 5th ed. American Society for Microbiology, Washington, DC.

Zolla-Pazner S. and Gomy M.K. (1992). Passive immunization for the prevention and treatment of HIV infection. AIDS 6: 1235-47.